ASPECT RATIO EFFECT ON HEAT TRANSFER IN ROTATING TWO-PASS RECTANGULAR CHANNELS WITH SMOOTH WALLS AND RIBBED WALLS

A Dissertation

by

WEN-LUNG FU

Submitted to the Office of Graduate Studies of
Texas A&M University
in partial fulfillment of the requirements for the degree of

DOCTOR OF PHILOSOPHY

May 2005

Major Subject: Mechanical Engineering

ASPECT RATIO EFFECT ON HEAT TRANSFER IN ROTATING TWO-PASS RECTANGULAR CHANNELS WITH SMOOTH WALLS AND RIBBED WALLS

A Dissertation

by

WEN-LUNG FU

Submitted to Texas A&M University
in partial fulfillment of the requirements
for the degree of

DOCTOR OF PHILOSOPHY

Approved as to style and content by:

J. C. Han (Chair of Committee)	S. C. Lau (Member)
H. C. Chen (Member)	N. K. Anand (Member)
D. L. O'Neal (Head of Department)	

May 2005

Major Subject: Mechanical Engineering

ABSTRACT

Aspect Ratio Effect on Heat Transfer in Rotating Two-Pass Rectangular Channels with Smooth Walls and Ribbed Walls. (May 2005)

Wen-Lung Fu, B.S., Chung Yuan Christian University;

M.S., Yuan-Ze Institute of Technology

Chair of Advisory Committee: Dr. Je-Chin Han

This study experimentally investigates the effects of rotation, the buoyancy force, and the channel aspect ratio on heat transfer in two-pass rotating rectangular channels. The experiments are conducted with two surface conditions: smooth walls and 45° angled ribbed walls. The channel aspect ratios include 4:1, 2:1, 1:1, 1:2 and 1:4. Four Reynolds numbers are studied: 5000, 10000, 25000 and 40000. The rotation speed is fixed at 550 rpm for all tests, and for each channel, two channel orientations are studied: 90° and 45° or 135°, with respect to the plane of rotation. Rib turbulators are placed on the leading and trailing walls of the channels at an angle of 45° to the flow direction. The ribs have a 1.59 by 1.59 mm square cross section, and the rib pitch-to-height ratio (*P/e*) is 10 for all tests.

The effects of the local buoyancy parameter and channel aspect ratio on the regional Nusselt number ratio are presented. Pressure drop data are also measured for both smooth and ribbed channels in rotating and non-rotating conditions. The results show that increasing the local buoyancy parameter increases the Nusselt number ratio on

the trailing surface and decreases the Nusselt number ratio on the leading surface in the first pass for all channels. However, the trend of the Nusselt number ratio in the second pass is more complicated due to the strong effect of the 180° turn. Results are also presented for this critical turn region of the two-pass channels. In addition to these regions, the channel averaged heat transfer, friction factor, and thermal performance are determined for each channel. With the channels having comparable Nusselt number ratios, the 1:4 channel has the superior thermal performance because it incurs the least pressure penalty. In this study, the author is able to systematically analyze, correlate, and conclude the thermal performance comparison with the combination of rotation effects on five different aspect ratio channels with both smooth walls and rib turbulated walls.

DEDICATION

This work is dedicated to my family.

ACKNOWLEDGMENTS

The author would like to express his deepest appreciation to Professor Je-Chin Han, the chair of his doctoral committee, for his support and guidance to complete this research successfully. The author also appreciates the assistance from the other doctoral committee members: Professor N. K. Anand, Professor S. C. Lau, and Professor H. C. Chen. Special thanks to my colleague, Ms. Lesley M. Wright, who provided me grateful suggestions during the research and helped me write this dissertation. This research was supported by the U.S. Department of Energy, Office of Fossil Energy, and the National Energy Technology Laboratory.

NOMENCLATURE

A	area of smooth wall
AR	aspect ratio, $W:H$
Bo_x	local buoyancy parameter, $(\Delta\rho/\rho)_x Ro^2 (R_x/D_h)$
D_h	hydraulic diameter
d_e	diameter of coolant exit hole
e	rib height
f	friction factor
f_o	fully developed friction factor in non-rotating smooth tube
h	heat transfer coefficient
H	channel height
k	thermal conductivity of coolant
Nu	local Nusselt number, hD_h/k
Nu_o	Nusselt number for fully-developed turbulent flow in smooth pipe
P	rib pitch
P_i	pressure at the inlet of the test section
P_o	pressure at the outlet of the test section
Pr	Prandtl number
Q	heat transfer rate at wall
R	mean rotating radius
Re	Reynolds number, $\rho V D_h/\mu$
Ro	rotation number, $\Omega 2D_h/V$

R_x	local rotating radius
$T_{b,x}$	local coolant temperature
$T_{f,x}$	local film temperature
$T_{w,x}$	local wall temperature
t_d	thickness of divider wall
V	bulk velocity in streamwise direction
W	channel width
x	distance in streamwise direction
α	rib angle
β	angle of channel orientation with respect to the axis of rotation
μ	dynamic viscosity of coolant
ρ	density of coolant
$(\Delta\rho/\rho)_x$	local coolant-to-wall density ratio
Ω	rotational speed

TABLE OF CONTENTS

Page

Page

LIST OF FIGURES

Page

Page

Page

LIST OF TABLES

Page

I INTRODUCTION

Background

Gas turbines are playing an increasingly important role throughout the industrialized world. While these engines are most notably used for aircraft propulsion and land based power generation, they are also used for marine propulsion, and a variety of other industrial applications. As the demand for power, in the form electricity or thrust, continues to increase, engineers must develop engines to meet this demand. The power output can be increased by raising the temperature of the gas entering the turbine. However, increasing the gas temperature must be done cautiously. The temperature of this hot mainstream gas is limited by the turbine components, namely the turbine blades and vanes. The extremely hot gases create excessive thermal stresses and result in premature failure of a blade or vane which is detrimental to the operation of the engine.

Various cooling techniques have been implemented in the engine design to increase the life of the turbine components. Air is extracted from the compressor (air which has not passed through the combustor) and injected into the blades and vanes of the turbine. This cooling air passes internally through the components. This coolant air removes heat from the blade before it is expelled out of the blade through discrete holes, known as film cooling holes. This relatively cool air forms a protective film on the surface of the blade protecting the blade from the hot mainstream gas.

This dissertation follows the style and format of ASME Journal of Turbomachinery.

A number of methods are commonly used in various combinations to remove heat from the blade internally. The leading edge of the blade sees the greatest heat load due to the stagnation of the mainstream flow. Therefore, this region must be cooled very aggressively. Internally, jet impingement is a common technique used for the leading edge. The impinging jets effectively remove heat from the blade surface, and after the impingement, as the spent air travels through the channel, additional heat is transferred from the walls of blade to the cooling air. Although the heat load near the trailing edge is less than that near the leading edge, it is still critical to cool this region. The very thin trailing edge poses several challenges for the turbine designers. The trailing edge must be effectively cooled without compromising the structure of the blade. One cooling technique for this region is pin-fin cooling. An array of pins (or cylinders) is cast into the blade, and as the coolant passes through the array, heat is removed from the blade. With the pins attached to both the pressure and suction sides of the cooling channel, they provide additional structural support while enhancing the heat transfer in the cooling passage.

With the leading and trailing edges of the blades being cooled, only the mid-chord region remains. A number of serpentine passages can be used as channels for the coolant air. The cooling channels are commonly lined with rib turbulators, or trip strips. These ribs enhance the heat transfer in the cooling channels by tripping the boundary layer and creating additional mixing of the warmer fluid near the channel wall with the relatively cooler air near the center of the channel. The cross-section of the channels varies depending on the where channel is located in the blade. In other words, channels

closer to the leading edge may be taller channels with a relatively large distance between the leading and trailing surfaces (in the cooling channel, the leading surface of the channel is on the suction side of the blade, and the trailing surface is on the pressure side). Near the trailing edge of the blade, the opposite may be true for the cooling channels; the channels are shorter with a very small distance between the leading and trailing surfaces. The channels near the center of the blade vary from the two extremes of the leading and trailing edges, and these channels may have cross-sections which are nearly square.

Although cooling the turbine components with air taken from the compressor effectively increases the life of the components, it also reduces the overall efficiency of the engine. The coolant air reduces the amount of the working fluid used to generate power. Therefore, a balance must be maintained between increasing the gas temperature and extracting gas for cooling. Understanding flow through the coolant channels can lead to effective cooling designs which minimize the amount of coolant. These optimized cooling schemes lead to engines which operate more efficiently with increased power output.

Researchers have spent many years trying to optimize the coolant flow through these internal channels. Han et al. [1] chronicles many studies that began with non-rotating channels with and without rib turbulators. The size, shape, and placement of the turbulators have been varied to determine the optimal design for given flow conditions. Early cooling designs used transverse ribs, or ribs placed 90° to the coolant flow. These ribs created more heat transfer enhancement than a smooth channel, but this

configuration was soon replaced with angled, or skewed, ribs. The angled ribs induce secondary flow along the ribs that further increase the heat transfer from the channel wall to the coolant. Although multiple rib configurations have been shown to increase the heat transfer beyond that of angled ribs, this geometry is commonly used in the engine due to the simplicity of the design.

Additional consideration must be given to the fact that many blades use serpentine passages. These cooling passages wind through the blade, and are not limited to a simple straight channel. A common serpentine channel may consist of a first pass with coolant flowing radially outward from the engine's hub. Near the tip of the blade, the coolant turns 180° where it travels radially inward from the tip to the hub in the second pass. Another turn would connect the second pass to the third pass with radially outward flow. Coolant flow in these turns is very complex, and the heat transfer is dependent on both the channel and turn geometry.

With the blade rotating, the coolant flow does not behave as the typical channel flow. The secondary flow patterns are strongly influenced by rotation. Heat transfer coefficients on leading surface and trailing surface are not equal in rotating channels. Due to the reversal of the Coriolis force, the coolant in channels with radially inward flow and in channels with radially outward flow has an opposite effect on the heat transfer.

In addition to the above mentioned factors, the channel aspect ratio can also affect the heat transfer in blade cooling passages. Therefore, it is imperative to

understand the combined effects of rotation, turn, channel geometry, and surface geometry on heat transfer in the internal cooling passages.

Literature Survey

Non-Rotating Channels

Earlier studies on cooling passages were primarily based on one-pass stationary models that study the surface roughness effect and the channel aspect ratio effect. The one-pass model did not include the turn effect which is a significant parameter in a multi-pass flow channel. Also the stationary models neglect the Coriolis and buoyancy effects which alter the velocity, turbulence, and temperature distributions. Metzger and Sahm [2] are pioneers who studied heat transfer in the multi-pass flow channels. They studied forced convection in a two-pass smooth rectangular channel by varying the divider location and the gap at the 180° turn. Fan and Metzger [3] extended the work by Metzger and Sahm [2] by varying the channel width. They concluded that increasing the channel aspect ratio results in smaller azimuthal heat transfer variations and increases overall channel heat transfer.

Han et al. [4] studied the local heat/mass transfer distribution in a non-rotating two-pass ribbed channel. Han and Zhang [5] studied the effect of rib-angle orientation on the local heat/mass transfer distribution in a non-rotating three-pass rib-roughened channel. It was observed that the rib angle, rib orientation, and the sharp 180° turn significantly affect the local heat/mass transfer distributions. Park et al. [6] studied the effects of rib angle on five different aspect ratio rectangular ducts under the non-rotating

condition. They found the order of heat transfer enhancement for the low aspect ratio ducts (AR=1:1, 1:2, and 1:4) is 60°, 45°, and 30°/90° angled ribs. For the high aspect ratio ducts (AR=2:1 and 4:1), the augmentation order is 90°/60°, 45° and 30° angled ribs.

Ekkad and Han [7] also applied the liquid crystal technique to measure the heat transfer distributions in different rib arrangements in a non-rotating square channel with a sharp 180° turn. One wall of the channel had periodically placed rib turbulators. They reported the broken V ribs have the highest heat transfer enhancement in the fist pass. However, the 60° parallel ribs produced higher enhancement in the turn and second pass. Chen et al. [8] used the naphthalene sublimation method to measure the detailed mass transfer along four walls of a square duct containing a sharp 180° bend with normal ribs on two opposite walls under the non-rotating condition. They found the ribbed walls have more span-wise uniformity than the smooth side walls.

Rotating Channels

All of the above studies are for non-rotating channels. It has been shown for non-rotating channels that the angled ribs have better heat transfer enhancement than normal ribs (90°), and the V-shaped ribs have better heat transfer than the angled ribs. In rotating channels, the heat transfer will be affected by the Coriolis force and buoyancy force.

Wagner et al. [9, 10] conducted a detailed experimental study to determine the effects of rotation (Coriolis and buoyancy forces) on the local heat transfer of a multi-pass square channel with smooth walls. They concluded that the first pass of the coolant

passage with rotation created a thinner boundary layer on the trailing surface and a thicker boundary layer on the leading surface resulting in increased heat transfer and decreased heat transfer on these two walls, respectively. In the second pass, the performance was different and opposite that of the first pass. The leading surface Nusselt number ratios in the second pass were higher than the trailing surface Nusselt number ratios because of the reversal of the Coriolis force direction. Taslim et al. [11, 12] investigated the heat transfer distribution in one-pass square and rectangular rib roughened channels under rotation. They found that the effects of rotation were more apparent in rib-roughened channels with a larger channel aspect ratio and a lower rib blockage ratio.

Han et al. [13] investigated the uneven wall temperature effect on local heat transfer in a rotating two-pass square channel with smooth walls. They concluded that uneven surface temperatures on the leading and trailing surfaces create unequal local buoyancy forces, which alter heat transfer coefficients. Johnson et al. [14, 15] performed a parametric experiment to investigate the effects of buoyancy and Coriolis forces on the heat transfer coefficient distribution of four-pass square channels with rib roughened walls. The experiments were conducted with rotation in both directions to simulate serpentine coolant passages with the rearward flow of coolant or with the forward flow of coolant. They concluded that both the rotation and channel orientation alter the leading and trailing surface heat transfer coefficients of the ribbed channel. Parsons et al. [16, 17] studied the effects of channel orientation and wall heating condition on the local heat transfer coefficients in a rotating two-pass square channel with ribbed walls. They

found that the effect of the Coriolis force and cross-stream flow were reduced as the channel orientation changed from the normal β=90° to an angled orientation of β=135°. Zhang et al. [18] analyzed the heating condition effects in a two-pass square duct with angled rib turbulators with rotation. They found that an uneven wall temperature had a significant impact on the local heat transfer coefficients.

Dutta and Han [19] also investigated the local heat transfer coefficients in rotating smooth and ribbed two-pass square channels with three channel orientations. Dutta et al. [20] presented experimental heat transfer results for turbulent flow through a rotating two-pass rib-roughened triangular channel for two channel orientations with respect to the axis of rotation. In addition, Park and Lau [21] and Park et al. [22] conducted experimental work using naphthalene sublimation to study the effects of the Coriolis force, 180° turn, channel orientation, and the different rib arrangements on local heat/mass transfer distributions on the leading and trailing walls of a two-pass square channel.

Murata et al. [23] excluded the turn effect by reversing the flow direction to obtain inward and outward flow in a one-pass square duct with rib roughened walls. Their data showed that the 60° rib has better heat transfer enhancement than the 90° rib. The effect of the radial flow direction did not show a difference in averaged Nusselt number. Liou et al. [24] performed heat transfer measurements using a liquid crystal technique in a rotating two-pass square duct with 90° in-line ribs. Their results are comparable with Parson et al. [16]. Al-Hadhrami and Han [25] studied the rotation effect on heat transfer in a rotating two-pass square duct with five different arrangements of

45° angled rib turbulators. They concluded that the parallel rib orientation (ribs in first and second passes are parallel and ribs on leading and trailing walls are parallel) provides higher overall Nusselt number ratio than crossed rib orientation, particularly, for increasing rotation numbers.

Almost all of the rotating studies have focused on square or close to square ducts. Recently, studies have moved to rotating rectangular ducts. A study of the buoyancy effect in a one-pass, high aspect ratio duct (AR=10:1) was conducted by Willett and Bergles [26]. Their duct was oriented at 60° to the r-z plane (150° respect to the rotation direction). They found the normalized Nusselt number ratio is a strong function of rotation number and buoyancy number. They also observed significant spanwise variation in the Nusselt number ratio under rotating conditions. The effect of rotation on the heat transfer distribution in a rotating, rectangular (AR=2:1), two-pass channel with ribs (45°) roughened walls was investigated by Azad et al. [27]. They showed the heat transfer coefficients decrease from the leading wall and increase from the trailing wall in the first pass. They also concluded that the effect of rotation is more apparent in the channel orientated at 90° then the channel oriented at 135° with respect to the direction of rotation. Al-Hadhrami et al. [28] studied the effect of rotation on heat transfer in rotating two-pass rectangular channels (AR=2:1) with rib turbulators for two channel orientations. They confirmed the conclusion from Azad et al. [27] that the 90°-channel orientation produces a greater rotating effect on heat transfer than a 135°-channel orientation.

Single-pass rectangular (AR=4:1) channels with rib roughened walls were studied by Griffith et al. [29] and Lee et al. [30]. Griffith et al. [29] concluded that this narrow rectangular passage creates more heat transfer enhancement than the smaller aspect ratio channels. They also found that significant spanwise variation is present across the width of the channel, and this variation is amplified by the use of angled ribs. Lee et al. [30] investigated six different rib configurations. They found the V-shaped ribs produce the greatest heat transfer enhancement in both rotating and non-rotating channels. They found in the rib-roughened channels all surfaces undergo heat transfer enhancement with an increased effect of rotation. They also confirmed the finding of Griffith et al. [29]: significant spanwise variation is present in the channels with angled ribs; however, this variation decreases in the channels with V-shaped ribs.

Cho et al. [31] used a mass transfer method to study the effect of rotation in a rotating two-pass rectangular channel (AR=1:2) with 70° angled ribs. Their results showed that the rotation effect diminished in the second pass due the 180° turn effect. An experimental result for a 1:4 rotating two-pass channel was reported by Agarwal et al. [32] using the mass transfer method. For a smooth surface, they found that the 1:4 channel has lower heat/mass transfer compared to square channel. For the 90° ribbed walls, the Sherwood number ratio shows a decreasing trend with increasing Reynolds number.

Summary and Objectives

From the literature survey, the existence of the rib turbulators enhances the heat transfer coefficient due to increased turbulent mixing, secondary flow, and, to some

extent, due to increased surface area. In general, the V-shaped ribs and the angled ribs yield more heat transfer enhancement than the normal ribs. Meanwhile, the 180° turn strongly affects the heat transfer behavior in the second pass of the two-pass channels. With the channel rotating, the heat transfer coefficients are not equal on the leading and trailing surfaces due to the effect of the Coriolis force. The previous studies also show that the effect of rotation on heat transfer is influenced by the channel orientation. However, these results are for square or higher aspect ratio (AR=2:1 and 4:1) channels. There is very limited data available for the lower aspect ratio (AR=1:2 and 1:4) channels.

In real turbine blades, the internal cooling passages are not limited to the high aspect ratio channels. Figure 1.1 shows the schematic of cooling channels and channel orientations in a typical turbine blade. The aspect ratios of the cooling channels vary from 1:4 to 4:1 with different channel orientations to fit the turbine blade profile. This range of cross-sections covers the majority of channels that could be seen in actual engines.

Therefore, the designers need more heat transfer information in different aspect ratio channels. They need to know how the rib geometry, turn geometry, channel orientation, and rotation affect the heat transfer in these channels. In additional, they need to know the overall thermal performance of the cooling scheme. In other words, the heat transfer enhancement comes at a sacrifice of pressure losses in the channel. Unfortunately, open literature cannot fulfill the designers' needs. Therefore, this study is an attempt to fill many of these needs.

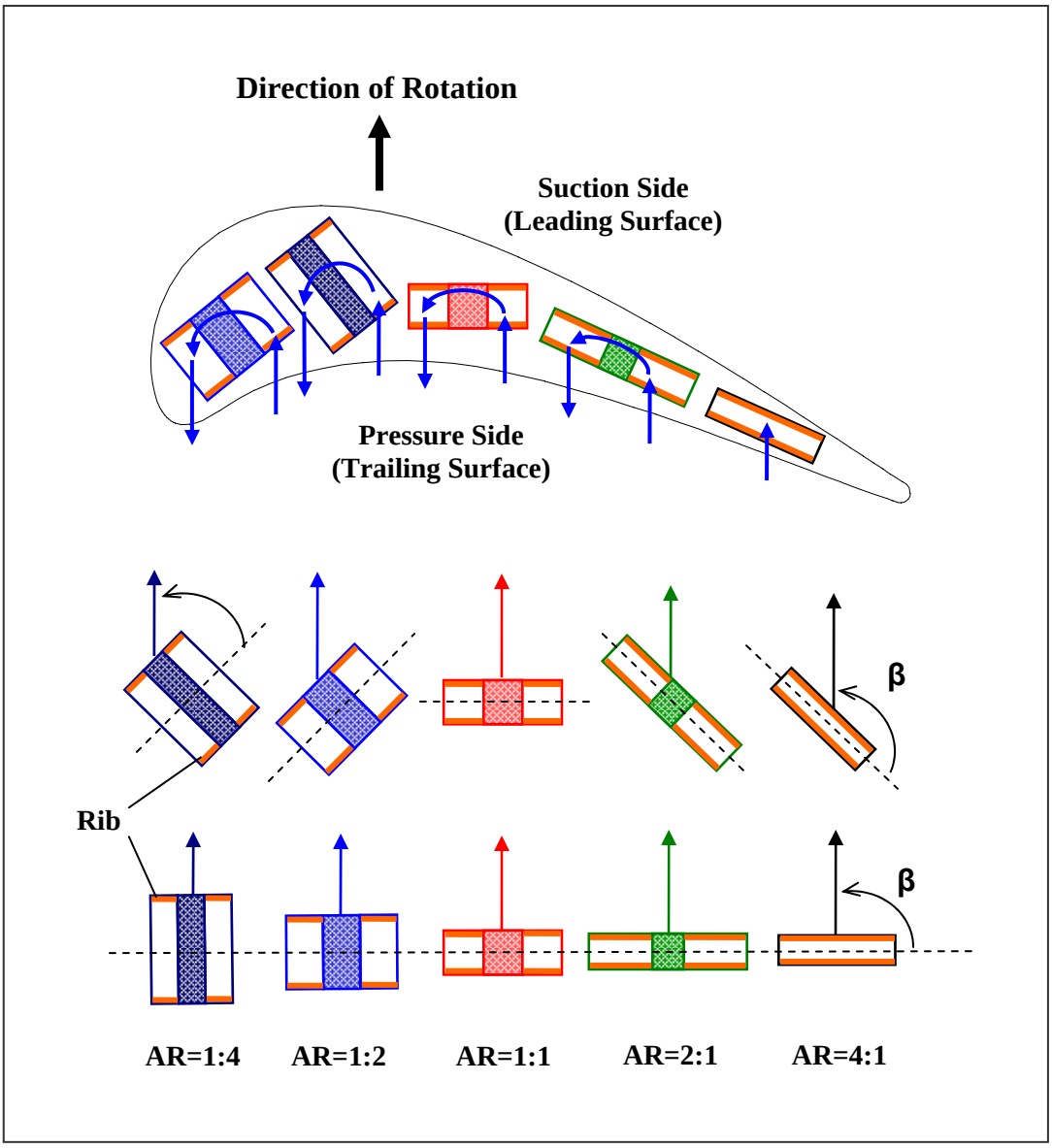

Figure 1.1 Internal Cooling Passages with Various Aspect Ratios

The experiments are conducted in five rectangular channels to study the effect of channel aspect ratios. The experiment includes channel aspect ratios of 1:4, 1:2, 1:1, 2:1, and 4:1. Due to geometrical constraints, the 4:1 channel has only one pass and the measurements have been taken separately by Griffith et al. [29]. The simple angled ribs would be a better choice than the complicated ribs (V-shaped ribs or broken ribs) for this study. Not only are they widely used in current engines, but also they are appropriate in the lower aspect ratio channels, due to the narrow width of the channel. This study provides more complete heat transfer and friction factor data in the rectangular channel for different aspect ratios with smooth walls and 45° angled ribbed walls. The objectives of this study are the following:

1. Study the effects of channel aspect ratio on heat transfer in rotating two-pass channels with smooth walls and 45° angled ribbed walls.
2. Study the effects of the 180° sharp turn on the heat transfer distribution in rotating two-pass channels with smooth walls and 45° angled ribbed walls.
3. Study the effects of the channel orientation (normal and 45° or 135°) with respect to the axis of rotation in rotating two-pass rectangular channels with smooth walls and 45° angled ribbed walls.
4. Study the friction factor in two-pass rotating channels with smooth walls and 45° angled ribbed walls.
5. Finally, with the complete heat transfer and friction data available, the overall thermal performance (ratio of heat transfer enhancement to friction losses) for each channel will be calculated and presented for comparison of the various channels.

II EXPERIMENTAL APPARATUS AND DATA REDUCTION

The experimental system was designed to simulate the rotating two-pass internal cooling channel. This system includes a rotating test rig, test sections, and data acquisition system. Temperature and pressure data are measured and used to obtain the heat transfer coefficient and friction factor in this study.

Rotating Test Rig

The rotating test rig is shown in Fig. 2.1. A variable frequency motor is connected via a gear-and-belt mesh to a hollow, rotating shaft. This shaft runs from the base of the test rig to the work platform and is attached orthogonal to the hollow, rotating arm. The test section is inserted inside the hollow rotating arm, which rotates in a plane orthogonal to the rotating shaft. A hand held optical tachometer is used to determine the rotation speed of the arm. Thermocouple and heater wires are connected to slip-ring assembly mounted to the rotating shaft. The output of the thermocouples is transferred to a data acquisition system. Power input to the heaters from the variable transformers is also transmitted through the slip ring assembly. A 48 channel Scanivalve pressure transducer is fixed to the rotating rig above the slip ring, on the axis of rotation. The signals to and from the transducer are transmitted through the slip ring, as with the thermocouples and heaters. Cooling air is pumped from a steady flow compressor, through an ASME orifice flow meter, then through the hollow rotating shaft, turning 90° and passing into the rotating arm, then through the test section, and is finally expelled into the atmosphere.

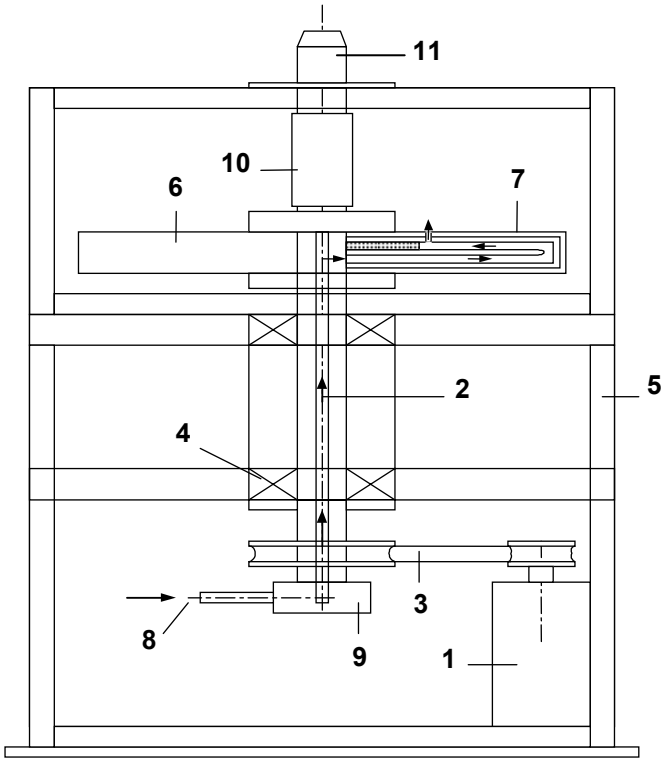

1. **Electrical Motor with Controller**
2. **Rotating Shaft**
3. **Belt Drive Pulley System**
4. **Bearing Support System**
5. **Steel Table**
6. **Rotating Arm**
7. **Test Section**
8. **Compressor Air**
9. **Rotary Seal**
10. **Slip Ring**
11. **Scanivalve Pressure Transducer**

Figure 2.1 Schematic of the Test Rig

Test Sections

This experiment contains four two-pass rectangular test sections: AR=1:4, AR=1:2, AR=1:1 and AR=2:1. All test sections are similar in geometry. The major difference is the channel aspect ratio (Width/Height). The dimensions of each test section are list in Table 1. Figure 2.2 shows the three dimensional view of the AR=1:2 test section. To show a clear view inside the channel, some portion of the test section has been removed. Each test section contains a 222.25 mm unheated entrance length to provide a hydrodynamic fully developed flow condition. Each pass has a 152.4 mm long heating section. The clearance of the 180° sharp turn from tip to end wall is identical to the channel width (W). The divider wall has a thickness of 12.7 mm with a 6.35 mm radius at the tip for all test sections except the AR=1:1 test section. The AR=1:1 test section has a 19.05 mm-thick divider wall. Cooling air is expelled to the atmosphere through a hole in the second pass. This hole is located 152.4 mm downstream of the end of heated section in the second pass. The mean rotating radius is 635 mm for all test sections.

The cross sectional views of each test section are shown in Fig. 2.3. In the AR=1:4 and AR=1:2 test sections, each of the inner and outer wall has two copper plates. The AR=1:1 and AR=2:1 test sections have only one copper plate in each of the inner and outer walls, because the dimension is smaller in these two test sections. Ribs are placed on the leading and trailing surfaces to enhance heat transfer. Pressure taps are also shown in the figures.

Table 1 Dimensions of Various Aspect Ratio Channels

Channel Aspect Ratio (AR)	1:4	1:2	1:1	2:1	4:1
Channel Width (W)	12.7	12.7	12.7	25.4	50.8
Channel Height (H)	50.8	25.4	12.7	12.7	12.7
Rib Height (e)	1.59	1.59	1.59	1.59	1.59
Hydraulic Diameter (D_h)	20.32	16.93	12.7	16.93	20.32
Rib Height to Hydraulic Diameter Ratio (e/D_h)	0.078	0.094	0.125	0.094	0.078
Rib Pitch to Rib Height Ratio (P/e)	10	10	10	10	10
Thickness of Divider Wall (t_d)	12.7	12.7	19.05	12.7	N/A
Diameter of Exit Hole (d_e)	12.7	12.7	19.05	9.53	N/A

Unit: mm

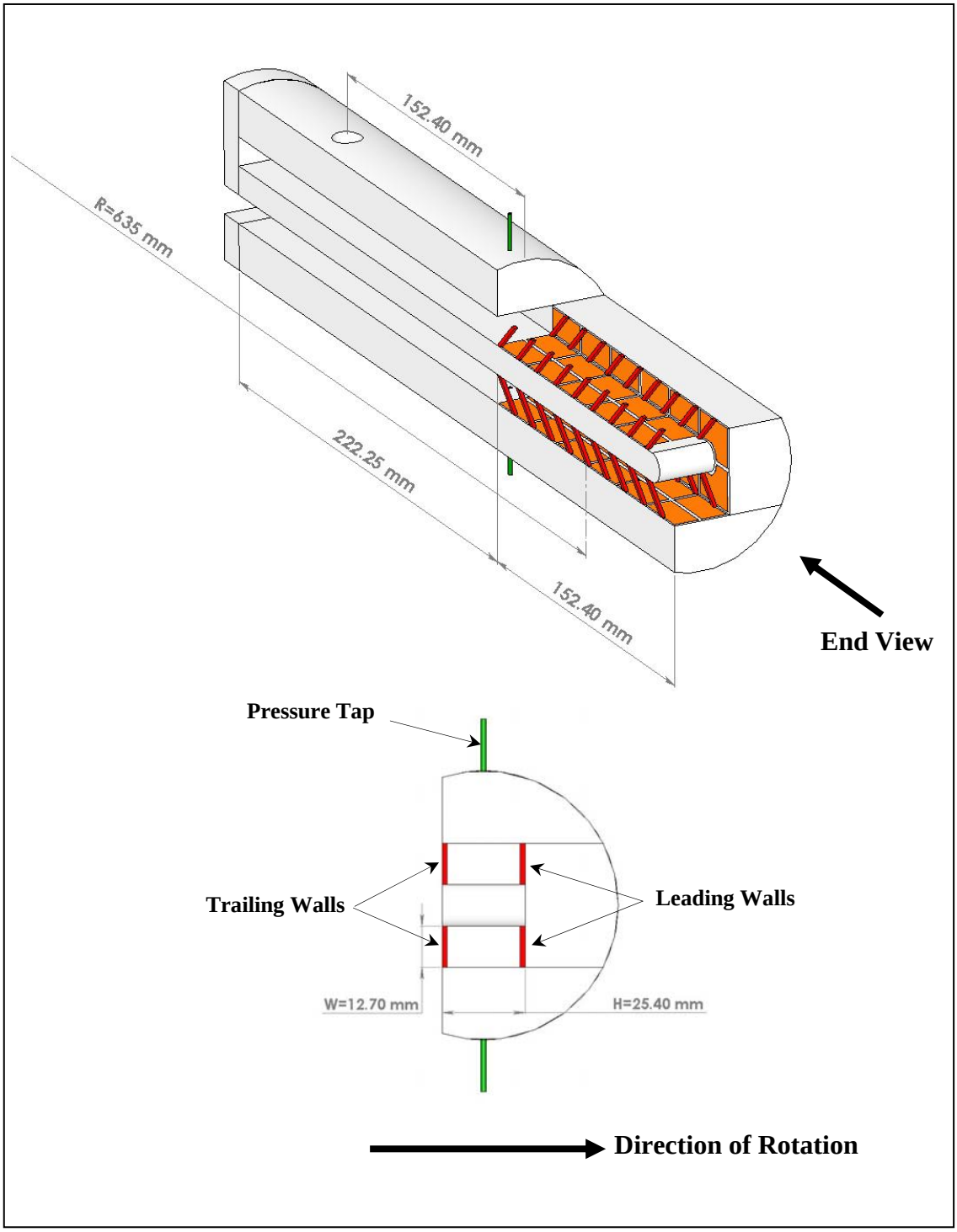

Figure 2.2 Geometry of the AR=1:2 Test Section with Angled Ribs

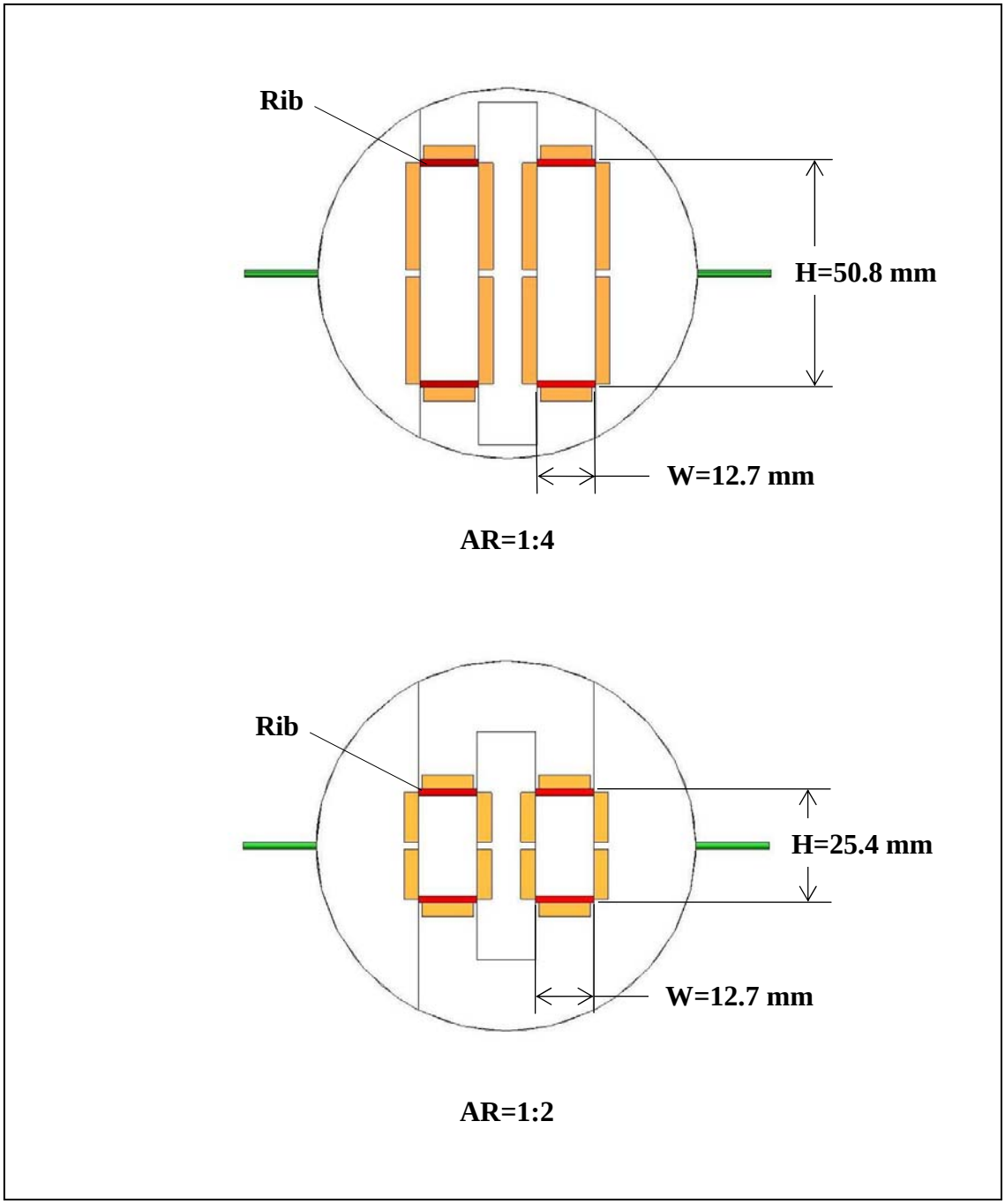

Figure 2.3 Cross Sectional View of the Test Sections

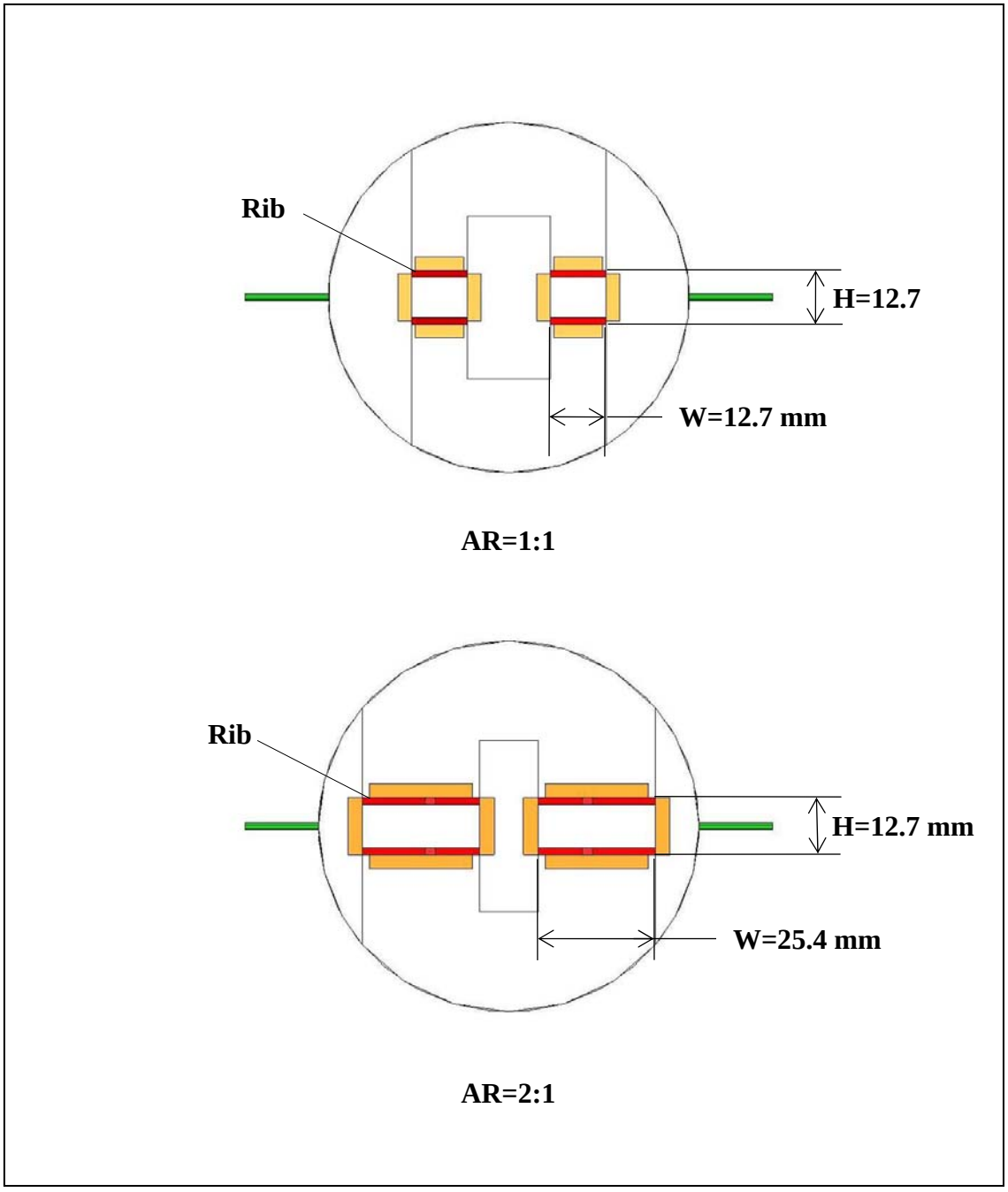

Figure 2.3 Cross Sectional View of the Test Sections (Continued)

Figure 2.4 shows the heat transfer model of the AR=1:1 test section. Each pass is divided into six segments. As described earlier, the AR=1:4 and AR=1:2 test sections should have six copper plates in each segment, but the AR=1:1 and AR=2:1 test sections have only four copper plates in each segment. The inner wall has only five segments in the flow direction because of the turn. The copper plates are mounted in a nylon substrate, which comprises the bulk of the test section. Pre-fabricated flexible heaters are installed beneath the copper plates. A total of 13 heaters are used for AR=1:2 test section and AR=1:4 test section. The AR=1:1 test section and AR=2:1 test section have only 9 heaters, because each inner and outer wall has only one heater. All heaters supply steady, uniform heat flux to the copper plates. Sufficient power is supplied in order to maintain a maximum wall temperature of nearly 65 °C for the corresponding section. Thermal conducting paste is applied between the heater and copper plates to promote heat transfer from the heater to the plates. Each 3.18 mm thick copper plate has a 1.59 mm deep blind hole drilled in the backside in which a copper-constantan thermocouple is installed 1.59 mm from the plate surface with thermal conducting glue. Thin nylon strips (1.59mm) between the copper plates reduce the conduction effect between the plates.

The ribs made of brass with a 1.59x1.59 mm cross section are glued on the leading and trailing walls at an angle of 45° to the flow direction. A thin layer of conductive glue is used so the thermal resistance between the brass ribs and the copper plates is negligible. The ratio of rib pitch-to-rib height is 10 for all tests. The entire test duct is surrounded by insulating nylon material and fits in a hollow cylindrical aluminum alloy arm for structural rigidity.

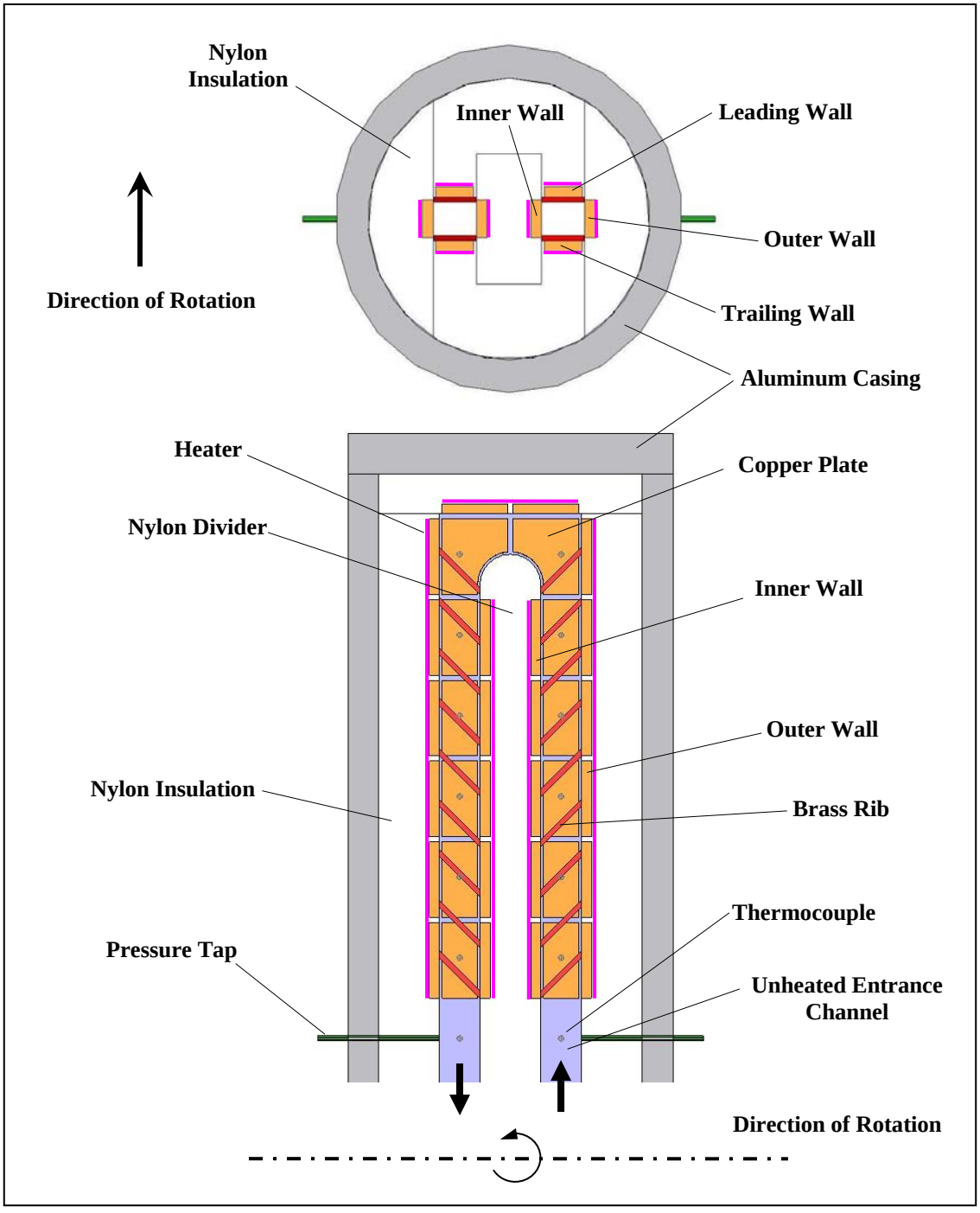

Figure 2.4 Heat Transfer Model (AR=1:1)

Static pressure taps are used to measure the pressure of the coolant at the inlet and outlet of the test section under isothermal condition. The inlet pressure tap is located on the outer wall near the inlet of the first pass, and likewise, the outlet tap is placed on the outer wall of the channel downstream of the copper plates. Each pressure tap is connected to a separate channel of the Scanivalve pressure transducer. From the calibration of the transducer with a standard U-tube manometer, the voltage signals obtained from the Scanivalve give the gauge pressure at both the inlet and outlet of the test section. From these measurements, the pressure drop incurred in the test section can be determined.

Table 2 lists the experimental conditions. For all test sections, the experiments were conducted for both smooth wall and 45° angled ribbed wall, and Reynolds numbers of 5000, 10000, 25000 and 40000. The test section rotates at a speed of 550 rpm, resulting in a range of rotation number (Ro) of approximately 0.015 to 0.3.

Data Reduction

Heat Transfer Enhancement

This study investigates the regionally averaged heat transfer coefficient at various locations within the rotating ducts. The heat transfer coefficient is determined by the net heat transferred from the heated plate, the surface area of the plate, the regionally averaged temperature of the plate, and the local bulk mean temperature in the channel. Therefore, the heat transfer coefficient is given as:

Table 2 Experimental Conditions

Parameter	Range
Channel Aspect Ratio (W:H)	1:4, 1:2, 1:1, 2:1, 4:1
Reynolds Number	5000, 10000, 25000, 40000
Rotational Speed (RPM)	550
Surface Geometry	Smooth and 45° Angled Ribs
Channel Orientation (β)	90°, 45° or 135°

$$h = \frac{Q_{net} / A}{\left(T_w - T_{b,x}\right)} \tag{1}$$

The net heat transfer is calculated using the measured voltage and current supplied to each heater from the variac transformers multiplied by the area fraction of the heater exposed to the respective plate minus the external heat losses escaping from the test section. The heat losses are predetermined by performing a heat loss calibration for both the rotational and stationary experiments. The heat loss calibration is performed by inserting insulation into the channel to eliminate natural convection. During the calibration, the heat transfer (in the form of power from the variac transformers) and

wall temperature of each plate is measured; therefore, from the conservation of energy principle it is possible to know how much heat is being lost to the environment.

The surface area used in this study is the projected surface area of the channel. In other words, the surface area of a smooth channel (the area increase due to the ribs is neglected). The regionally averaged wall temperature ($T_{w,x}$) is directly measured using the thermocouple installed in the blind hole on the backside of each copper plate. Because the plates are made of copper, which has a high thermal conductivity, the temperature of each plate is assumed uniform. One thermocouple at the inlet and one thermocouple at the outlet of the test section measure the inlet and outlet bulk temperatures, respectively. Therefore, the bulk temperature at any location in the test section can be calculated using linear interpolation. The results presented from this study are based on the linear interpolation method. Figure 2.5 shows typical heat flux and temperature distributions for the square channel. The data was collected for both rotating and non-rotating channels with smooth and angled ribbed channels, and the Reynolds number of the flow is 10000. Although linear interpolation is the method of choice for determining the coolant temperature at various locations in the channel, the coolant temperature can also be calculated using the conservation of energy principle. For the present study, both methods compare very well. The energy balance equation is:

$$T_{bx} = T_{bi} + \sum_{j} \left(Q - Q_{loss} \right) / \dot{m} c_p \qquad (2)$$

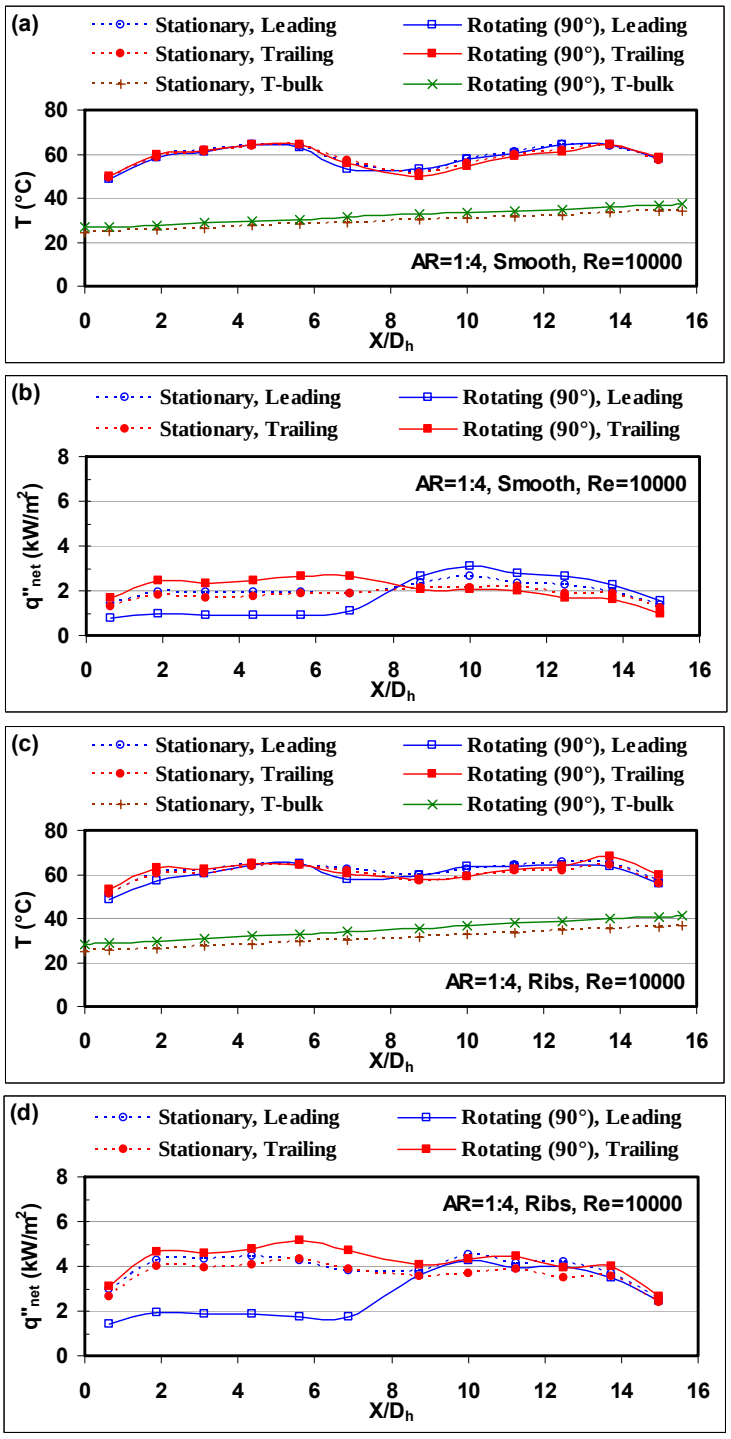

Figure 2.5 Sample Temperature and Net Heat Flux Distributions in the AR=1:4 Test Section

The Dittus-Boelter/McAdams correlation for heating ($T_{w,x} > T_{b,x}$) is used in this study to provide a basis of comparison. The Dittus-Boelter/McAdams correlation is used to calculate the Nusselt number for fully developed turbulent flow through a smooth stationary circular tube. Therefore, the Nusselt number ratio is given as:

$$\frac{Nu}{Nu_o} = \left(\frac{hD_h}{k}\right)\left(\frac{1}{0.023\,\mathrm{Re}^{0.8}\,\mathrm{Pr}^{0.4}}\right) \tag{3}$$

All air properties are taken based on the bulk air temperature with a Prandtl number (Pr) for air of 0.71.

Frictional Losses

The frictional losses in the cooling channel are determined by measuring the pressure drop from the inlet to the outlet of the heated test section. The friction factor is calculated using the measured inlet and outlet pressures as shown in equation 4.

$$f = \frac{P_i - P_o}{4\left(\frac{L}{D_h}\right)\left(\frac{1}{2}\rho V^2\right)} \tag{4}$$

The friction factor ratio can then be calculated by dividing the fiction factor by the turbulent friction factor in a smooth tube as given by the Blasius equation. This ratio is shown in equation 5.

$$\frac{f}{f_o} = \frac{f}{0.079\,\mathrm{Re}^{-1/4}} \tag{5}$$

Thermal Performance

Based on the heat transfer enhancement (Nu/Nu_o) and the pressure loss penalty (f/f_o), the thermal performance, η, of each channel can be calculated. Equation 6 shows the thermal performance based on the constant pumping power condition as used by Han et al. [33].

$$\eta = \frac{Nu/Nu_o}{\left(f/f_o\right)^{1/3}} \tag{6}$$

Uncertainty Analysis

An uncertainty analysis is performed based on the method described by Kline and McClinton [34]. By substituting equation (1) into equation (3), the Nusselt number ratio can be expressed as

$$\frac{Nu}{Nu_o} = \left(\frac{D_h}{k}\right)\left(\frac{Q_{net}}{A(T_x - T_{bx})}\right)\left(\frac{1}{0.023\,\mathrm{Re}^{0.8}\,\mathrm{Pr}^{0.4}}\right) \tag{7}$$

The uncertainty of each variable in equation (7) is estimated below:

Heat Transfer Area (A): ±1.5%

Air Conductivity (k): ±2%

Hydraulic Diameter (D_h): ±1.5%

Net Heat Input (Q_{net}): ±3%~±15%

Prandtl Number (Pr): ±0.5%

Reynolds Number (Re): ±1.5%~±5%

Temperature (T): ±0.5 °C

From the uncertainty analysis, the uncertainty of the Nusselt number ratio is influenced most by the temperature measurement, heat input measurement, and the flow rate measurement (Reynolds Number). The typical uncertainty of the Nusselt number ratio is approximately ±4 to ±7% for the highest Reynolds number cases. The uncertainty increases in the lower heat flux cases, especially on the reduced heat transfer wall (leading wall in the first pass and trailing wall in the second pass) under rotation. The maximum uncertainty can be up to 20% at Reynolds number of 5000. The temperature difference between the copper plate and air mean temperature varies from 7 °C to 40 °C.

Similar to the Nusselt number ratio, the uncertainty of friction factor ratio can be estimated using the same method. By substituting equation (4) into equation (5), the friction factor ratio can be rewrite as

$$\frac{f}{f_o} = \frac{\Delta P}{4\left(\frac{L}{D_h}\right)\left(\frac{1}{2}\rho V^2\right)} \times \frac{1}{0.079\,\mathrm{Re}^{-0.25}} \qquad (8)$$

The uncertainty of each variable in equation (8) is estimated as below. The pressure losses are measured at Reynolds number of 10000, 25000, and 40000. The uncertainty of each variable in equation (8) is estimated as bellow.

Channel Length (L): ±1.2%

Air Density (ρ): ±1%

Velocity (V): ±1% to ±3%

Reynolds Number (Re): ±1.5% to ±3.5%

Pressure Loss (ΔP): ±0.3% to ±2.5%

It is clear that the Reynolds number, pressure losses, and velocity measurement have about the same level of uncertainty. However, the velocity measurement attributes more uncertainty in the friction factor ratio because the velocity has a power of 2 in the denominator. The uncertainty for the friction factor ratio is approximately ±2.5% to ±6.5%.

III CONCEPTUAL SECONDARY FLOW BEHAVIORS

The flow through a serpentine, rotating passage is influenced by many factors, each increasing the complexity of the flow. To have a better understanding of the heat transfer in a two-pass rotating internal channel, it is necessary to discuss the secondary flows and their effects on heat transfer in the rotating channel.

Rotation Effect in Internal Channels

Figure 3.1 shows how the coolant flow through a rotating channel is altered by both Coriolis force and buoyancy. The Coriolis force alters both the velocity and temperature profiles of the coolant through the channel. In a channel with radial outward flow (first pass in present study), the coolant is forced toward the trailing surface of the channel, and in channels with radial inward flow (second pass in present study), the core of the coolant is forced toward the leading surface. The strength of the Coriolis force is dependent upon the velocity of the coolant, the channel geometry, and the rotational speed of the channel. These factors can be combined to define the rotation number, Ro, and are shown in equation (9).

$$Ro = \frac{\Omega D_h}{V} \tag{9}$$

In aircraft engines, the rotation number may vary up to 0.25.

The buoyancy parameter due to the centrifugal force and temperature difference is important because of the high rotating speed and large temperature difference in the actual engine. For the radial outward flow, the rotation-induced buoyancy force aids the

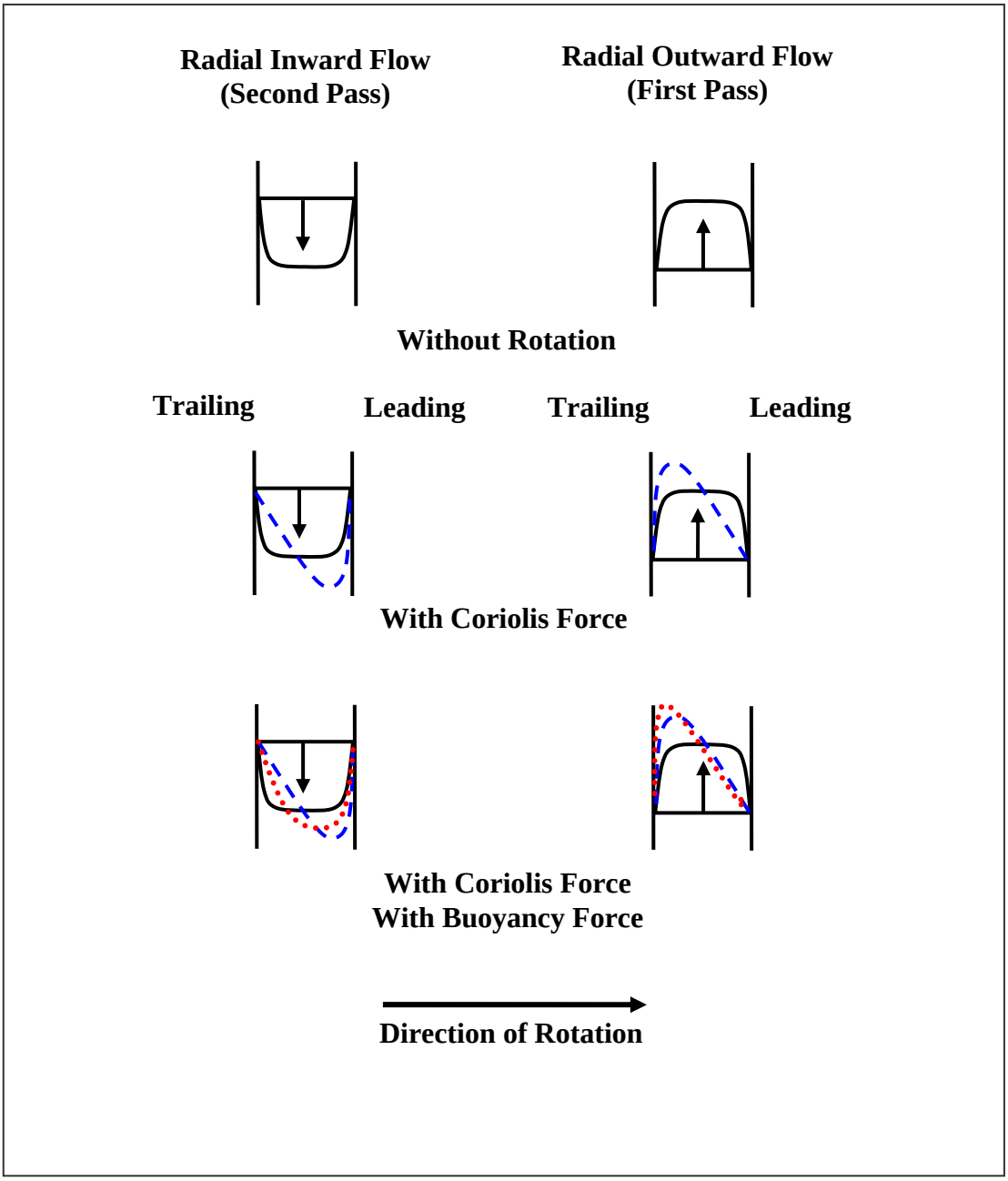

Figure 3.1 Rotation Effect in the Internal Channel

inertia force. This force opposes the inertia force in the second pass because the flow direction is reversed. A local buoyancy parameter is used to present the combined effects of the Coriolis and buoyancy forces, and in aircraft engines this parameter typically varies from 0 to 1.

$$Bo_x = (\frac{\Delta\rho}{\rho})(Ro)^2 \frac{R}{D_h} \tag{10}$$

This local buoyancy parameter can be re-written incorporating the measured wall and coolant temperatures as shown in equation (11).

$$Bo_x = \frac{T_{w.x} - T_{b,x}}{T_{f,x}} (Ro)^2 \frac{R_x}{D_h} \tag{11}$$

The first term on the right hand side of equation (11) represents the buoyancy force due to temperature gradient. This term is the primary source in natural convection heat transfer. The reference temperature is defined as the local film temperature which is the average of the local wall and the local coolant temperatures.

$$T_{f,x} = \frac{T_{w.x} + T_{b,x}}{2} \tag{12}$$

A secondary effect of the Coriolis force is the formation of a pair of counter-rotating vortices, conceptually drawn in Fig. 3.2. The Coriolis induced vortices circulate toward the trailing wall for radial outward flow and toward the leading wall for radial inward flow. This cross-stream secondary flow pattern significantly increases heat transfer on the trailing wall of the first pass (radial outward flow) and the leading wall of the second pass (radial inward flow), while the heat transfer decreases on the leading

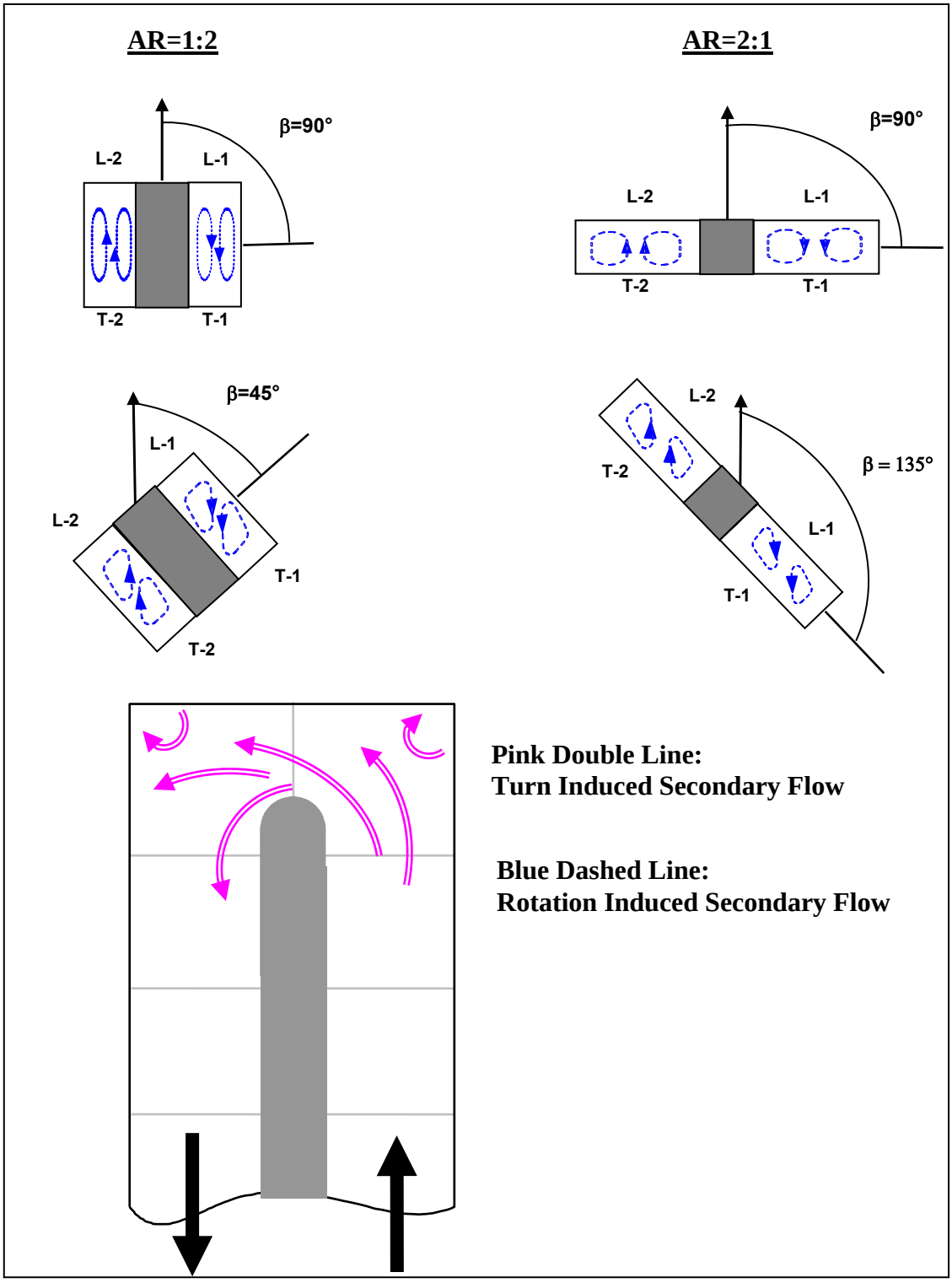

Figure 3.2 Conceptual Secondary Flow Patterns in Smooth Channel

wall of the first pass and the trailing wall of the second pass. As a result, the rotation effect causes a difference in heat transfer between the leading wall and the trailing wall in a rotating channel.

When the channel orientated in an angle (β=45° or 135°) to the rotation direction, the Coriolis induced vortices do not circulate normally toward the trailing wall nor the leading wall. The rotation effect in heat transfer is less than the channel orientates at a normal angle.

Turn Induced Secondary Flow

When the coolant travels through the 180° turn of a serpentine passage, areas of impingement, separation, and recirculation are created, as shown in Figure 3.2. On the outer walls, where the flow impinges, the heat transfer coefficients are typically elevated. However, near the inner wall, were flow separation occurs, the heat transfer coefficients typically decrease. Depending on the turn geometry, pockets of recirculation may also appear in the corners of the turn.

Rib Induced Secondary Flow

Angled rib turbulators induce secondary flow patterns that have been shown to increase the heat transfer in the cooling channel. Not only do the angled ribs effectively trip the boundary layer of the coolant, they also induce secondary flow vortices (also shown in Fig. 3.3) which further enhance the heat transfer. The rib induced vortices impinge on the outer wall in the first pass and on the inner wall in the second pass as a result of the rib orientation. In addition to the leading and trailing wall,

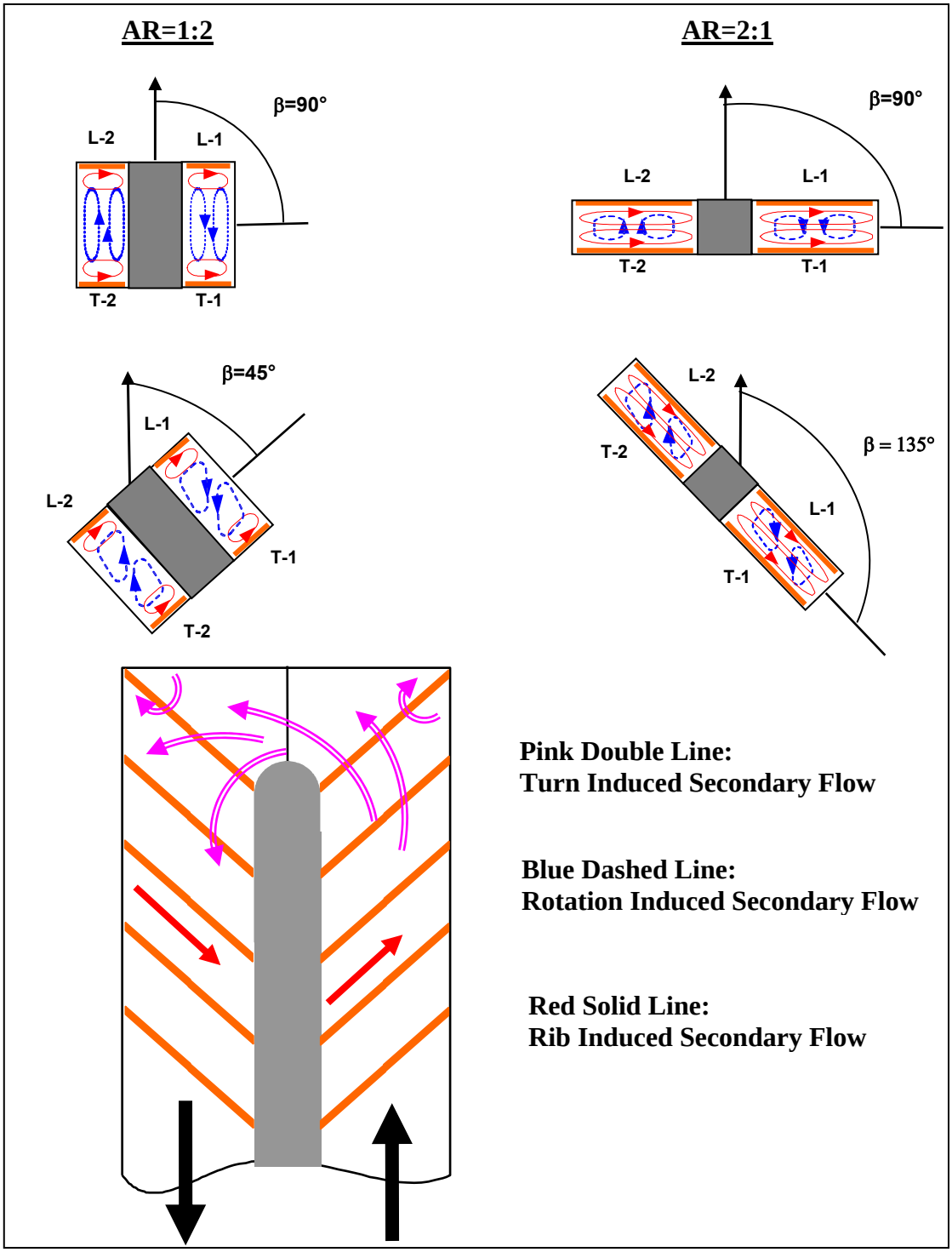

Figure 3.3 Conceptual Secondary Flow Patterns in Ribbed Channel

heat transfer enhancement is expected on the outer wall in the first pass and on the inner wall in the second pass due to the rib induced secondary flow.

These secondary flow patterns in a rotating internal channel have been confirmed by previous studies [35, 36] in square and AR=2:1 channels. As the channel aspect ratio becomes smaller, the secondary vortices induced by the Coriolis force, rib, and the 180° sharp turn could be distorted. Heat transfer in these channels may have different behavior. A conceptual secondary flow patterns for all five different aspect ratio channels is shown in Fig. 3.4.

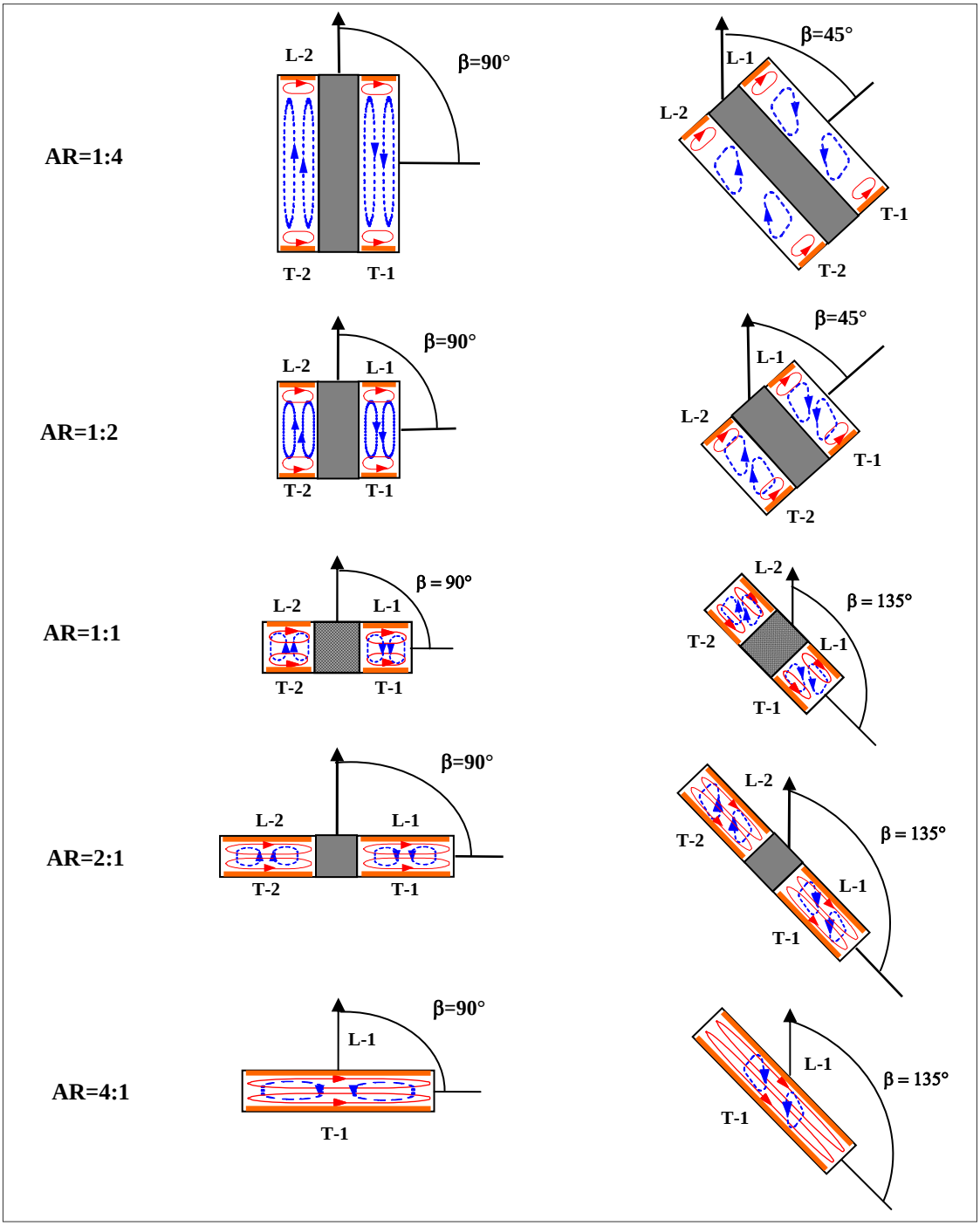

Figure 3.4 Conceptual Views of the Secondary Flow Vortices Induced by Rotation (Blue Dashed Line) and Induced by Ribs (Red Solid Line)

L: Leading; T: Trailing; 1: 1st Pass; 2:2nd Pass

IV HEAT TRANSFER RESULTS FOR SMOOTH WALLS

As described earlier, the secondary flow patterns are influenced by the rotation, turn and channel aspect ratio in a smooth rotating two-pass channel. This section discusses the heat transfer results for smooth channels. The experiments are conducted for both non-rotating and rotating channels with two channel orientations. Each test includes four Reynolds number: 5000, 10000, 25000 and 40000.

Regionally Averaged Nusselt Number Ratio Distributions

The leading and trailing walls are the most interesting surfaces in rotating channels. Not only are these two walls closer to the blade pressure side and suction side, they also influenced by rotation. Figures 4.1 - 4.4 show the heat transfer results on the leading and trailing walls for all smooth channels that have been tested in the present study. The figures contain both non-rotating and rotating (β = 90° and 45° or 135°) heat transfer distributions.

For the AR=1:4 channel (Fig. 4.1), the Nusselt number ratios approach a value of unity when the flow becomes fully developed in non-rotating channel. As expected, the leading wall and trailing wall have approximately the same Nusselt number ratio distribution. Through the turn, the values are elevated, and as the flow redevelops in the second pass the Nusselt number ratios gradually decrease. There is only 6 hydraulic diameter-long in the second pass in this channel. If X/D_h were longer, the Nusselt number ratio would decrease to about the fully developed value.

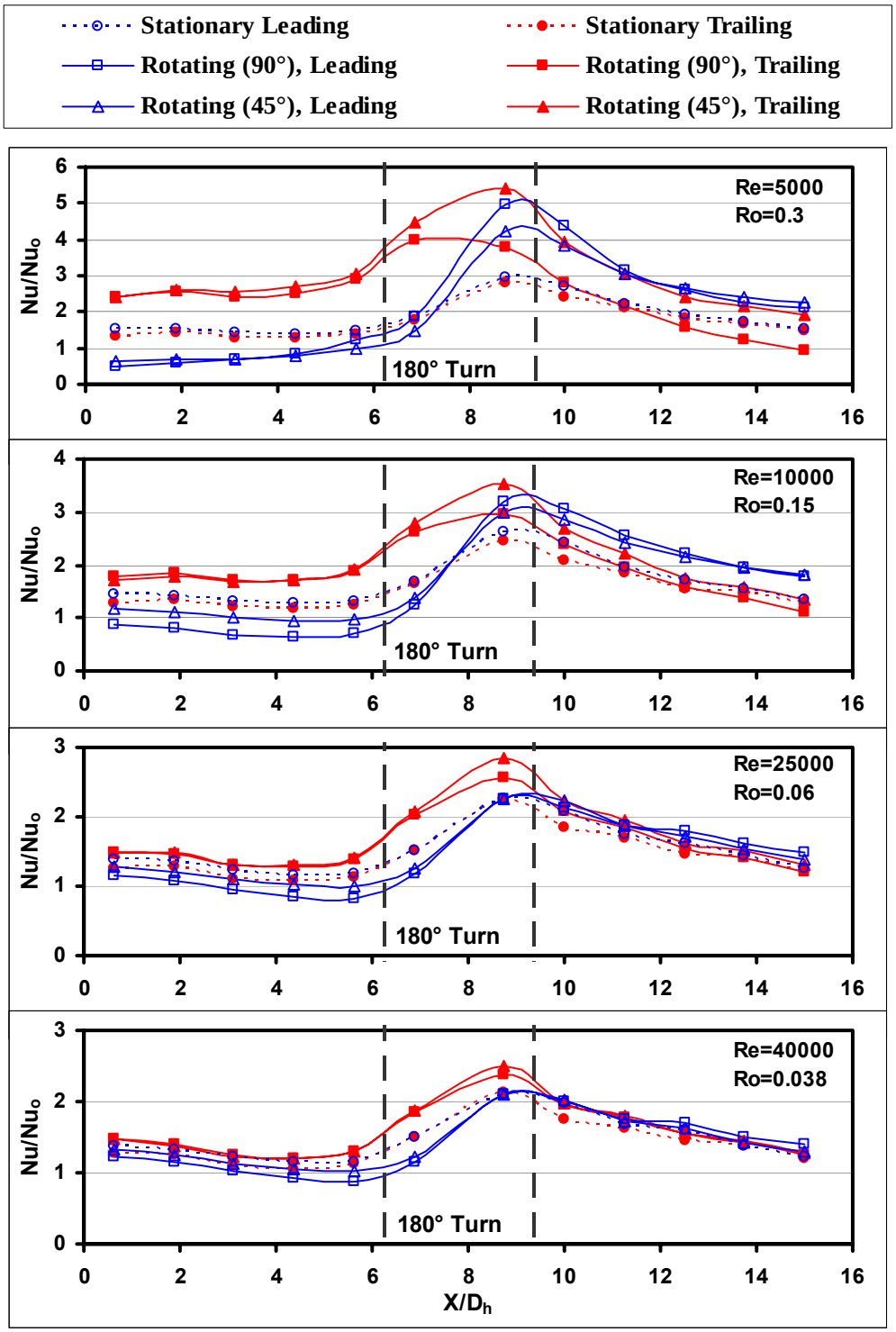

Figure 4.1 Regionally Averaged Nusselt Number Distributions for the AR=1:4 Channel with Smooth Walls

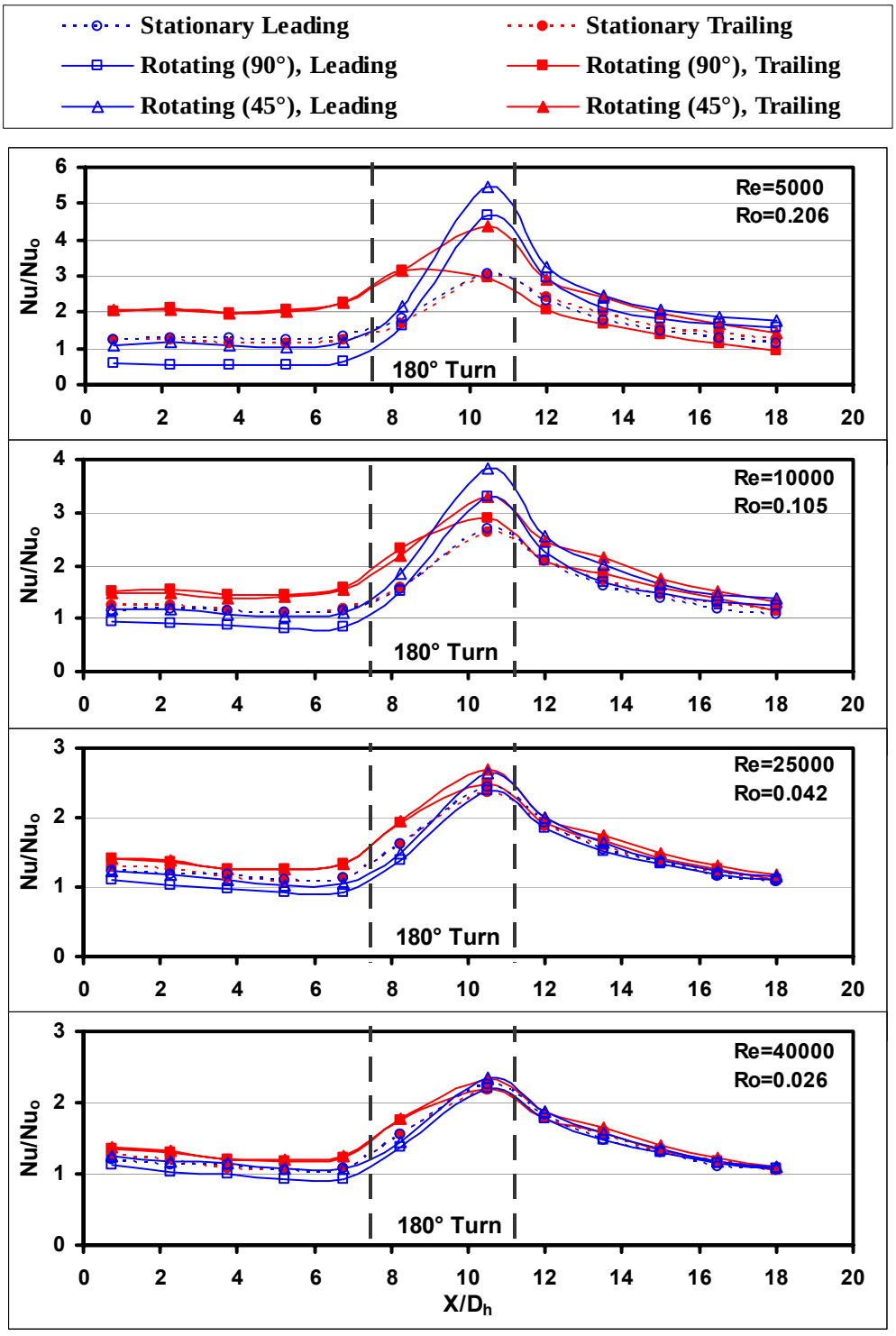

Figure 4.2 Regionally Averaged Nusselt Number Distributions for the AR=1:2 Channel with Smooth Walls

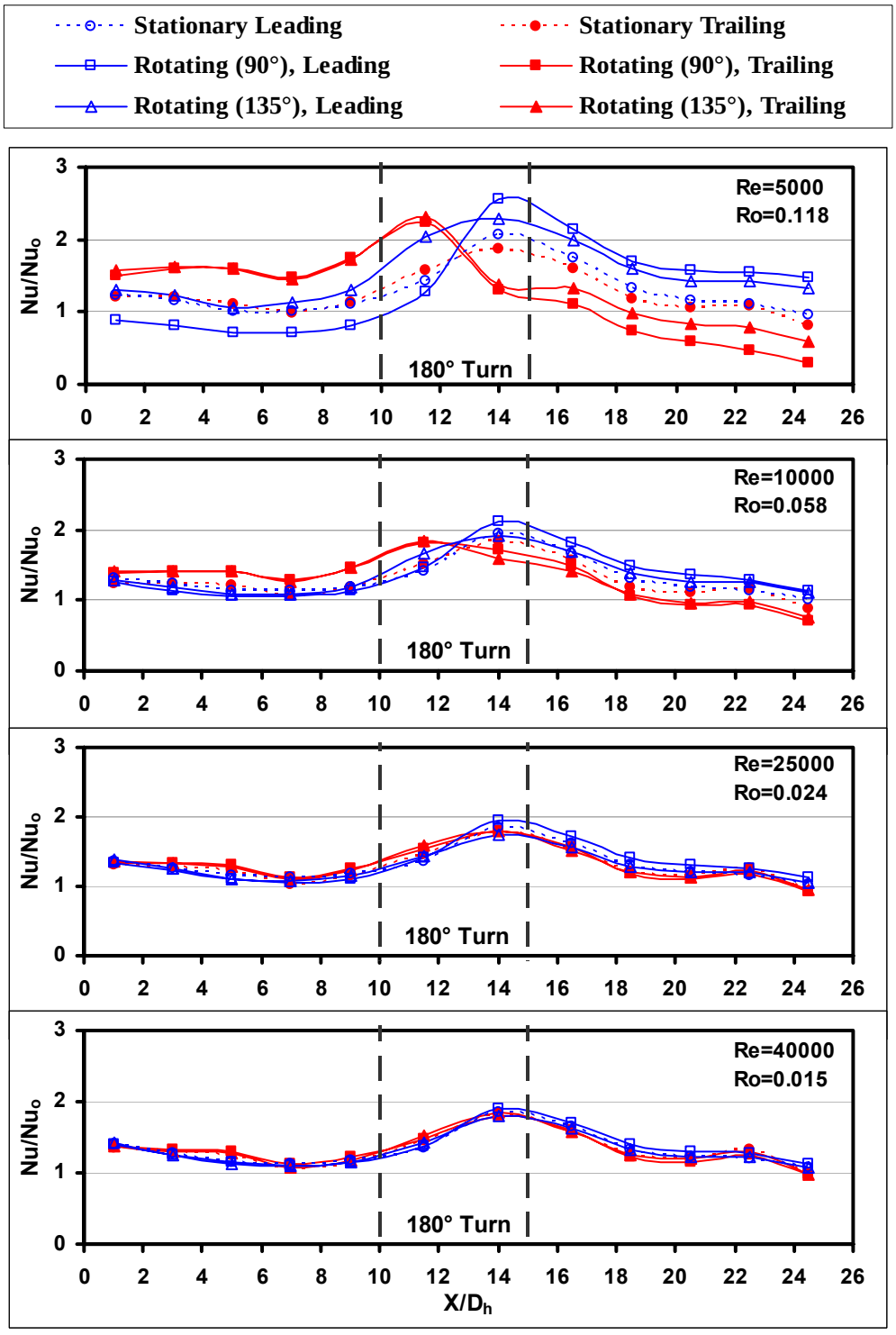

Figure 4.3 Regionally Averaged Nusselt Number Distributions for the AR=1:1 Channel with Smooth Walls

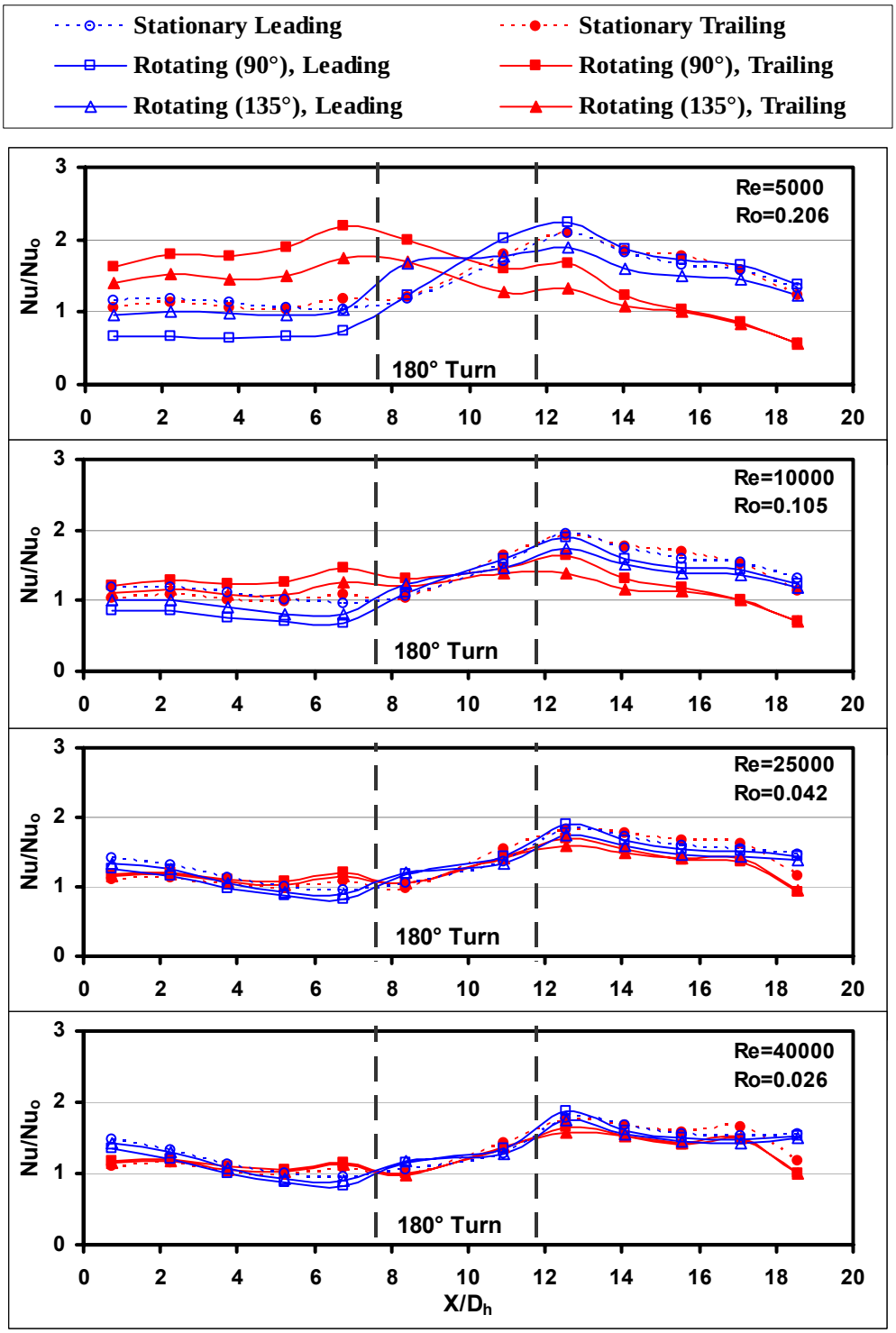

Figure 4.4 Regionally Averaged Nusselt Number Distributions for the AR=2:1 Channel with Smooth Walls

As one would anticipate, the rotation effect enhances heat transfer on the trailing surface in the first pass, and the leading surfaces experiences a declination in heat transfer. At Re=5000, the heat transfer from the trailing surface of the first pass is clearly enhanced above the non-rotating channel, while the first pass leading surface decreases. In the second pass, the trends are reversed, with rotating enhancing the heat transfer from the leading surface.

In general the Nusselt number ratios for both the leading and trailing surfaces under the rotating condition are higher than those of the non-rotating case in the second pass of present 1:4 channel. Not only is the enhancement on both the leading and trailing surfaces greater than that of the non-rotating channel, there is less difference between the leading and trailing surfaces in the second pass. The numerous studies involving square channels indicate the leading surface of the second pass experiences heat transfer enhancement above that of a non-rotating channel, while the trailing surface experiences decreased heat transfer. For the present 1:4 channel, less variation between the leading and trailing surfaces is seen due to the turn. The 180° sharp turn has a more dominant effect on the heat transfer of the second pass than rotation. Therefore, the rotation induced vortices which result in the heat transfer difference between the leading and trailing surfaces are not as strong as the secondary flow induced by the turn. Because the second pass is not long enough (about 6 D_h) for flow to develop, the Nusselt number ratio is always higher than the fully developed value in the 1:4 channel.

In the turn region, the heat transfer enhancement is greater than that of the non-rotating value due to the combined effect of rotation and 180° sharp turn. This heat transfer trend is true for both channel orientations (β=90° and 45°).

The effect of rotation is most clearly shown for the Reynolds number of 5000. Because the experiments were performed at a constant rotational speed of 550 rpm, the rotation number varies inversely with the Reynolds number. Therefore, as the Reynolds number increases, the effect of rotation decreases. As shown in Fig. 4.1, the variation between the leading and trailing surfaces decreases with increasing Reynolds number as both surfaces approach the non-rotating value of Nusselt number ratio.

The rotation effect in heat transfer is stronger in the channel oriented at 90° than in the channel oriented at 45°. Because the rotation induced vortices circulate directly toward the leading or trailing walls with channel orientated at 90° (as shown in Fig. 3.4), the effect of rotation in heat transfer is higher. The effect of rotation diminishes for both channel orientations as the Reynolds number increases to 40000 (rotation number decreases).

Figure 4.2 shows the Nusselt number ratio distributions for the AR=1:2 channel. The heat transfer in non-rotating channel behaves similar to the 1:4 channel. Like the 1:4 channel, significant variation due to rotation is observed in the first pass of the 1:2 channel. However, the difference between the leading and trailing surfaces is less in this 1:2 channel than the 1:4 channel. Because the rotating experiments are conducted at a constant angular velocity of 550 rpm, the rotation numbers vary between the two channel sizes (the channels have different hydraulic diameters). Therefore, the rotation

numbers of the 1:2 channel are less than those of the 1:4 channel. As the rotation number decreases (Reynolds number increases), the difference between the leading and trailing surfaces decreases for both channel orientations (β = 90° and 45°). A diminished variation of heat transfer difference in the second pass is also observed in this 1:2 channel.

As shown in Fig. 4.3, the heat transfer behavior in the 1:1 non-rotating channel is similar to the 1:4 and 1:2 channels. The 1:1 channel has the smallest hydraulic diameter among the present studied channels. Therefore, this channel has the smallest rotation number. As expected, the variation in heat transfer due to rotation is smaller in this square channel. However, the heat transfer variation is greater in the second pass than in the first pass. This different heat transfer behavior could attribute to the turn geometry and channel geometry. This square channel has a thicker divider wall (19.05 mm) and smallest hydraulic diameter. The flow sees a relatively smooth turn in this square channel, when it flows through the turn. In other words, the turn effect in heat transfer is less in this square channel compared to the other channels. Therefore, the rotation effect in heat transfer is clearly seen in the second pass of this square channel compared to the other channels.

Figure 4.4 shows the Nusselt number ratio distributions for the AR=2:1 channel. Again, the non-rotating channel has similar heat transfer behavior as the other channels do. The rotation effect creates a significant heat transfer variation in the first pass and a slightly less heat transfer variation in the second pass. Similar to all other channels, the heat transfer variation due to rotation diminishes at high Reynolds number (low rotation

number). However, the highest Nusselt number ratio is observed outside the turn region in the AR=2:1 channel. It may attribute to the turn geometry, because this 2:1 channel has the largest turn gap.

In general, the Nusselt number ratio distributions for 1:2, 1:1, and 2:1 channels are similar to the 1:4 channel. The major difference is that the rotation effect creates less heat transfer variation in the second pass than in the first pass for the low aspect ratio channels (1:4 and 1:2). However, the square and 2:1 channels have about the same variation in the first pass and the second pass due to the rotation effect. The heat transfer variation reduces as the Reynolds number increase for all channels.

Comparison with Previous Studies

The diminished variation between the leading and trailing surfaces of the second pass has also been observed by Cho et al. [31] in 1:2 rotating channels. Figure 4.5 compares the heat transfer/mass transfer behaviors in the smooth 1:2 channel of Cho et al. [31] to the smooth results of the present 1:2 channel. The Reynolds number of both the non-rotating and rotating channel is 10000, and the rotation number of the rotating case is about 0.1 for both the previous study and the present study.

As shown in Fig. 4.5, the present study is in close agreement with the previous study for the non-rotating smooth channel. The most significant difference between the two data sets is in the 180° turn. The study of Cho et al. [31] is performed using mass transfer; therefore, a detailed distribution can be obtained. With the copper plate method of the present study, only two regionally averaged points are recorded for the turn, so the detailed distribution cannot be obtained to capture the slightly higher values presented in

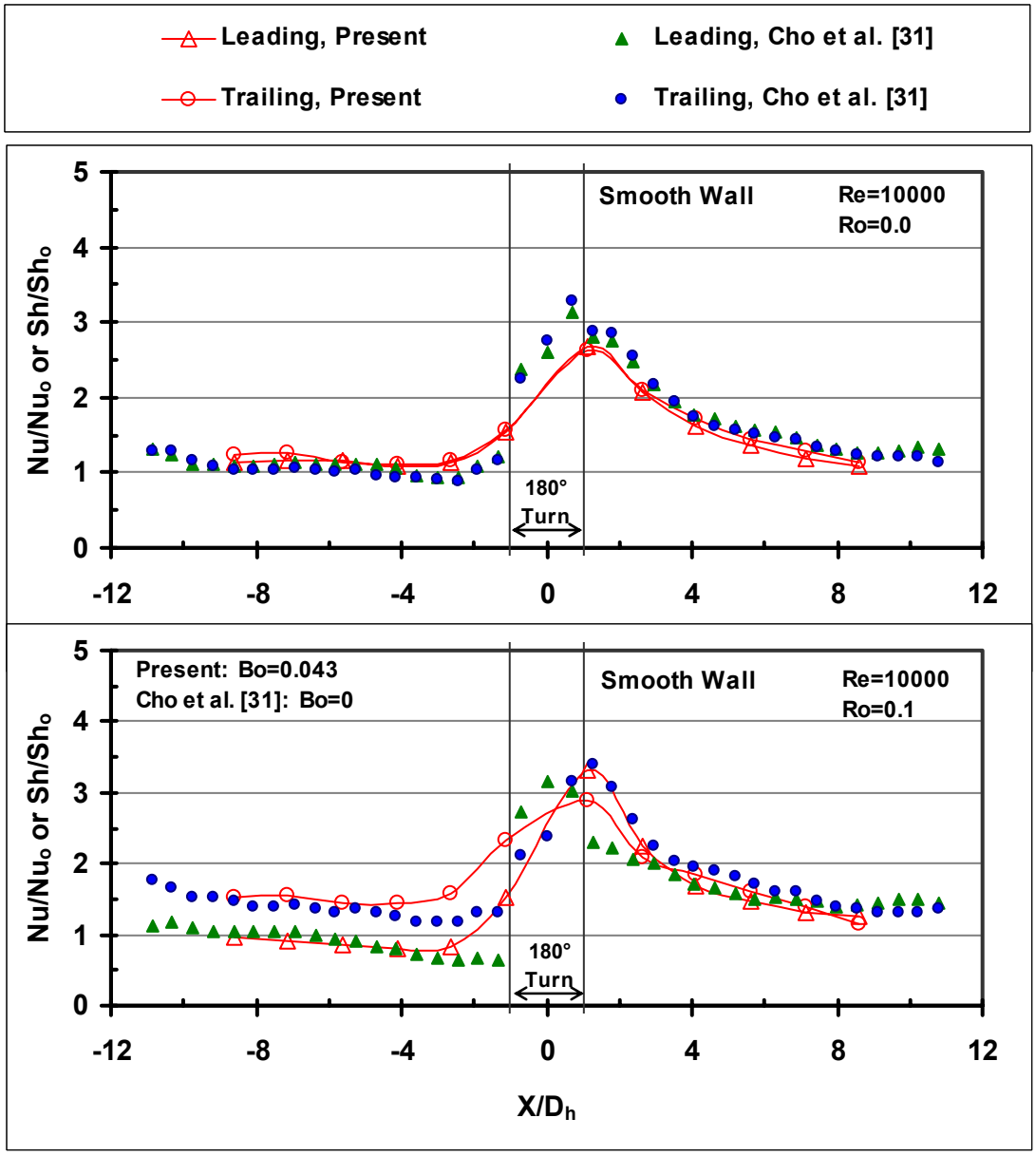

Figure 4.5 Comparison of the Nusselt Number Ratio Distributions for the AR=1:2 Channel with Smooth Walls

the previous mass transfer study.

The rotating results of the present 1:2 channel are also comparable to the previous study. As shown in Fig. 4.5, both studies (using different experimental methods) reveal the same results for both the leading and trailing surfaces of the first and second passes. This confirms the heat transfer in the second pass is dominated by the 180° turn. As with the current study, Cho et al. [31] reported only negligible variation between the leading and trailing surfaces of the second pass.

When considering the flow structure of the coolant in the rotating two-pass channels, it has been shown in Fig. 3.4 that the circulation direction of the rotation induced vortices reverses in the second pass due to the reversed direction of the Coriolis force. The strength of the vortices begins growing just downstream out the turn. While the strength of the rotation induced vortices is growing, the effect of the turn is diminishing through the second pass. With a relatively large distance between the leading and trailing surfaces of the 1:2 and 1:4 channels (compared to square and 2:1 channels), more distance is required for the effect of the sharp 180° turn to diminish. Therefore, the length of the second pass of the present study is not long enough for the entrance effect to diminish and allow the effect of rotation to become more apparent. The X/D_h is approximately 6 and 9 in the second pass for the 1:4 channel and 1:2 channel, respectively. Therefore, the effect of rotation is significantly reduced in the second pass of the low aspect ratio channels.

Secondary Flow Effect on Circumferential Heat Transfer

As discussed in previous section, the complicated secondary flows could affect the circumferential heat transfer distribution. It is interesting to compare the local data between different channels. However, due to the tremendous amount of data, only the most interesting data are compared in this section. Figure 4.6 shows the data regions of the test section. The cross-sectional view of the AR=1:2 channel shows six circumferential copper plates for each pass. They are labeled as L (leading), T (trailing), OL (outer-leading), OT (outer-trailing), IL (inner-leading), and IT (inner-trailing). The construction of the AR=1:4 channel is identical to the 1:2 channel. The 2:1 channel and 1:1 channel have four circumferential copper plates. Only one copper plate one each of the inner and outer walls. In the streamwise direction, the channel is divided into twelve segments, six in the first pass and six in the second pass. As shown in Fig. 4.6, the number next to the segment indicates the data region. Region 4 and 11 should represent the fully develop flow in the first pass and the second pass, respectively.

The rotation induced secondary flow has a strong effect on the circumferential heat transfer of the channel. Figure 4.7 shows the rotation induced secondary flow patterns, as well as the circumferential regionally averaged Nusselt number ratios at the Reynolds number of 10000. The circumferential distribution is shown at two locations in the channel: at the fourth region in the first pass and the fifth region in the second pass (eleventh point overall). These two regions are considered as the fully developed flow region in each pass of the two-pass channel. The numbers marked next to each surface of the different aspect ratios, orientations, and rotation numbers are the Nusselt

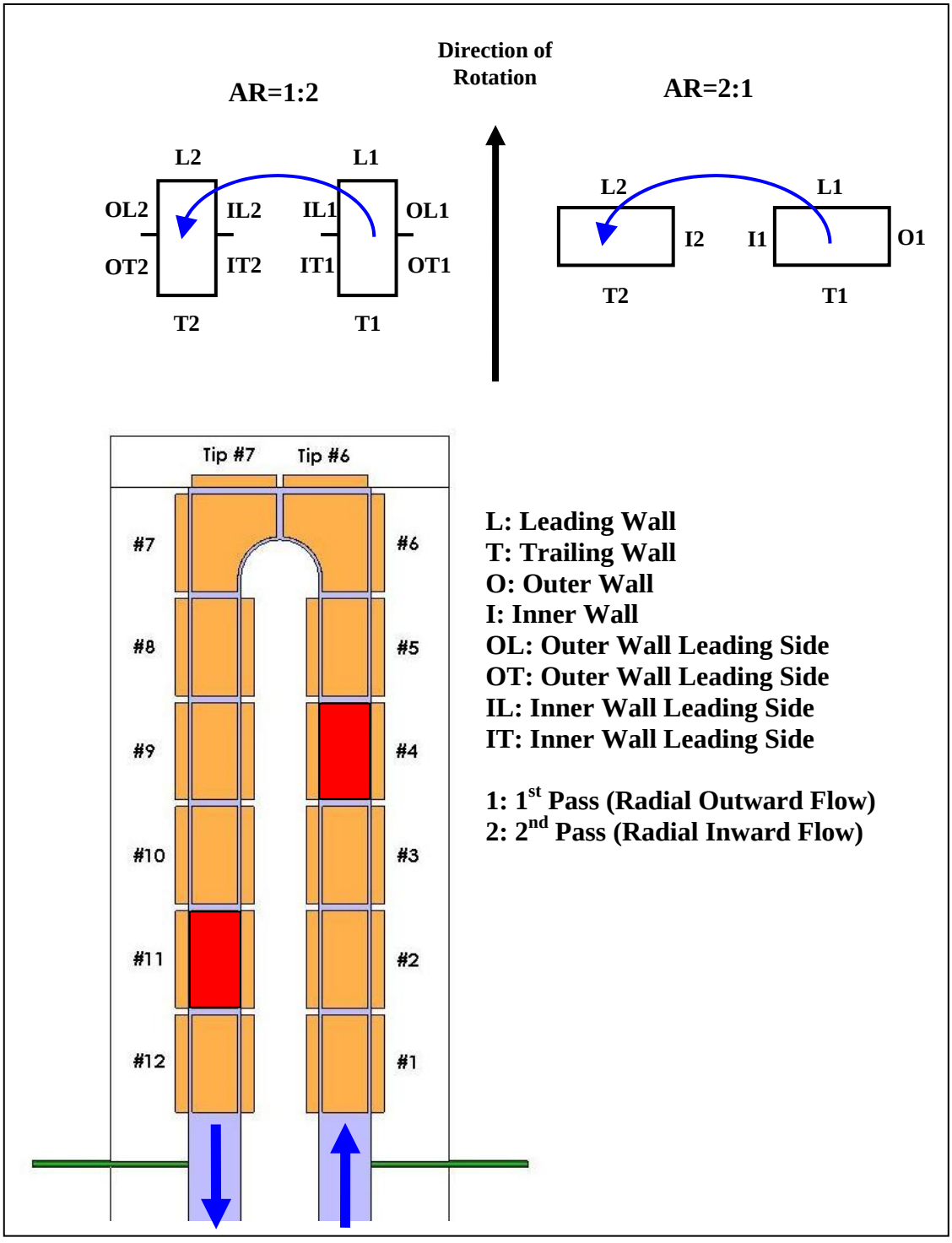

Figure 4.6 Regions of Interest in the Smooth Channels

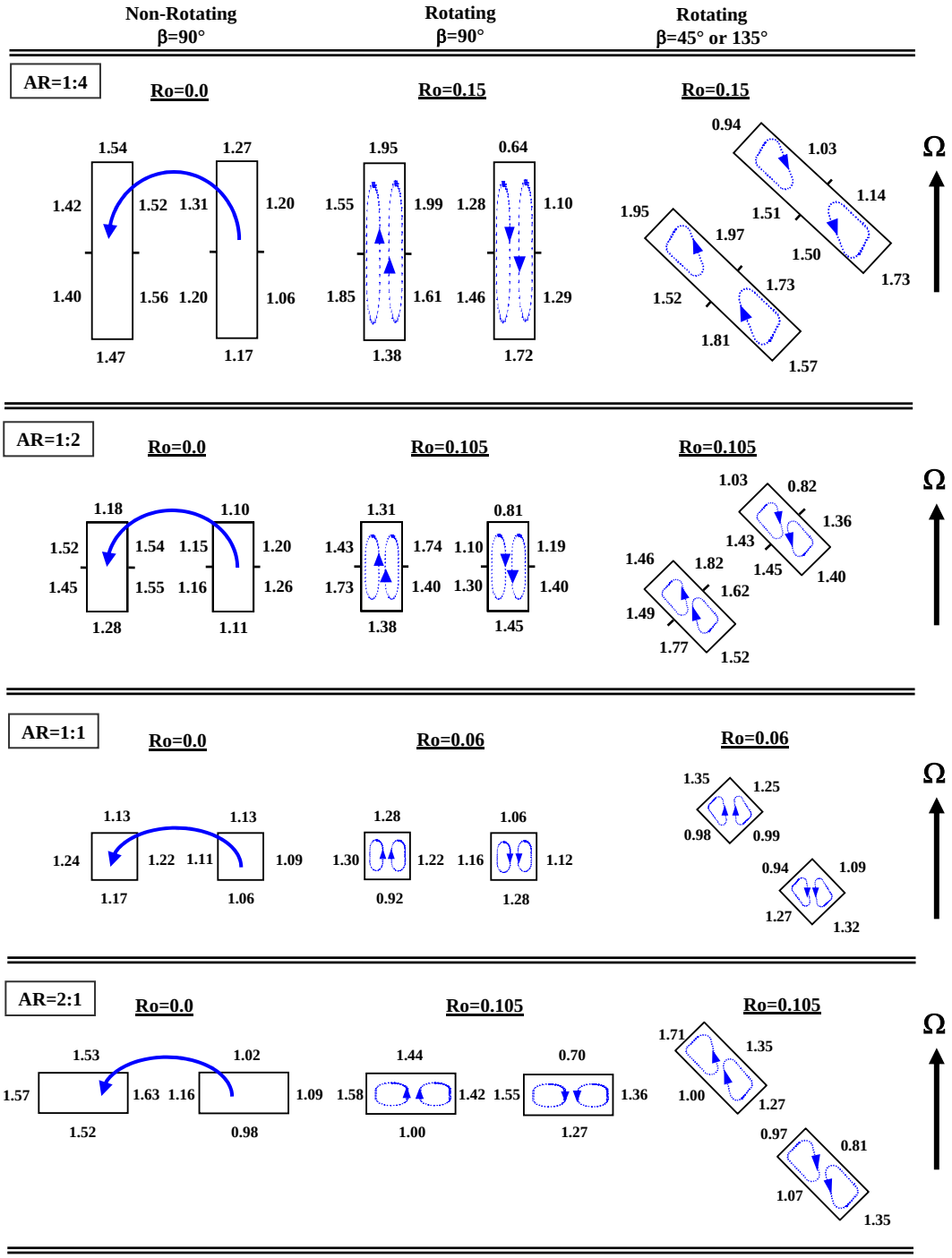

Figure 4.7 Secondary Flow Effect on Circumferential Heat Transfer (Re=10000) with Smooth Walls (Number Represents the Nusselt Number Ratio)

number ratios on these surfaces. The arrow indicates the direction of rotation induced vortices.

For the non-rotating case (as shown in Fig. 4.7), the regionally averaged heat transfer is uniform around the perimeter walls in the first pass for all channels. In the second pass, it is generally true, except the heat transfer level is slightly higher than in the first pass due to the 180° turn effect.

As the channel rotated, a pair of vortices induced by the Coriolis force enhances the heat transfer on the trailing surface and reduces the heat transfer on the leading surface in the first pass. The effect is reversed in the second pass due to the reversed direction of the Coriolis force. Section 3 has discussed the secondary flow patterns in detail. For the low aspect ratio channels (1:4 and 1:2), the trailing (T), outer-trailing (OT), and inner-trailing (IT) surfaces in the first pass undergo a heat transfer enhancement under rotating conditions, while the leading (L), outer-leading (OL), and inner-leading (IL) surfaces experience reduced heat transfer. In general, the heat transfer in the second pass follows this trend; however, the turn effect created a more complicated result. The difference between the leading and trailing surfaces is relatively small in the second pass than that in the first pass. There is almost no difference in the second pass of the AR=1:2 channel. In addition, the outer-trailing (OT) wall in the second pass has higher heat transfer than the outer-leading wall. For the high aspect ratio channels (1:1 and 2:1), the rotation effect is clearly seen on the leading wall and the trailing wall in the first pass and the second pass. Because there is only one copper plate

on each of the inner and outer walls, the rotation effect on side walls can not be identified.

The rotation effect reduced for the channel orientation of 45° or 135° (when compared to β=90°). Therefore, the difference of heat transfer between the leading and trailing surfaces reduced. Higher heat transfer enhancement can be seen on the side walls due to the rotation induced secondary flow impinging on the side walls.

Aspect Ratio Comparison – Regional Comparisons

All of the two-pass channels contain six copper plates in the first pass and six copper plates in the second pass. The location of each region has been shown in Fig. 4.6. A 4:1 single pass test section is also compared to the first pass of the other test sections, and this single pass test section consists of six copper plates in the streamwise direction. Because the test sections have similar construction, the Nusselt number ratios are compared at specific regions, rather than at a given X/D_h location. The regions chosen for comparison are 4, 11, 6, and 7. Regions 4 and 11 should represent fully developed flow in the first and second passes, respectively. Regions 6 and 7 are interesting, as they give more insight to the complexities of the 180° turn. For regions 4 and 11, the Nusselt number ratios are presented on the leading, trailing, inner, and outer walls. At regions 6 and 7, similar results are shown including the leading, trailing, outer, and tip surfaces. These local comparisons are completed to show how the heat transfer enhancement varies with the increasing buoyancy parameter, and the comparisons are made for channels positioned normal and skewed to the direction of rotation. The non-rotating Nusselt number ratios are also given at a Reynolds number of 40000 as references. The

reference values are the averaged value of the leading and trailing surfaces, since they are approximately the same in the non-rotating cases. For the inner, outer, and tip regions, each value is given in the figures.

Figure 4.8 shows the effect of the buoyancy parameter on the Nusselt number ratios at region 4, in the smooth channels oriented at $\beta = 90°$. The separation of the leading and trailing surfaces is clearly seen in Fig. 4.8(a). For the 1:2, 1:1, and 2:1 channels, the Nusselt number ratios on the trailing surface continue to increase with the increasing buoyancy parameter, while the leading surfaces experience a gradual decrease in the heat transfer coefficients. However, in the 1:4 channel, the trailing surface behaves as expected, while the leading surface decreases to a minimum at $Bo = 0.08$, and then the Nusselt number ratios increase with the increasing effect of rotation. The 4:1 channel behaves similarly, with less degradation on the leading surface.

In general, the rotation effect creates greater heat transfer variation in the lower aspect ratio channel than in the high aspect ratio channel for the same hydraulic diameter. In other words, the 1:4 channel has larger heat transfer variation than the 4:1 channel, and the 1:2 channel has larger heat transfer variation than the 2:1 channel. The square channel has the lowest heat transfer variation due to rotation. This can be attributed to the geometry of the rotation induced vortices. As shown in Fig. 3.4, the rotation induced vortices have a narrow elongated shape in lower aspect ratio channels (1:4 and 1:2). The flow becomes warmer while traveling from the trailing surface to the leading surface. Therefore, the heat transfer difference between these two surfaces is large. In high aspect ratio channels (4:1 and 2:1), the rotation induced vortices most

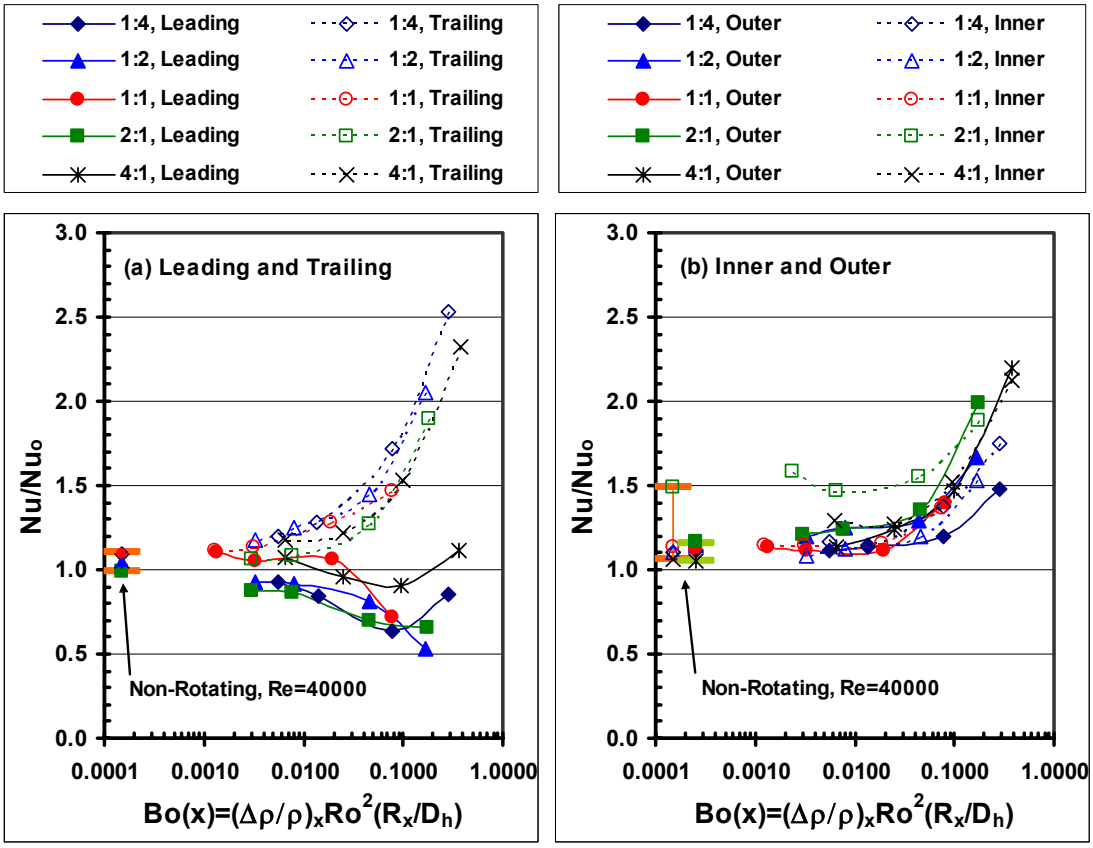

Figure 4.8 Nusselt Number Ratio Comparison at Region 4 in the Smooth Channels (β=90°)

have a circular shape. The coolant is well mixed between the leading and trailing surfaces. The heat transfer difference is small between these two surfaces in the high aspect ratio channels.

The trends for the outer and inner walls are less decisive than the leading and trailing surfaces. As Fig. 4.8(b) shows, the heat transfer enhancement on both the outer and inner walls increases with rotation for all channels. The level of enhancement for the inner and outer walls of a given aspect ratio is comparable, with the largest separation of the two surfaces occurring in the 1:4 channel.

As expected, the trends for the heat transfer enhancement in the second pass are opposite of those in the first pass. Figure 4.9 shows the Nusselt number ratios at region 11 in the second pass. As the effect of rotation increases, the heat transfer on the leading surfaces increases and decreases on the trailing surfaces. The level of enhancement and declination is reduced as the effect of rotation is reduced in the second pass. Unlike region 4, the channel aspect ratio effect on the heat transfer variation is not seen in region 11. Because the flow is affected by the strong turn, the heat transfer distribution is more complicate in the second pass than in the first pass.

In general, the heat transfer from both the inner and outer surfaces increases with the buoyancy parameter. Figure 4.9(b) shows the exception is with the inner wall of the 2:1 channel; however, it appears as the buoyancy parameter continues to increase, the Nusselt number ratios will continue to rise, after the initial decline.

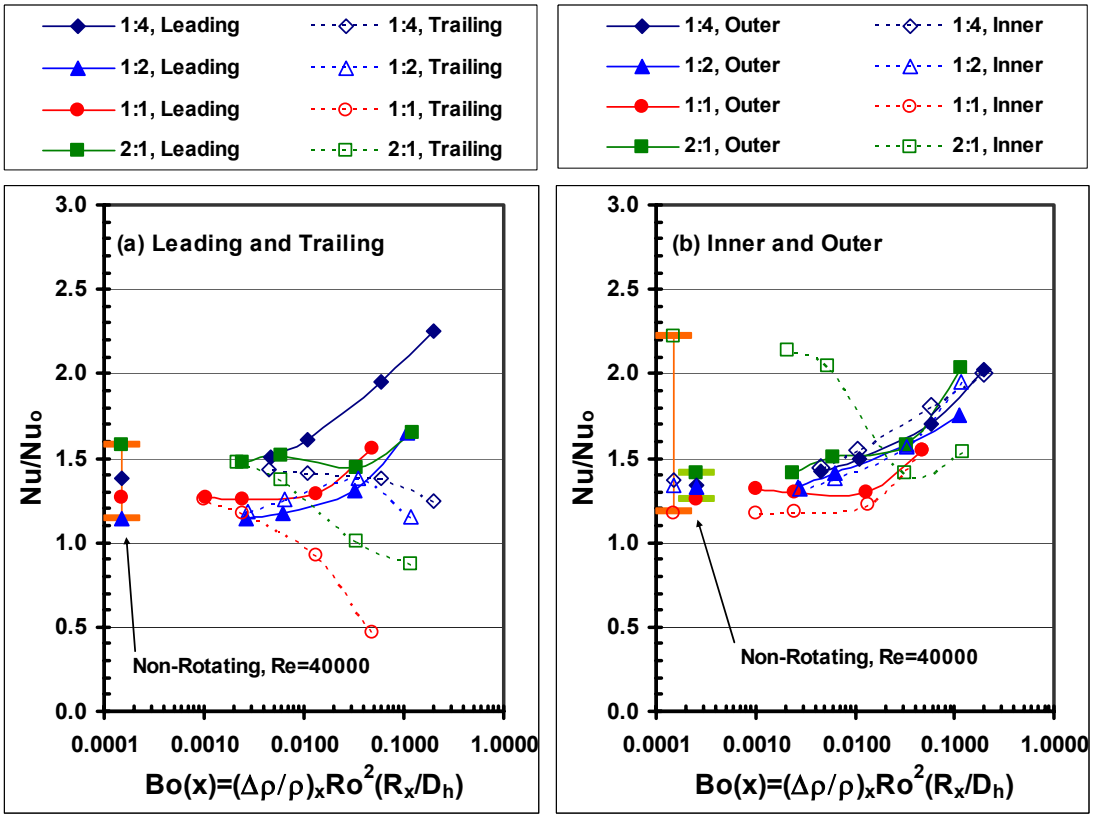

Figure 4.9 Nusselt Number Ratio Comparison at Region 11 in the Smooth Channels (β=90°)

Figures 4.10 and 4.11 show the Nusselt number ratios in the 180° turns. In region 6 (Fig. 4.10), both the leading and trailing surfaces experience heat transfer enhancement with rotation, with the trailing surfaces enhanced more than the leading surfaces. In Fig. 4.10(b) it can be seen that the Nusselt numbers on the tip also increase as the rotation number increases. The enhancement on the tip is greater than the leading and trailing surfaces, and this is expected as the coolant flow impinges on the tip. The secondary flow inside the turn has been shown in Fig. 3.2. Results for the outer wall are also shown for the 1:1 and 2:1 channels; data were not recorded for this location in the 1:4 and 1:2 channels. It is clear the level of enhancement on this outer wall is much less than on the tip. In the corner of the turn an area of recirculation exists which hurts the heat transfer performance, and the impingement that occurs on the tip is absent on the outer walls.

Figure 4.11 shows the Nusselt number ratios for the second half of the turn. As with region 11, the heat transfer on the leading surfaces is enhanced. It is more difficult to make a blanket statement for the trailing surface, as both enhancement and declination are shown depending on the channel aspect ratio. An important observation is the comparison of the heat transfer coefficients in region 7 with those in region 6. The level of enhancement in region 7 is significantly greater than in region 6. Figure 4.11(b) shows the tip and outer wall results. The Nusselt number ratios on the outer wall are much higher than those on the outer wall of region 6. As the flow travels through the turn, it now impinges on this outer wall. In general, the level of enhancement on the tip is the same at both locations in the turn.

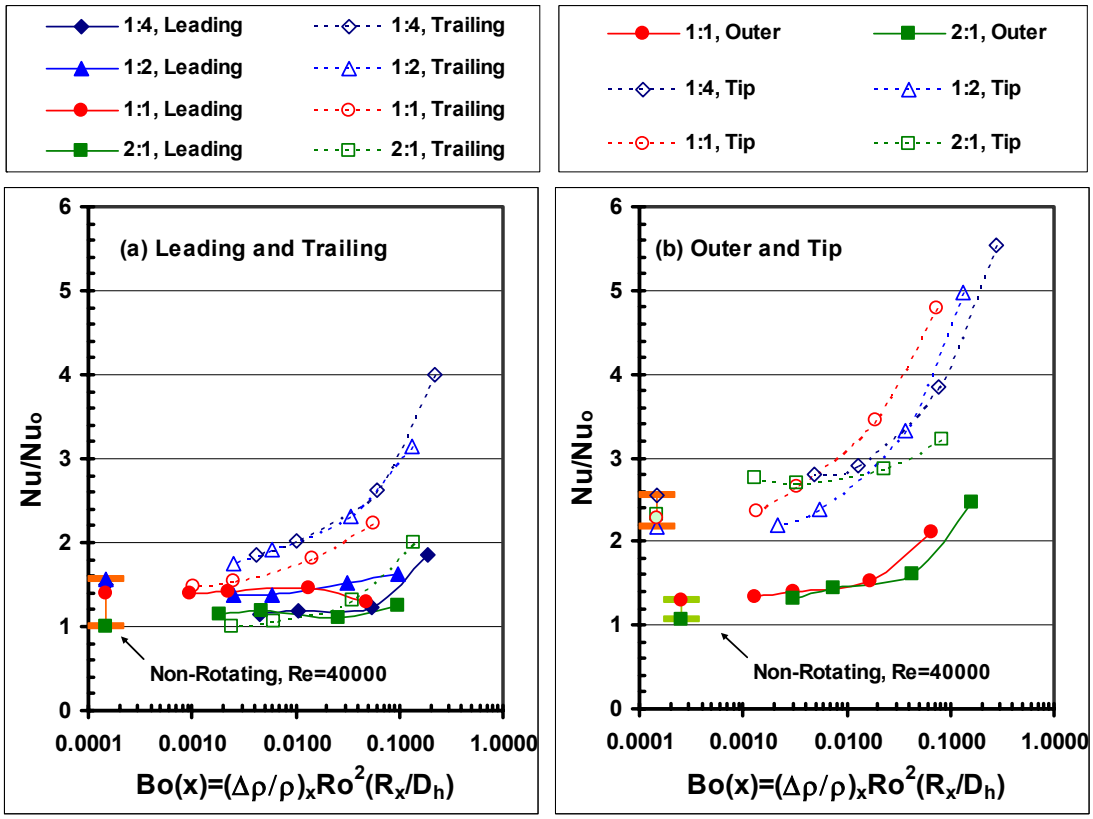

Figure 4.10 Nusselt Number Ratio Comparison at Region 6 in the Smooth Channels (β=90°)

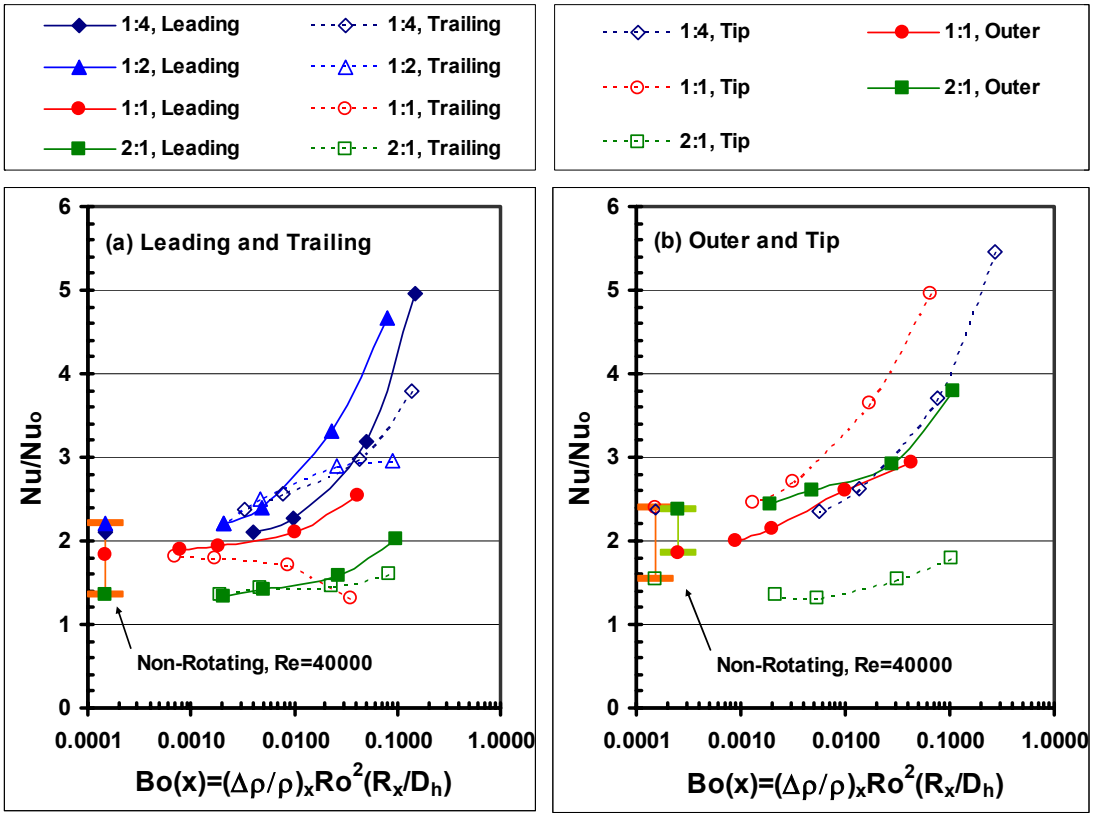

Figure 4.11 Nusselt Number Ratio Comparison at Region 7 in the Smooth Channels (β=90°)

Local comparisons were also made for the smooth channel with varied orientations. To model the location of the cooling channels in the blade, the 1:4 and 1:2 channels oriented at 45°, the 1:1 channel maintaining its orientation of 90°, and the 2:1 and 4:1 channels oriented at 135°, with respect to the direction of rotation (as shown in Fig. 1.1). Immediately seen in Fig. 4.12(a) is that the effect of rotation decreases in the skewed channels. The heat transfer on the trailing surfaces increases at region 4 in every channel. While on the leading surface, the Nusselt number ratios increase for the 4:1 and 2:1 channels, and see a slight declination in the 1:4 and 1:2 channels.

The general increase that was seen for the inner and outer surfaces in the normal channel is not seen for the skewed channels. The rotation induced vortices are altered, as shown in Fig. 3.2, and they do not impinge directly on the trailing surface of the first pass (as they do when the orientation angle is 90°). In the 1:4 and 1:2 channels, with β = 45° the rotation induced vortices travel from the leading-outer corner to the trailing-inner corner. Therefore, the secondary flow impinges on the inner wall of these channels; thus increasing the heat transfer coefficients on the inner surface. However, the 2:1 and 4:1 channels are oriented at 135°, so the secondary induced vortices travel from the leading-inner wall to the trailing-outer all. For this orientation, the coolant impinges on the outer surface, rather than the inner, and the heat transfer coefficients increase on the outer wall. For region 11, the heat transfer coefficients on the leading surface are greater than the trailing surface for all channels, as shown in Figure 4.13. With the skewed channel, both the leading and trailing surfaces of the 1:4 and 1:2 channels experience heat transfer enhancement with rotation. The trends for the inner and outer wall are similar to those of

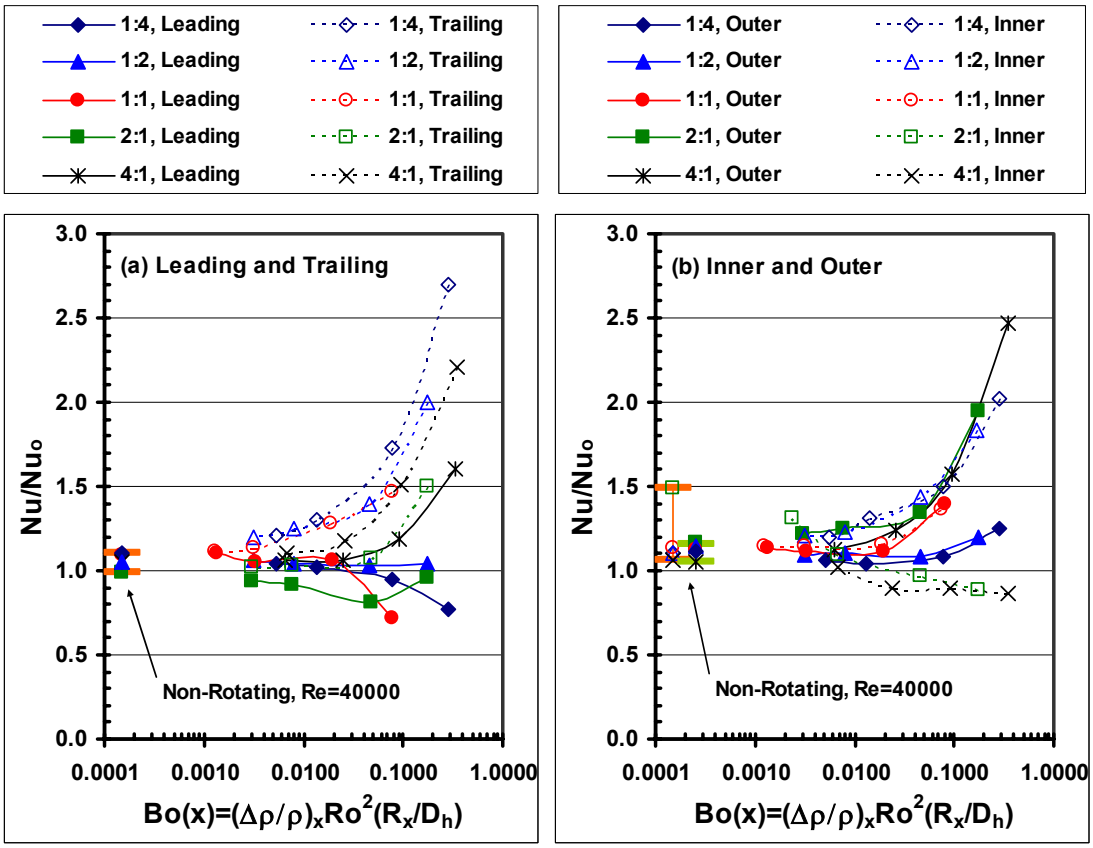

Figure 4.12 Nusselt Number Ratio Comparison at Region 4 in the Smooth Channels (β=45° or 135°)

region 4. Again, due to the shifting of the rotation induced vortices, the inner walls of the 1:2 and 1:4 are the recipients of impingement of the coolant, and therefore, the enhancement is greater for the inner walls than the outer walls. The opposite is true for the 2:1 channel where the rotation induced secondary flow impinges on the outer wall.

The turn results are shown in Figures 4.14 and 4.15 for regions 6 and 7, respectively. The trends for region 6 are similar to those of region 4; the difference lies with the level of enhancement. The heat transfer enhancement of region 6 is much greater than of region 4. The same can be said for the trends of regions 7 and 11. The orientation angle does not have a significant effect on the Nusselt number ratios of the tip and outer walls of the points in the turn (Figs. 14(b) and 15(b)). The level of trends for the heat transfer enhancement on both outer and tip wall are very similar to the results for the channels oriented normal to the direction of rotation (Figs. 4.10(b) and 4.11(b)).

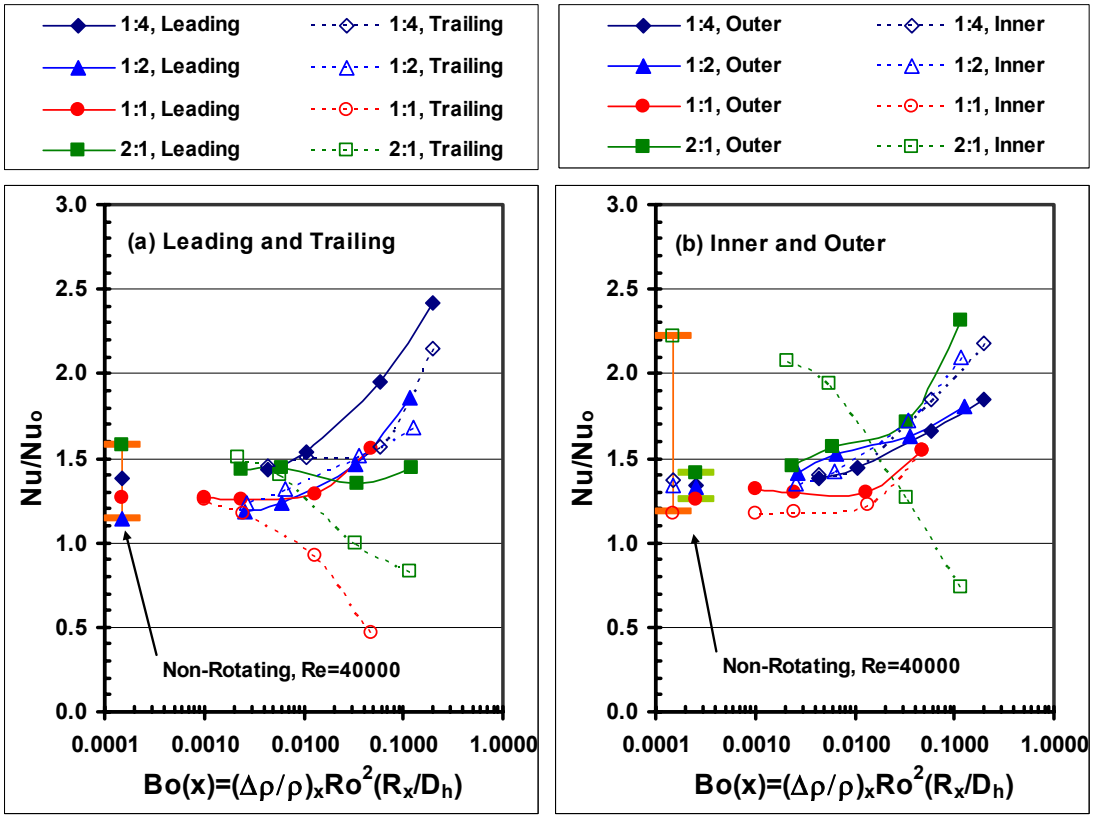

Figure 4.13 Nusselt Number Ratio Comparison at Region 11 in the Smooth Channels (β=45° or 135°)

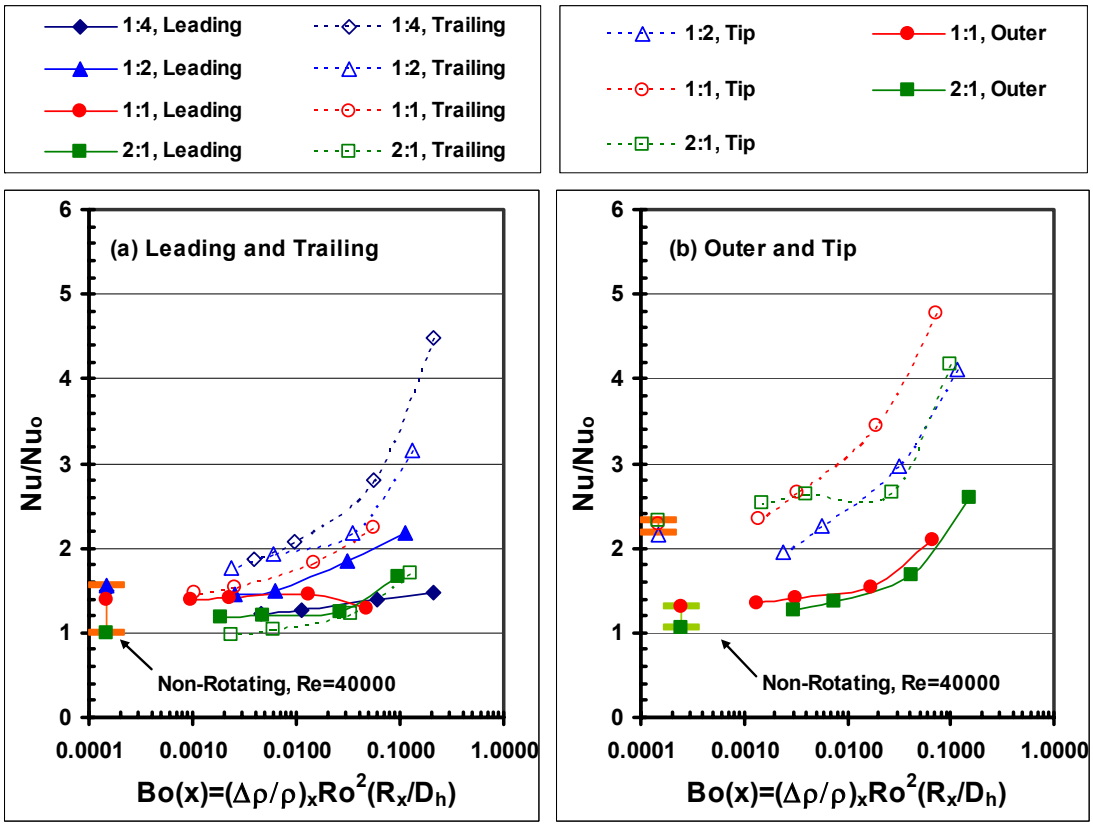

Figure 4.14 Nusselt Number Ratio Comparison at Region 6 in the Smooth Channels (β=45° or 135°)

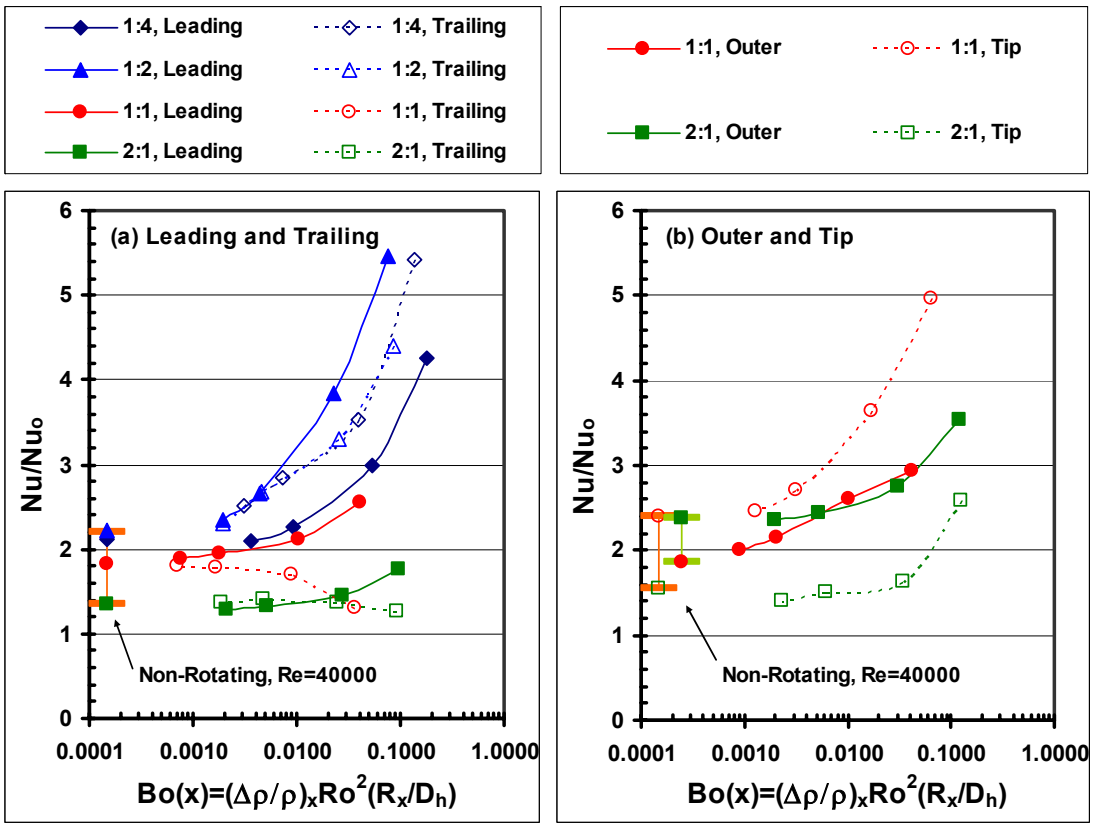

Figure 4.15 Nusselt Number Ratio Comparison at Region 7 in the Smooth Channels (β=45° or 135°)

V HEAT TRANSFER RESULTS FOR RIBBED WALLS*

In addition to the rotation induced vortices, the angled ribs also create secondary flow that affects the heat transfer of the internal channel. This section discusses the heat transfer results for the 45° angled ribbed walls. The experimental conditions are identical to that of the smooth wall channels. The sequence of figures 5.1 – 5.15 is the same as figures 4.1 – 4.15. Whereas the previous figures compared the heat transfer results in smooth channels, the following figures compare the results in channels with 45° angled ribs.

Regionally Averaged Nusselt Number Ratio Distributions

The Nusselt number ratio distributions for 45° angled ribbed channels are shown in Fig. 5.1 - 5.4. Similar to Fig. 4.1 – 4.4, each figure contains both non-rotating and rotating (β=90° and β=45° or 135°) Nusselt number ratio distributions for both the leading and trailing surfaces at four Reynolds numbers.

Fig. 5.1 shows the Nusselt number ratio distributions for the AR=1:4 channel. The level of heat transfer enhancement by the angled rib remains relatively constant throughout the entire non-rotating channel, and as expected, the leading and trailing surfaces experience the same level of enhancement. The 45° angled rib enhances heat transfer about three times more than the smooth channel at Re=5000. Unlike the smooth

* Part of data reported in this section is reprinted with permission from "Heat Transfer in Two-Pass Rotating Rectangular Channels (AR=1:2 and AR=1:4) with 45 Deg Angled Rib Turbulators" by Wen-Lung Fu, Lesley M. Wright, and Je-Chin Han, 2005, Journal of Turbomachinery, 127, pp. 164-174. Copyright © 2005 by ASME.

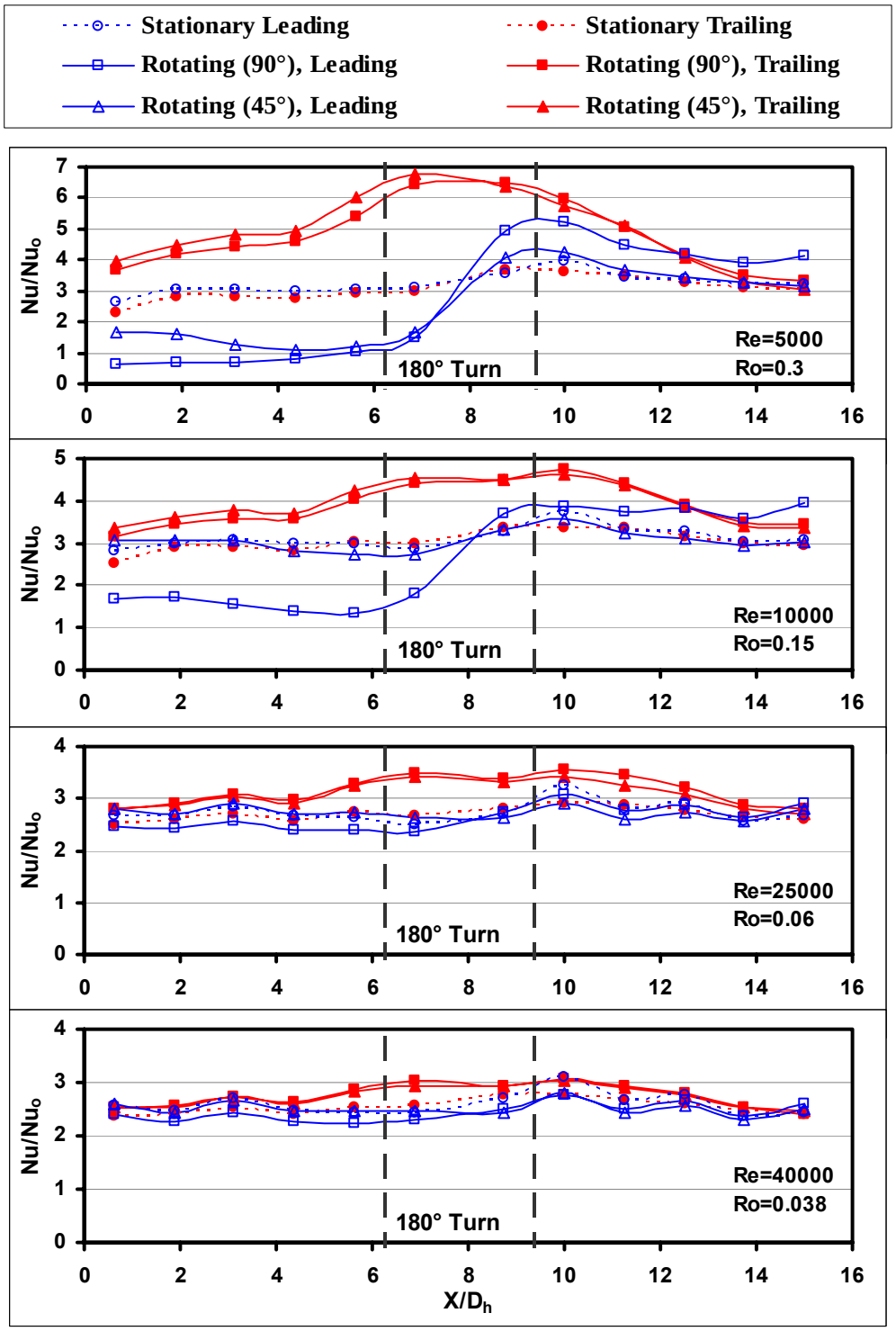

Figure 5.1 Regionally Averaged Nusselt Number Distributions for the AR=1:4 Channel with Ribbed Walls

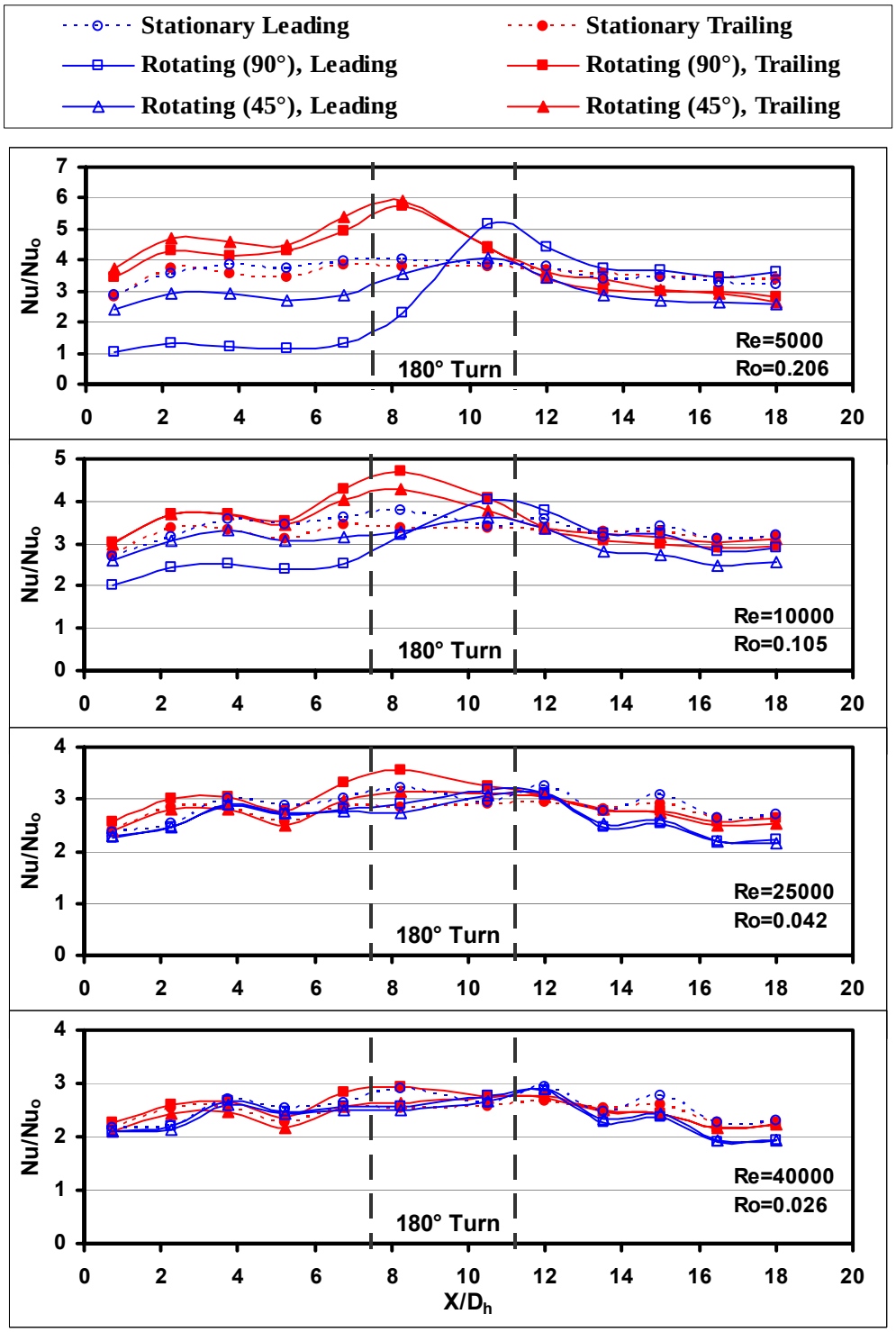

Figure 5.2 Regionally Averaged Nusselt Number Distributions for the AR=1:2 Channel with Ribbed Walls

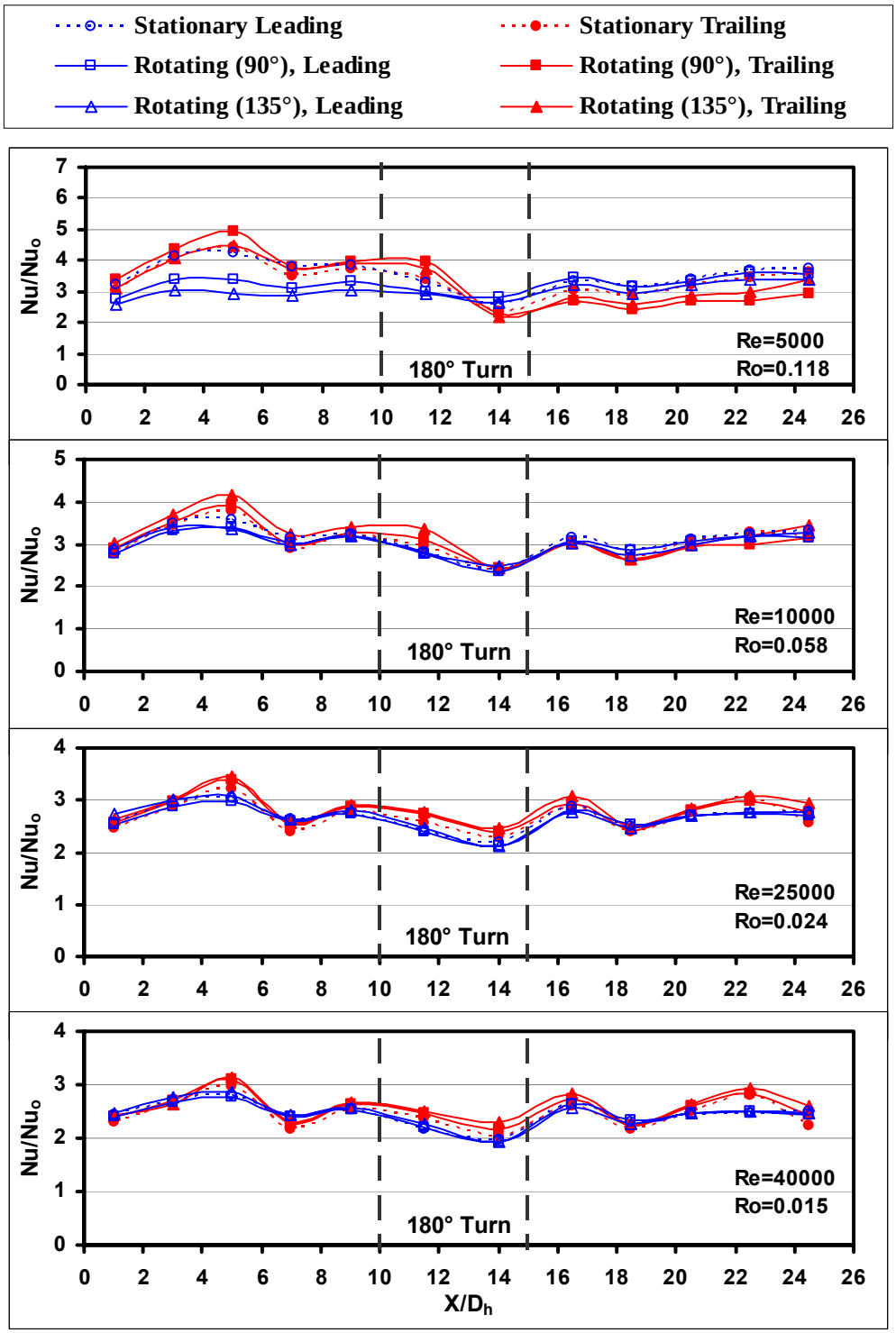

Figure 5.3 Regionally Averaged Nusselt Number Distributions for the AR=1:1 Channel with Ribbed Walls

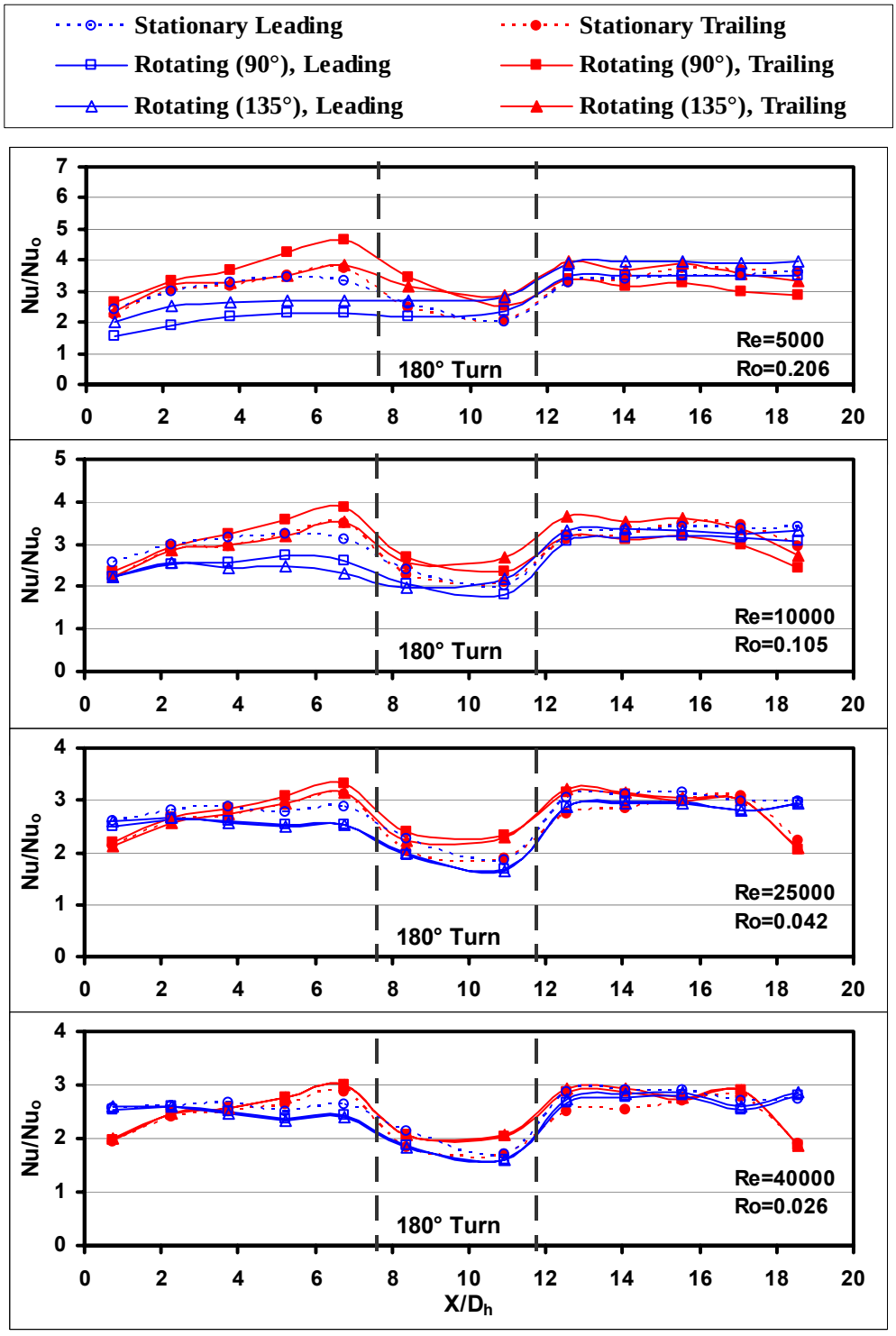

Figure 5.4 Regionally Averaged Nusselt Number Distributions for the AR=2:1 Channel with Ribbed Walls

channel (Fig. 4.1), the elevated enhancement due to turn is not seen in the ribbed channel. Because there are fewer ribs in the turn region, the heat transfer enhancement in the turn region is attributed to the turn effect which is merged into a flat level in the ribbed channel. In the second pass, the enhancement is about the same as in the first pass. It is also clearly seen that as the Reynolds number increases, the Nusselt number ratios decrease.

The effect of rotation can be seen in Fig. 5.1. Similar to the smooth channel, the heat transfer enhancement on the trailing surface is greater than that of the non-rotating channel in the first pass, and the leading surface experiences a declination in heat transfer. However, the difference between the leading and trailing surfaces is much greater in the ribbed channel than in the smooth channel (Fig. 4.1). As described in section 3, the velocity profile is skewed toward the trailing surface in the first pass due to rotation effect (Fig. 3.1). With ribs on the leading and trailing surfaces, the enhancement and declination due to the ribs is enlarged. The heat transfer enhancement on the trailing surface is greater than on the leading surface due to ribs. Therefore, the heat transfer difference between the leading and trailing surfaces is greater in the ribbed channel than in the smooth channel. This trend is true for both channel orientations ($\beta = 90°$ and $45°$).

The diminished rotation effect in the second pass is also observed in this ribbed channel. It has been discussed in the previous section. The 1:4 channel is only about six hydraulic diameters long in the second pass. It is not sufficient for flow to develop after the flow pass the turn. Therefore, the heat transfer in the second pass is still affected by the turn effect. As the Reynolds number increases (rotation number decreases), the

difference between the leading and trailing surfaces decreases. In general the Nusselt number ratios of both the leading and trailing surfaces are greater than those of the non-rotating channel in the second pass. This offers positive information for designers in that the declination of heat transfer traditionally seen on the trailing surface of the second pass is not present in the 1:4 channel.

The Nusselt number ratio distributions for the 1:2 channel are shown in Fig. 5.2. As with the 1:4 channel (Fig. 5.1), the heat transfer enhancement in the non-rotating channel is relatively constant throughout the entire channel. However, the level of heat transfer enhancement in the 1:2 non-rotating channel is more than that of the 1:4 channel. The height of the ribs is the same for both channels; however, the height of the 1:4 channel is twice that of the 1:2 channel. Therefore, the effect of the angled ribs is more in the 1:2 channel than the 1:4 channel. As the Reynolds increases, the level of heat transfer enhancement decreases.

Similar to the 1:4 channel (Fig. 5.1), the significant effect due to rotation is observed in the first pass of the 1:2 channel. However, the difference between the leading and trailing surfaces is less in this 1:2 channel than in the 1:4 channel. The reason is the same as described earlier. The channel has larger rotation number because of the larger hydraulic diameter, since the rotating speed is constant in present study. The difference between the leading and trailing surfaces decreases significantly in the second pass of the 1:2 channel (Fig. 5.2). At the higher rotation numbers (lower Reynolds numbers), a difference between the leading and trailing surfaces can be observed, but this difference quickly diminishes as the rotation number decreases

(Reynolds number increases). In this case the flow has less than nine hydraulic diameters to develop downstream of the turn. This short distance is insufficient for the rotation induced vortices to overcome the dominant secondary flow induced by the 180° sharp turn. Unlike the 1:4 channel, the Nusselt number ratios of both the leading and trailing surfaces are less than those of the non-rotating channel in the second pass of the 1:2 channel. This is different than the trends shown for the 1:4 channel where the ratios were greater than the non-rotating channel. As the Reynolds number increases (Rotation number decreases), the difference between the leading and trailing surfaces decreases for both channel orientations ($\beta = 90°$ and 45°).

Figure 5.3 shows the Nusselt number ratio distribution for the square channel. Similar to the 1:4 and 1:2 ribbed channels, the Nusselt number ratio distribution for the square ribbed channel is relatively constant. However, the level of enhancement is more in this square channel than in the 1:4 and 1:2 channels. Again, it is attributed to the higher ratio of rib height-to-channel height (e/H) in this square ribbed channel. Similar to 1:4 and 1:2 channels, the rotation effect creates a heat transfer difference between the leading and trailing surface in the first pass. However, the variation is smaller than the other two channels because of the smaller rotation number in this square channel. In the second pass, the variation is smaller than in the first pass. Again, it is due to the combined effects of the turn, angled rib and rotation.

The Nusselt number ratio distributions for the 2:1 ribbed channel are shown in Fig. 5.4. The rib height and channel height are the same as the square channel. However, the angled ribs enhance less heat transfer in the 2:1 non-rotating ribbed channel than in

the square channel. As the coolant flows along the rib, the thermal boundary layer becomes thicker. Therefore, the heat transfer enhancement reduces along the rib. The rib length in the 2:1 channel is twice that of the square channel. Therefore, the regionally averaged Nusselt number ratio is less in the 2:1 ribbed channel. In the turn region, the enhancement is even less, since there are fewer ribs in the turn but larger smooth area.

It is clearly seen that the rotation effect creates a heat transfer variation in the first pass. However, the variation is smaller in the 2:1 ribbed channel than in the 1:2 ribbed channel. It is attributed to the channel geometry. In the 1:2 channel, the channel is narrow and the rotation induced vortices are in the circular shape (as shown in Fig. 3.4). Therefore, the heat transfer difference between the leading and trailing surfaces is less. The heat transfer variation in the second pass decreases significantly as seen in the other channels.

In general, the 45° angled ribs enhance the heat transfer approximately 2.5 to 4 times the non-rotating channels. The rotation effect on heat transfer is similar to that of the smooth channels. However, the heat transfer variation is larger in the first pass of the ribbed channels. The reduced heat transfer variation in the second pass is also observed in the ribbed channel. As the Reynolds number increases, the heat transfer variation due to rotation is reduced.

Comparison with Previous Studies

Figure 5.5 compares the angled rib results of the present 1:2 channel to those of the 1:2 ribbed channel used by Cho et al. [31]. Although the channel geometry of both studies is similar, the rib geometry of the two studies differs. The angled ribs of the

previous studies are oriented at 70° to the mainstream flow. The rib pitch-to-height ratio (P/e) is 7.5, and the rib height-to-hydraulic diameter ratio (e/D_h) is 0.075; for the current study P/e is 10 and e/D_h is 0.094. When comparing the non-rotating results of the current study to those of the previous study, it can be seen that Nusselt number ratios of the current study are greater than those of the previous study in both the first and second passes, but the trends of the two studies are similar. Therefore, the difference in enhancement levels can be attributed to the difference in rib geometry. It should also be reiterated, that the previous study utilizes mass transfer. The results of mass transfer experiments are traditionally lower than those of other experimental techniques because the area atop the ribs is not measured using the mass transfer method. The highest heat transfer occurs on top of the ribs, and this area of very high heat transfer is not considered using mass transfer; therefore, the average values are different between these two measurements.

The comparison of the 1:2 rotating channels with angled ribs is also shown in Fig. 5.5. As with the smooth channel comparison, the difference between the leading and trailing surfaces in the first pass is clearly seen. However, in both the present study and the previous study of Cho et al. [31], almost no variation exists in the second pass.

The comparison confirms that the interaction between the rib induced secondary flow, rotation induced secondary flow, and turn induced secondary flow result in diminished heat transfer difference between the leading and trailing surfaces in the second pass of the low aspect ratio channel.

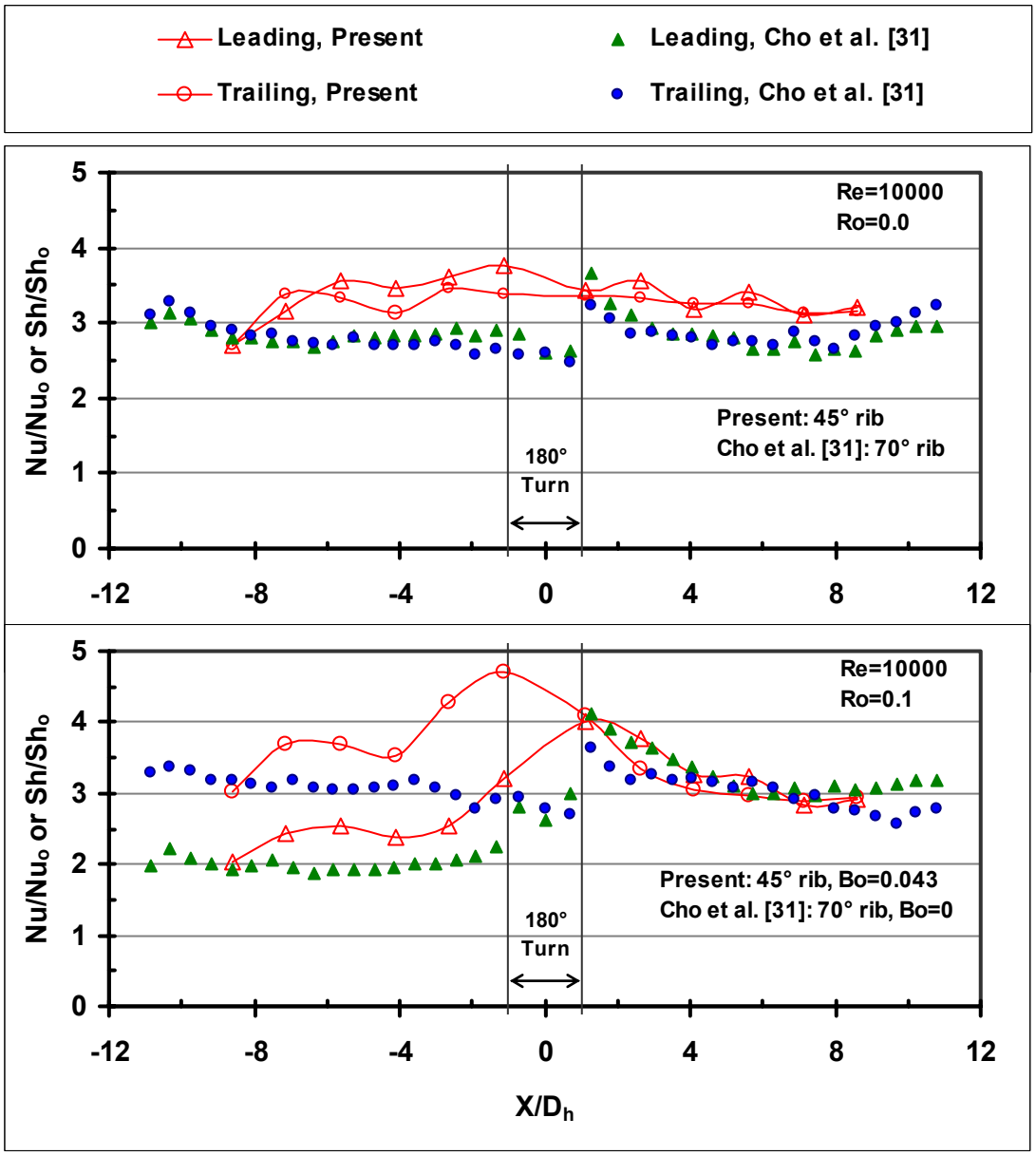

Figure 5.5 Comparison of the Nusselt Number Ratio Distributions for the AR=1:2 Channel with Ribbed Walls

Secondary Flow Effect on Circumferential Heat Transfer

Similar to Fig. 4.6, Fig. 5.6 shows the locations of data regions in the ribbed channel. The 45° angled ribs are placed on the leading and trailing surfaces. The labels are the same as used in the smooth channels. In the streamwise direction, the channel is divided into twelve segments, six in the first pass and six in the second pass. The regions chosen to compare are identical to those chosen for the smooth channels; regions 4, 11, 6, and 7. Region 4 and 11 represent the fully develop flow in the first pass and the second pass. Region 6 and 7 are inside the turn.

In rotating ribbed channels, both the rib induced and the rotation induced secondary flows could affect the circumferential heat transfer in the channel. Figure 5.7 shows the angled rib induced vortices (Red Solid line) and rotation induced vortices (Blue Dashed line), as well as the circumferential regionally averaged Nusselt number ratios at the Reynolds number of 10000. The first pass outward flow is the right hand segment and the second pass inward flow is the left hand segment. The circumferential distribution is shown at two regions in the channel: region #4 and region #11. The numbers marked next to each surface of the different aspect ratios and orientations are the Nusselt number ratios on these surfaces. The ribs are also shown in the figure.

As shown in Fig. 5.7, the leading (L) and trailing (T) surfaces experience significantly greater heat transfer enhancement than the inner (IL and IT) and outer (OL and OT) walls of all non-rotating channels. This should be expected as the rib roughened walls trip the boundary layer resulting in increased turbulence and increased heat transfer (over the smooth inner and outer walls).

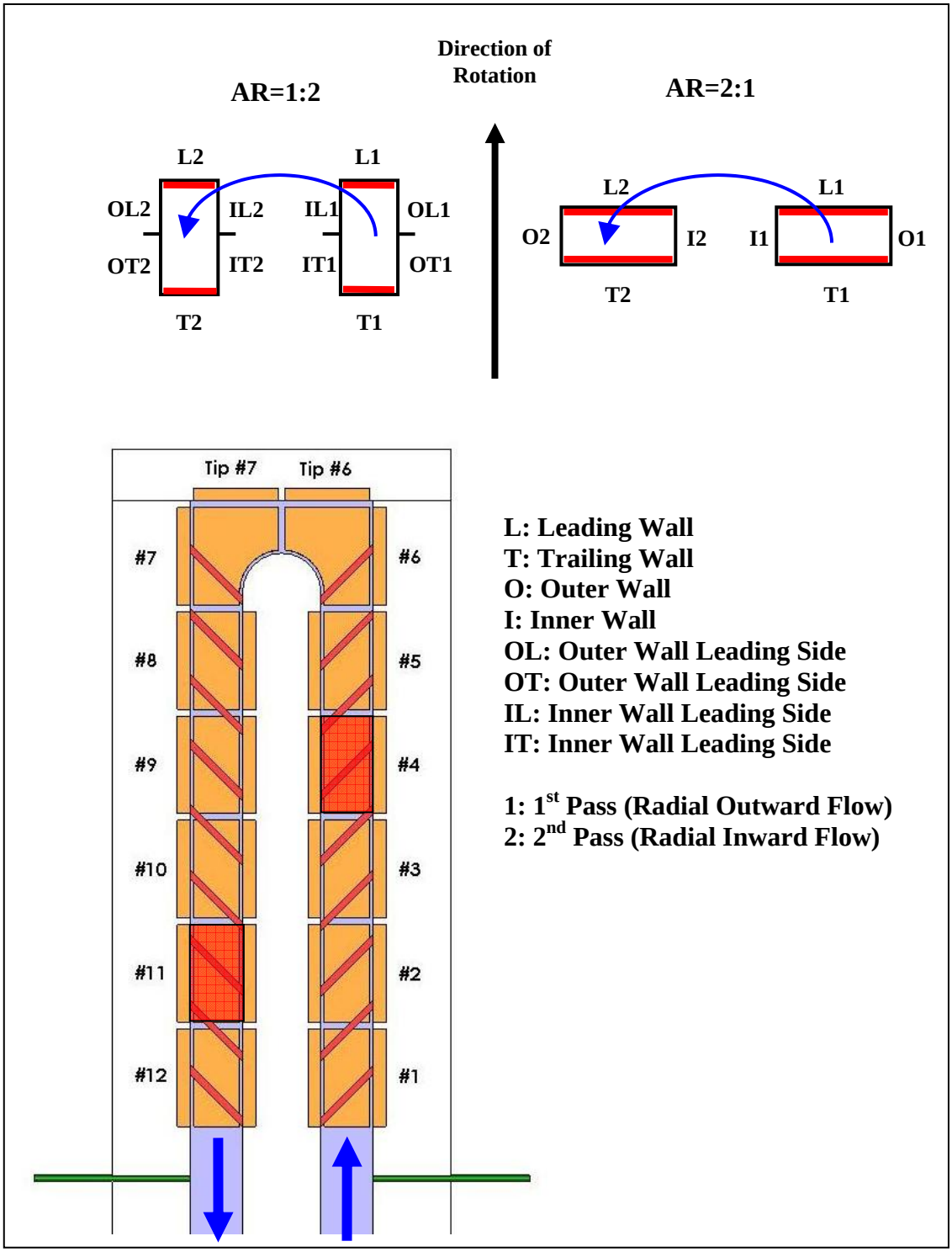

Figure 5.6 Regions of Interest in the Ribbed Channels

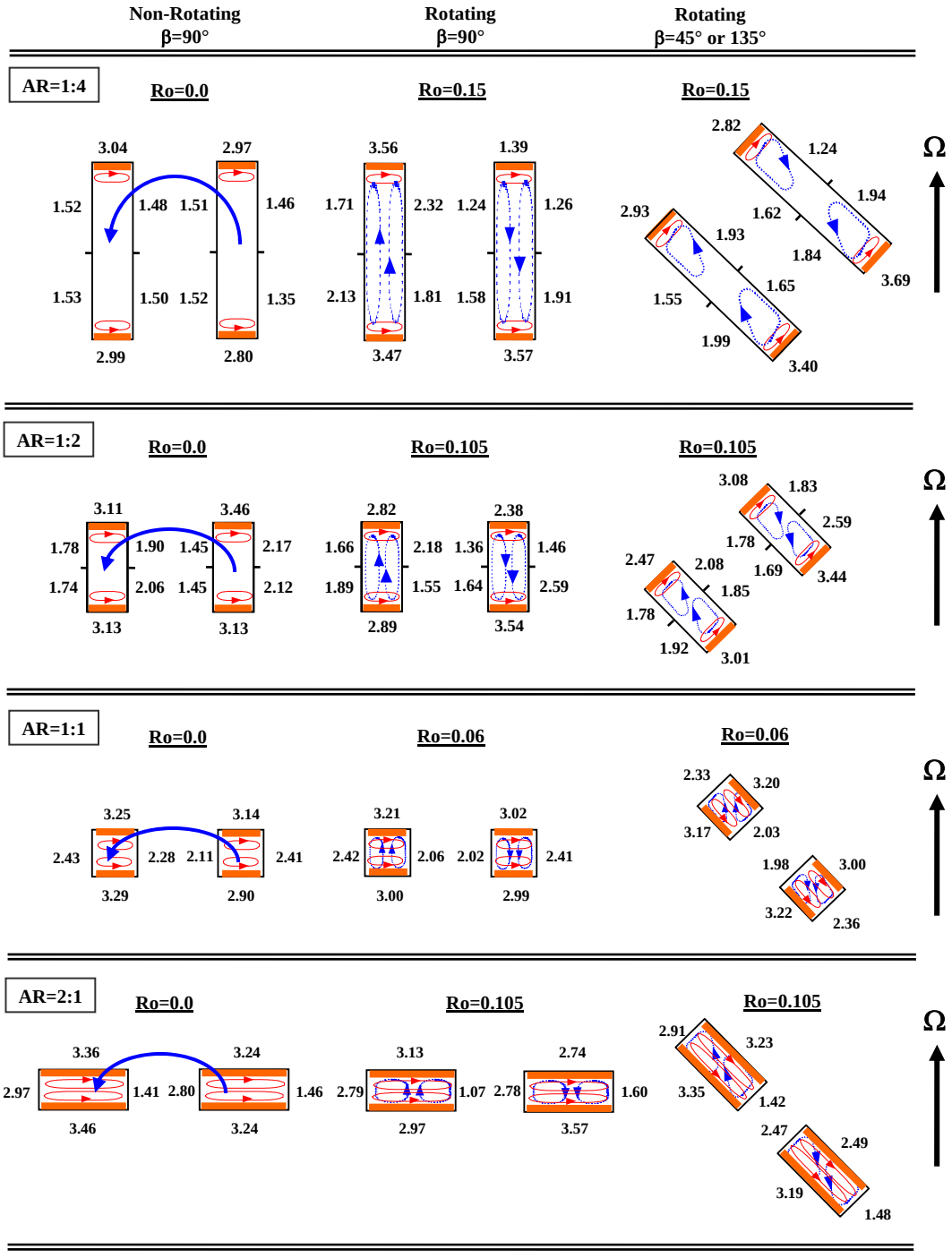

Figure 5.7 Secondary Flow Effect on Circumferential Heat Transfer (Re=10000) with Ribbed Walls (Number Represents the Nusselt Number Ratio)

The ribs also enhance heat transfer on the smooth side walls in non-rotating channels. In general, the enhancement on smooth side walls increase as increasing aspect ratio. This can be attributed to the blockage effect. The channel with a higher blockage ratio (e/H) could have stronger turbulence flow. Therefore, the heat transfer enhancement is greater. In the present study, the height of the ribs are the same for all channels, the higher aspect ratio channel has a higher blockage ratio.

The heat transfer on the smooth side walls of the non-rotating channels are also influenced by the rib arrangement. For example, the outer walls of the first pass experience more enhancement than the inner walls of the first pass and enhancement of the second pass inner walls is greater than that of the outer walls in the 1:2 channel. This can be explained by considering the rib induced secondary flow. In the first pass, the ribs are placed so the coolant is forced from the inner wall to the outer wall. The coolant impinges on the outer wall and circulates back to inner wall. Therefore, the enhancement on the outer wall of the first pass is greater than that on the inner wall. Similarly, in the second pass, the coolant is forced from outer wall to the inner wall, where it impinges on the inner wall and circulates back around to the outer wall. Therefore, in the second pass, the enhancement on the inner wall is greater than the outer wall.

When comparing the non-rotating Nusselt number ratios for the 1:2 channel to those of the 1:4 channel. It can be seen that the values in the 1:4 channel are lower than those of the 1:2 channel, especially on the inner and outer walls. The heights of the ribs are the same for both channels; therefore, the height of the ribs is less significant in the very narrow 1:4 channel than the 1:2 channel. Only a very small area of the inner and

outer walls is effected by the rib induced secondary flow, and the effect is reduced due to the regional heat transfer measurements.

However, this behavior is reversed in 2:1 channel. The side walls, with coolant impingement, have lower enhancement. This can be explained by considering the coolant flow along the ribs. The coolant becomes warmer as it flows along the ribs. When the warm coolant finally impinges on the smooth side wall, the heat transfer enhancement could be less.

For the rotating channel, the effect of rotation is clearly seen in the first pass. The rotation effect enhances heat transfer on the trailing surface but reduces heat transfer on the leading surface in the first pass. The effect of rotation diminished in the second pass as shown on previous sections.

The constructive interaction between the rib induced vortices and the rotation induced vortices is clearly seen in the enhancement of the outer-trailing (OT) surface of the first pass and the inner-leading (IL) surface of the second pass. On both surfaces, the combined effect of the ribs and rotation result in significant enhancement above the enhancement in the non-rotating channels. This is clearly seen in both the 1:2 and 1:4 channels. This effect can not be identified in the square and 2:1 channels due to limited measurements on the side walls. In general, the heat transfer behavior is similar in both channel orientations. However, the rotation effect on heat transfer is reduced in the channels skewed to the rotation direction.

Aspect Ratio Comparison – Regional Comparisons

Similar to the smooth channels, the heat transfer enhancements at the same regions (#4, #11, #6, and #7) are compared in the ribbed channels. The location of each region is shown in Fig. 5.6.

Figure 5.8 shows the Nusselt number ratios at region 4 in the ribbed channel with $\beta = 90°$. For all aspect ratios, heat transfer from the trailing surfaces is enhanced with rotation. However, the trends on the leading surfaces vary significantly depending on the aspect ratio. The heat transfer coefficients on the leading surface decrease in the 2:1, 1:2, and 1:4 channels. The most severe declination clearly occurs in the 1:4 channel. The predictions of Su et al. [36] showed two vortices are formed from the interactions of the rotation and rib induced secondary flow. One vortex encompasses the majority of the channel, while the second, much smaller vortex, is limited to a small area near the leading surface of the channel. With limited interaction of the coolant core with the leading wall, this would explain why the Nusselt number ratios on the leading surface are very low.

Similar to the smooth channels, the non-rotating Nusselt number ratios are also shown in the figure for references. For the leading and trailing surfaces, the averaged values are shown.

The heat transfer on all of the inner and outer walls in region 4 is enhanced with rotation. The ribs are placed so the coolant near the wall travels from the inner wall to the outer wall. With the varying aspect ratios, the actual length of the ribs varies. In other

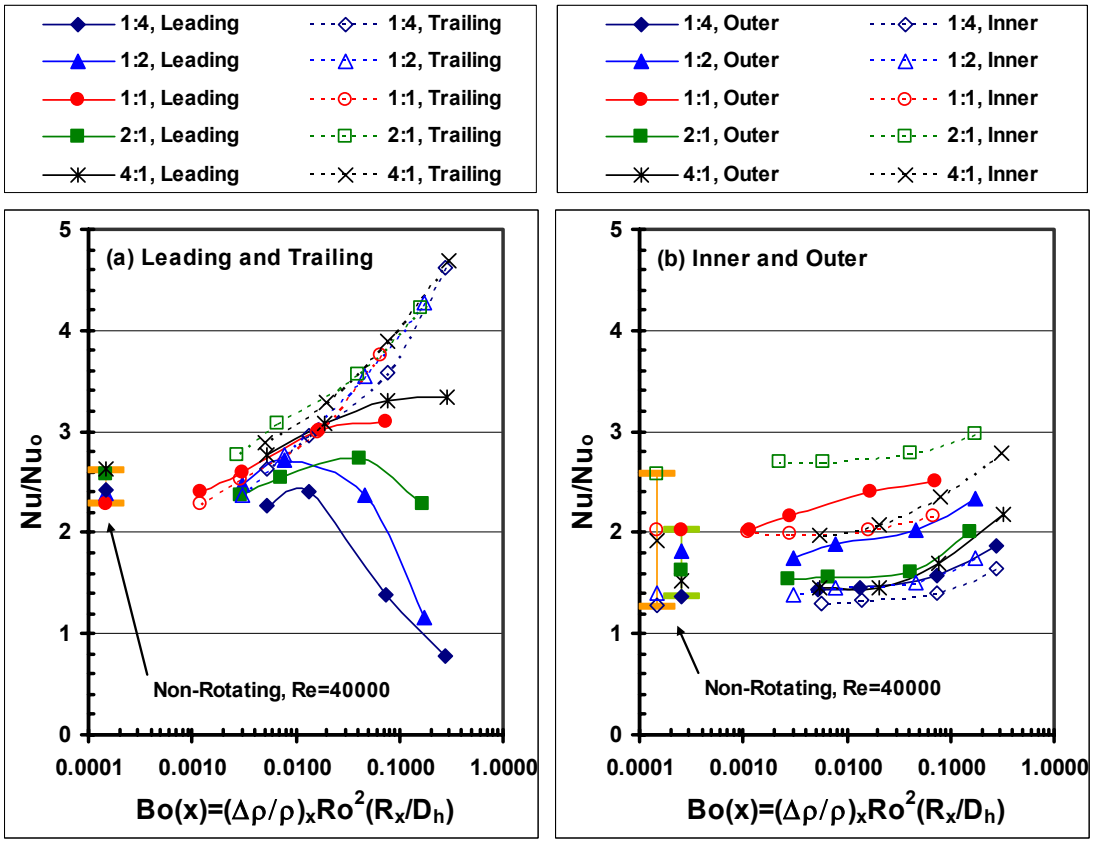

Figure 5.8 Nusselt Number Ratio Comparison at Region 4 in the Ribbed Channels (β=90°)

words, the ribs in the 1:2 and 1:4 channels are much shorter than those in the 2:1 and 4:1 channels. In the 1:2 and 1:4 channels, the heat transfer on the outer walls is greater than the inner walls. The coolant travels along the rib from the inner wall and impinges on the outer surface; thus, increasing the heat transfer. Although the secondary flow pattern in the 2:1 and 4:1 channels is the same as for the 1:2 and 1:4 channels, the heat transfer coefficients on the inner surface are greater than those on the outer surface. In this case the ribs are much longer, and as the coolant travels along the rib, the thermal boundary layer becomes thicker, and the heat transfer decreases as the coolant temperature increases. Therefore, the impingement of the relatively warmer fluid on the outer wall is less effective than in the 1:2 and 1:4 channels.

Figure 5.9 shows the results for region 11 in the ribbed channels. In the second pass, the heat transfer on both the leading and trailing surfaces increases with rotation. In the second pass, the ribs are placed so the secondary flow travels from the outer to the inner wall. However, the clear distinction between the outer and inner walls is not seen in the second pass as it is in the first pass. The extreme drop in the Nusselt number ratios on the inner wall of the 2:1 channel is unusual, and this result must be further investigated to establish the validity of the trend.

The data collected in the 180° turns of the ribbed channels are shown in Figures 5.10 and 5.11. As shown in Fig. 5.6, the ribs do not extend all the way to the tip of the turn. The trends for the leading and trailing surfaces of region 6 (Fig. 5.10(a)) are similar to those of region 4. In this location the Nusselt numbers are much greater than those at region 4. The tip and outer wall of region 6 are shown in Fig. 5.10(b), the increase with

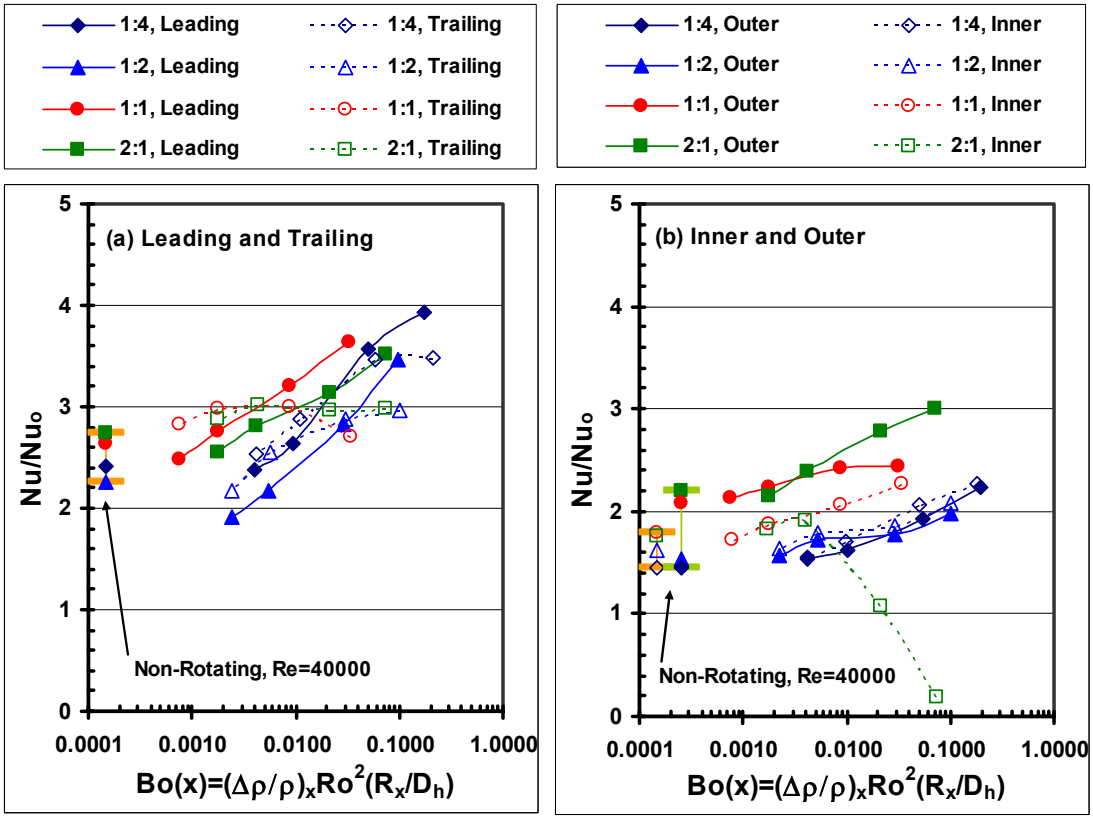

Figure 5.9 Nusselt Number Ratio Comparison at Region 11 in the Ribbed Channels (β=90°)

with rotation is less than for the smooth channel, but this is expected as the effect of rotation decreases with the use of rib turbulators. All surfaces at region 7 are increasing with rotation (Fig. 5.11). As with the smooth channel, the Nusselt number ratios are greater after the turn than before the turn.

The final group of plots (Figs. 5.12 - 5.15) shows the Nusselt number ratios in ribbed channels with varying orientations. Combinations of the various trends shown previously are shown in these plots. The effect of rotation is reduced with the varied orientation. With only a couple of exceptions, the heat transfer from all surfaces at all locations is enhanced with rotation. This offers positive information for the engine designers. The most glaring exception occurs in the 1:4 channel. The low heat transfer from the leading surface is the result of the interaction of the rotation and rib induced secondary flow. The combined effect traps the warm air near the surface, resulting in decreased heat transfer on the leading surface in the first pass.

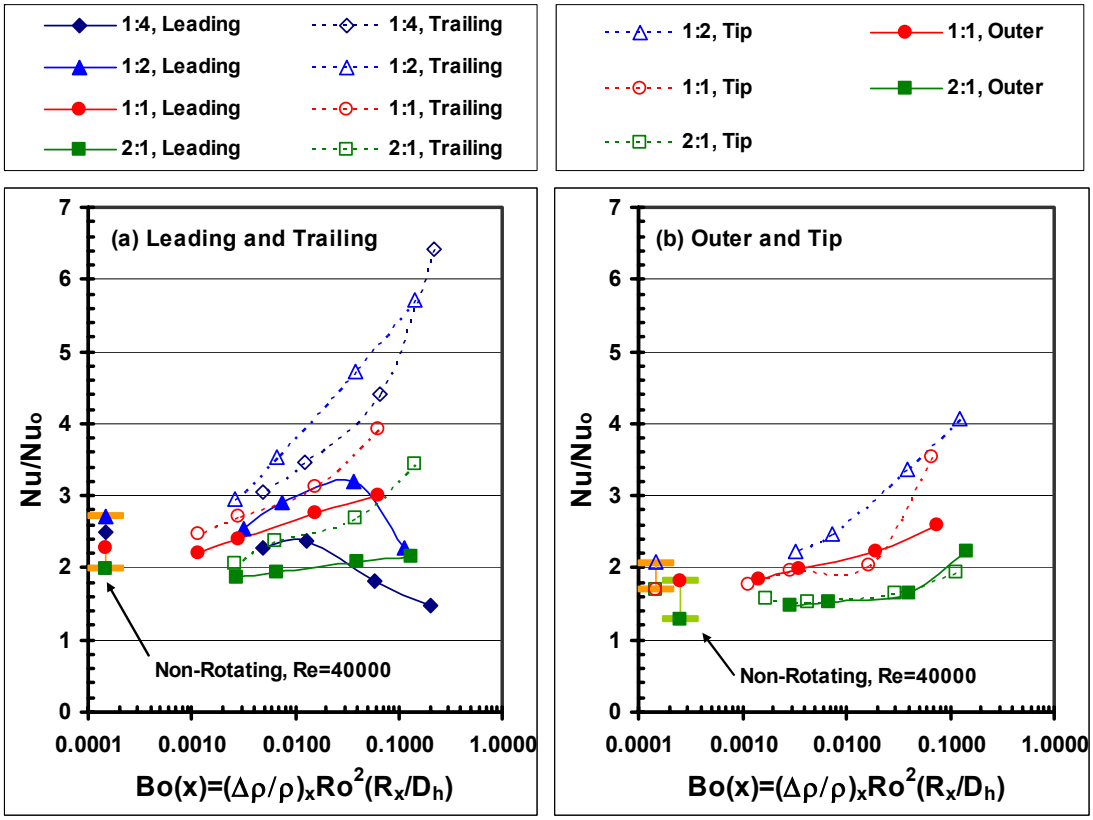

Figure 5.10 Nusselt Number Ratio Comparison at Region 6 in the Ribbed Channels (β=90°)

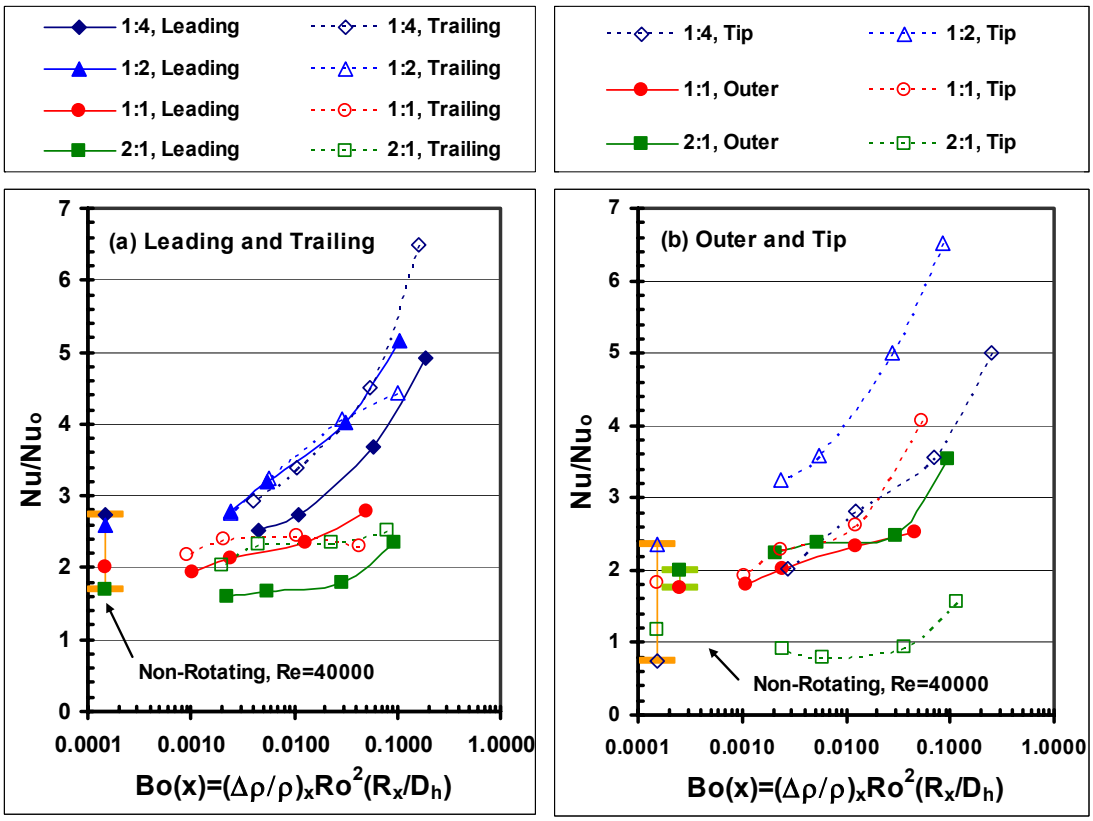

Figure 5.11 Nusselt Number Ratio Comparison at Region 7 in the Ribbed Channels (β=90°)

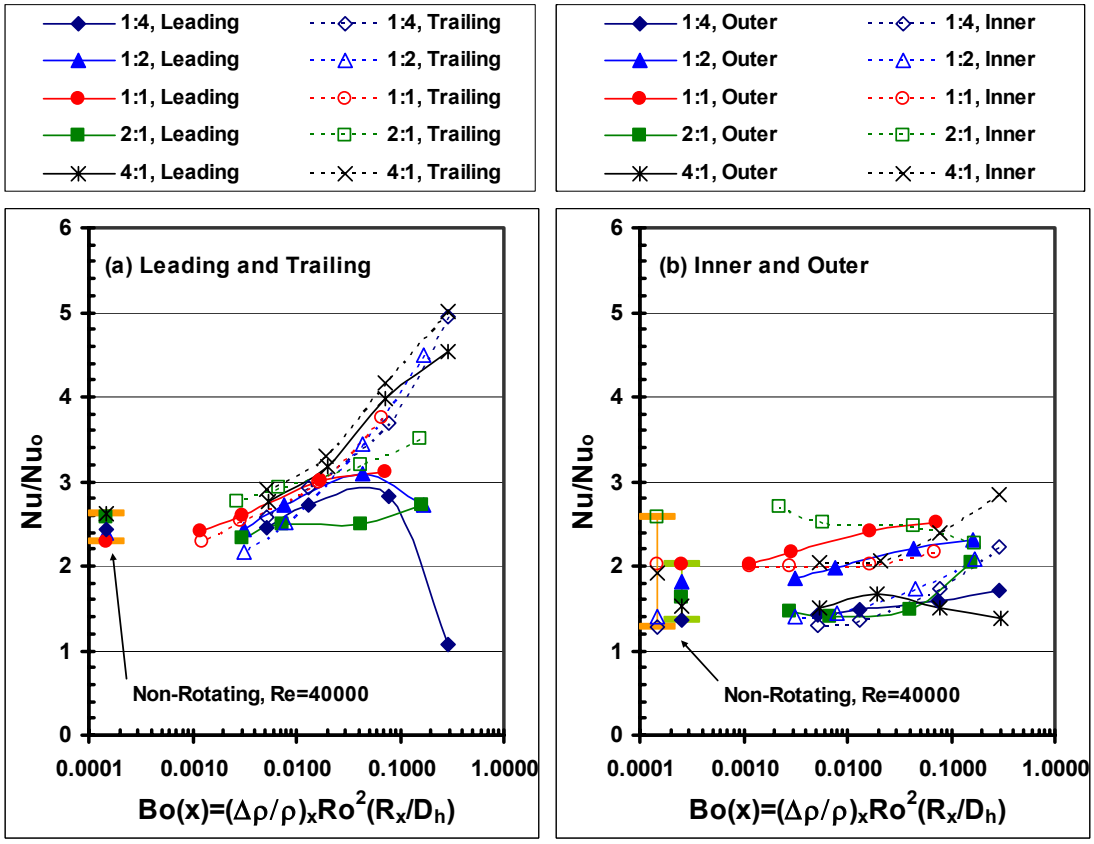

Figure 5.12 Nusselt Number Ratio Comparison at Region 4 in the Ribbed Channels (β=45° or 135°)

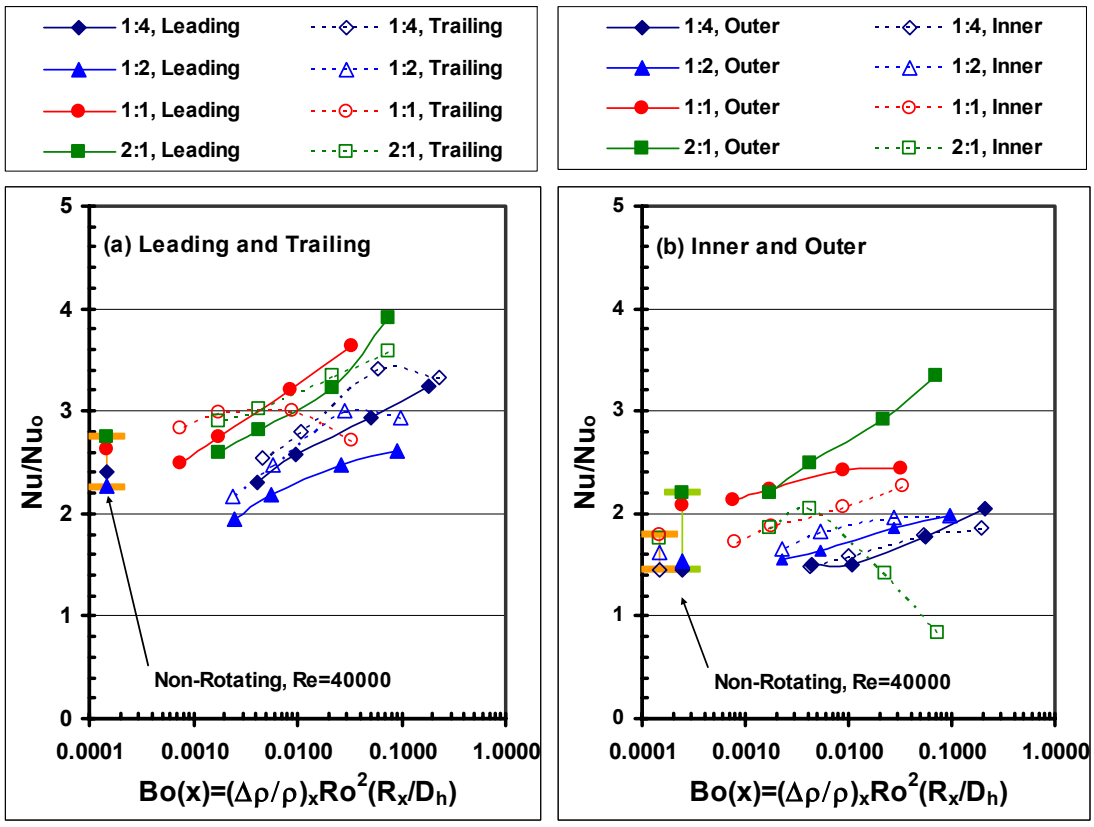

Figure 5.13 Nusselt Number Ratio Comparison at Region 11 in the Ribbed Channels (β=45° or 135°)

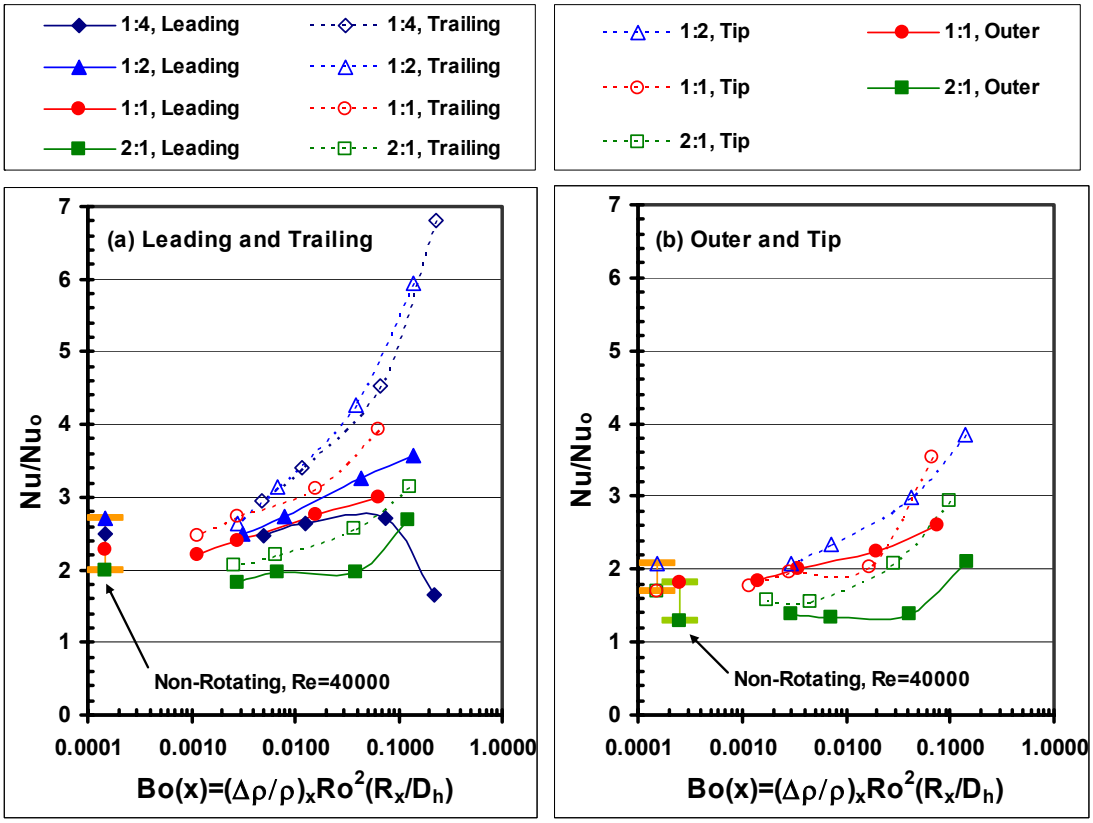

Figure 5.14 Nusselt Number Ratio Comparison at Region 6 in the Ribbed Channels (β=45° or 135°)

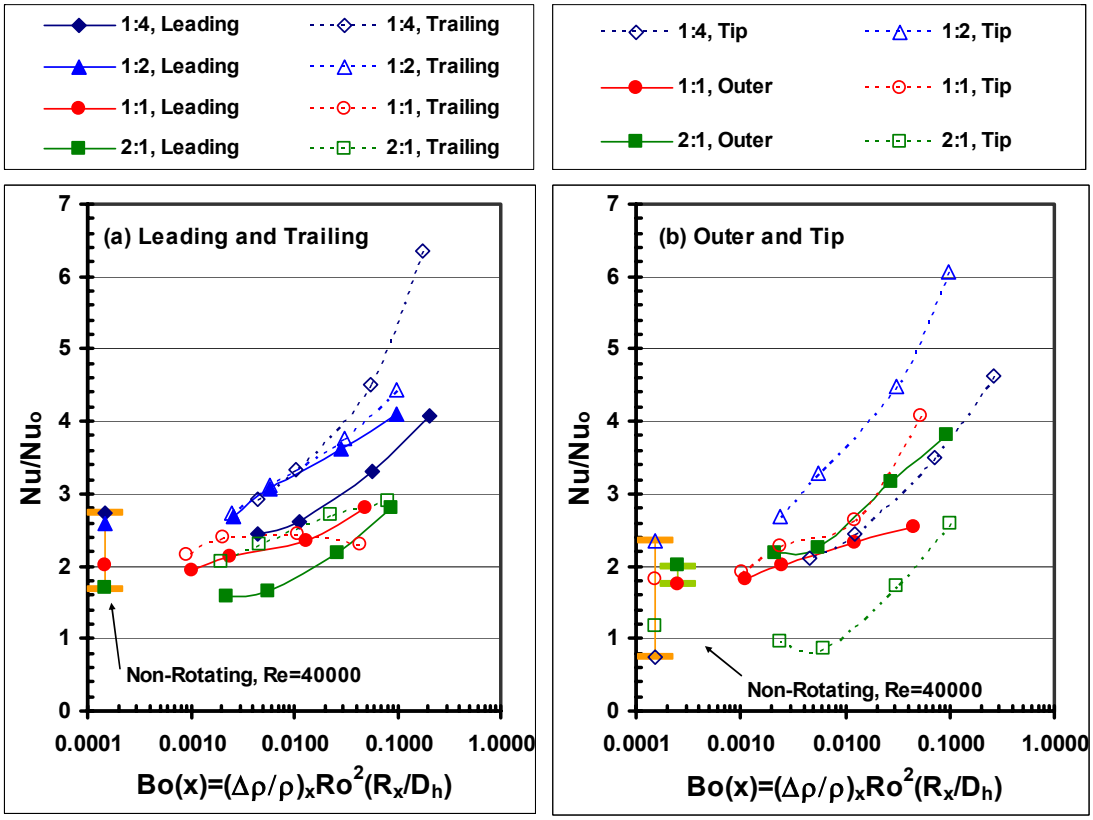

Figure 5.15 Nusselt Number Ratio Comparison at Region 7 in the Ribbed Channels (β=45° or 135°)

VI OVERALL THERMAL PERFORMANCE

The final goal of this study is to compare the thermal performance in different aspect ratio channels. Ribs enhance heat transfer in the cooling channels by disturbing the near wall flow. Most likely the pressure drop penalty is also higher. For designers, the heat transfer performance afforded by the ribs must be weighed against the pressure drop to ensure the efficiency of the design. The definition of thermal performance has been given in equation (6).

Because the cooling channels of the blades vary as the cross-section of the blade changes, designers need measurements for a wide range of channels. Four aspect ratios are considered: 1:4, 1:2, 1:1, and 2:1 in this study. The channel aspect ratios and orientations that were used to obtain data are shown in Fig. 1.1. Measurements were taken in channels with both smooth walls and ribbed walls. In addition, both non-rotating and rotating channels are considered, and the orientation of the rotating channels is varied. The 1:4 and 1:2 channels are rotated at β=90° and 45°, and the 1:1 and 2:1 channels are rotated at β=90° and 135°. The orientation angles are comparable to the actual alignment of the various cooling passages in the turbine blades.

Channel Average Nusselt Number Ratio

The first comparisons are done for the overall, or channel averaged, heat transfer. Figure 6.1 presents the channel averaged Nusselt number ratios for smooth and ribbed channels, and the figure is separated by the channel aspect ratio. The channel averaged Nusselt number ratio is obtained by averaging the leading and trailing surfaces of every

region (12 regions on each surface). In Figure 6.1(a), the Nusselt number ratios in the smooth, rotating channels are greater than the non-rotating channels. The ratios never reach the expected value of unity due to the elevated values at the entrance and in the turn. As the Reynolds number increases, the difference between the rotating and non-rotating results decreases. Similar trends are seen for the 1:2, 1:1, and 2:1 channels in Figs. 6.1 (b), (c), and (d), respectively. However, the difference between the rotating and non-rotating averaged Nusselt number ratios is less in the high aspect ratio channels (square and 2:1). As also shown in Fig. 6.1, the lower aspect ratio channels has higher averaged Nusselt number ratio in non-rotating case.

The similar trend is clearly seen in the ribbed channels. However, the averaged Nusselt number ratio decreases faster in the ribbed channels than in the smooth channels with increasing Reynolds number. The averaged Nusselt number ratio is approximately 2.5 to 3.5 in ribbed channels.

Friction Factor Ratio

Although the level of heat transfer enhancement for the various aspect ratios is comparable, more information is needed for a complete comparison. Figure 6.2 shows the friction factor ratio for each of the channels. The pressure penalty for the smooth channels ranges from approximately 2 to 4. These friction ratios are elevated above unity due to the pressure loss incurred in the 180° turn. As shown in Fig. 6.2(a), the friction factor ratio for the 1:4 ribbed channels are only 1.5 to 2 times greater than the 1:4 smooth channels. This is a stark contrast to the 2:1 channels shown in Fig. 6.2(d).

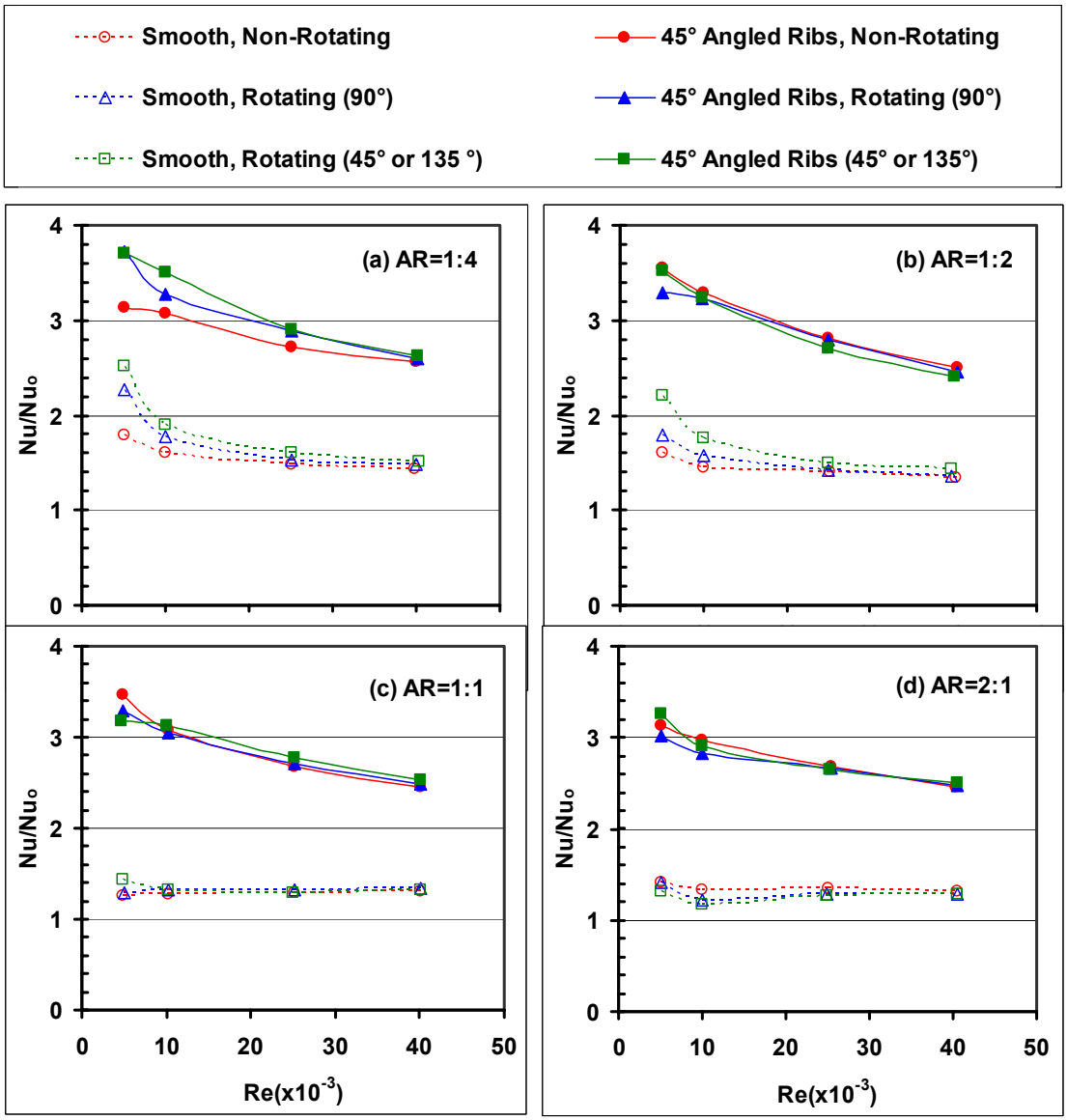

Figure 6.1 Channel Averaged Nusselt Number Ratios for Non-Rotating and Rotating Channels

The pressure penalty for the 2:1 ribbed channels is 4 times greater than the smooth channels. The size of the rib turbulators is the same for every channel. Therefore, the ribs placed on the leading and trailing walls of the 1:4 channel only affect a very small portion on the coolant flow. However, in the 2:1 channels, these ribs block a significant part of the flow area; therefore, the flow is obstructed, and a significant pressure drop is incurred. In other words, the blockage effect is greater in the 1:2 ribbed channel than in the 1:4 ribbed channel. Therefore, the pressure drop is higher in the 1:2 ribbed channel. The difference between the ribbed and smooth surfaces increases from the 1:4 to the 1:2 channels, and similarly to the 1:1 channel.

Thermal Performance

Finally, with the channel averaged Nusselt number and friction factor ratios, the thermal performance for each channel can be calculated. As shown in Figure 6.3, the trends for the thermal performance are similar to those for the friction factor ratios. This should be expected as no significant variations are present with the Nusselt number ratios, so the friction factor ratios strongly impact the performance. The performance for all the smooth channels is approximately 1. Both the Nusselt number ratios and the friction factor ratios are elevated above unity, and when they are combined with the constant pumping power expression, the performance of the smooth channels is approximately one. As shown in Figure 6.3, the thermal performance in the ribbed channel decreases as the aspect ratio increases. Therefore, the 1:4 channel has the superior thermal performance. This is directly related to the increasing friction factor ratio with the increasing aspect ratio.

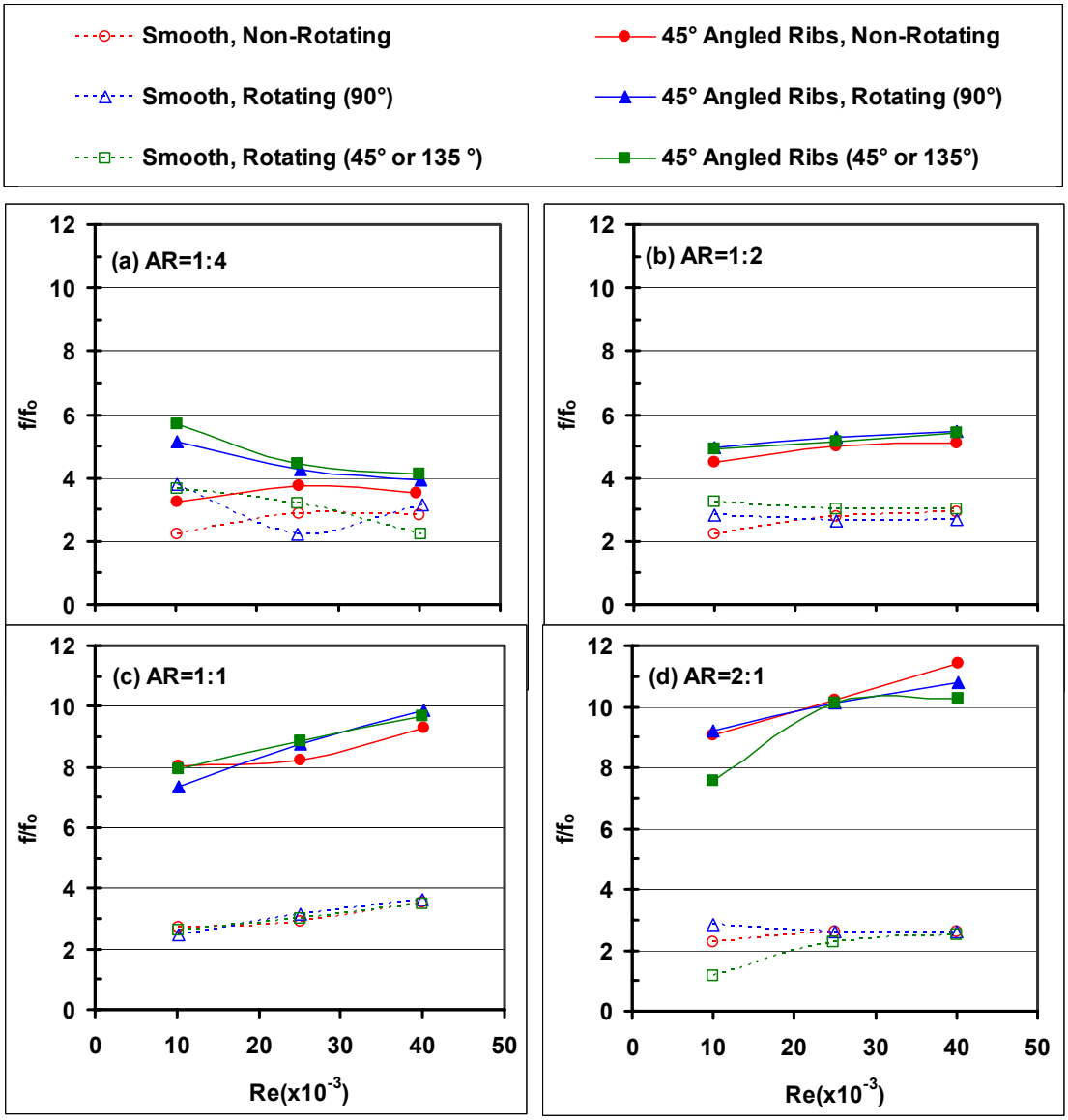

Figure 6.2 Overall Friction Factor Ratios for Non-Rotating and Rotating Channels

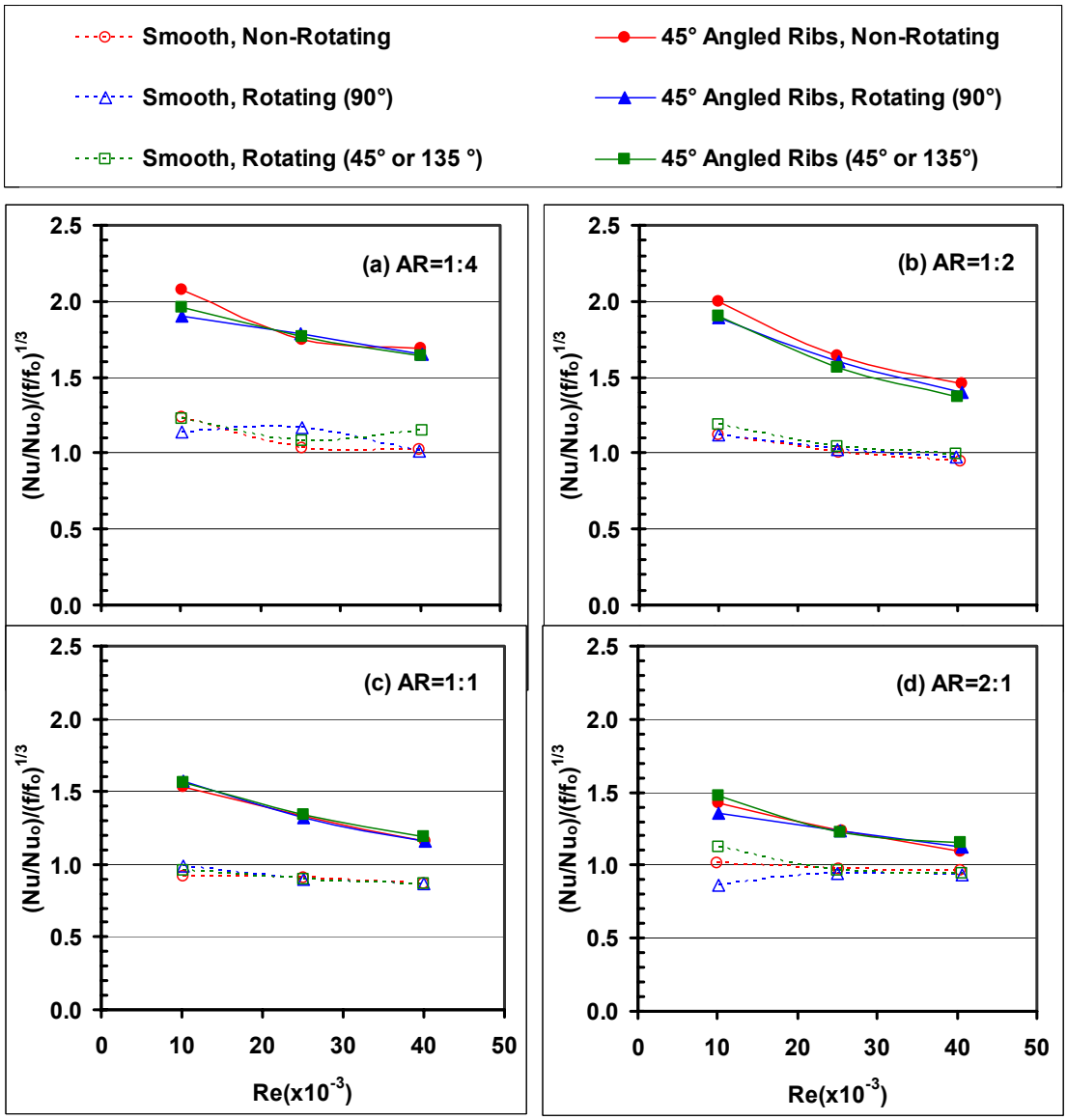

Figure 6.3 Overall Thermal Performance for Non-Rotating and Rotating Channels

VII CONCLUSIONS AND RECOMMENDATIONS

This study presents a variety of heat transfer results in a wide range of turbine blade two-pass internal cooling channels. Both smooth and angled ribs, overall channel averaged and regional results are shown for aspect ratios ranging from 1:4 to 4:1. This range of cross-sections covers the majority of channels that could be seen in actual engines. The experiments were performed for Reynolds number from 5000 to 40000. The rotating speed was fixed at 550 rpm for all tests. The effects of rotation and channel aspect ratio on heat transfer were discussed in detailed. Based on the limited parametric study, the main conclusions can be drawn.

Conclusions

1. The 45° angled ribs enhanced heat transfer approximately 2.5 to 4 times greater than the smooth circular pipe in the fully developed region for the non-rotating channels. The enhancement reduced as increasing Reynolds number. Smooth side walls also benefited from the ribs with heat transfer enhancement. The enhancement in ribbed channels could be attributed to the blockage effect and the rib induced vortices.
2. The rotation effect created heat transfer differences between the leading and trailing walls for both smooth and ribbed channels. In general, the heat transfer variation depends on the channel geometry (aspect ratio). The 1:4 channel has larger variations than the 4:1 channel, the 1:2 channel has larger variations than the 2:1 channel, and the square channel has the smallest heat transfer variations for both smooth and ribbed channels. It is because the channel geometry restricts

the rotation induced vortices that result in different heat transfer distributions in rotating channels. This provides important information to designers that the low aspect channel may have very low heat transfer on heat transfer reducing surface under rotating. The rotation effect also reduced with increasing Reynolds number (decreasing rotation number).

3. In general, the rotation effect was reduced in the second pass for both smooth and ribbed channels. This is attributed to the effect of the 180° sharp turn.
4. The 45° or 135° channel orientation creates less heat transfer difference between the leading and trailing walls than the 90° channel orientation for both smooth and ribbed channels.
5. The Nusselt number ratio decreases with increasing Reynolds number in both non-rotating and rotating channels with smooth and ribbed walls.
6. The overall level of heat transfer enhancement for all the ribbed channels is comparable. However, significant differences arise with the pressure losses incurred in the channels. The 1:4 channel incurred the lowest pressure penalty; therefore, the thermal performance of the 1:4 channel is superior to 1:2, 1:1, and 2:1 channels, respectively.

Recommendations

Due to the number of test sections, only limited parameters were investigated in this study. For example, the Reynolds number ranged from 5000 to 40000. However, the Reynolds number can be up to hundreds thousands in aircraft engines. For all tests, the rotating speed was fixed at 550 rpm. Therefore, the rotation effect is not independent

from Reynolds number in this study. In addition, the rib height is the same for all tests. To have better understanding of the heat transfer behavior in internal channels, the following works are recommended for future studies.

1. Investigate the effect of rib geometry (rib height, profile, and spacing) on heat transfer by varying rib geometry while keeping the channel geometry the same.
2. Investigate the rotation effect on heat transfer by varying the rotating speed at constant Reynolds number.
3. Investigate the heat transfer behavior at the higher Reynolds Number to reveal the effect of Reynolds number.

REFERENCES

[1] Han, J. C., Dutta, S., and Ekkad, S. V., 2000, *Gas Turbine Heat Transfer and Cooling Technology*, Taylor and Francis, New York.

[2] Metzger, D. E., and Sahm, M. K., 1986, "Heat Transfer around Sharp 180° Turns in Smooth Rectangular Channels," ASME J. Heat Transfer, **108**, pp. 500–506.

[3] Fan, C. S., and Metzger, D. E., 1987, "Effects of Channel Aspect Ratio on Heat Transfer in Rectangular Passage Sharp 180° Turn," ASME Paper No. 87-GT-113.

[4] Han, J. C., Chandra, P. R., and Lau, S. C., 1988, "Local Heat/Mass Transfer Distributions Around Sharp 180 Deg. Turns in Two-Pass Smooth and Rib-Roughened Channels," ASME J. Heat Transfer, **110**, pp. 91–98.

[5] Han, J. C., and Zhang, P., 1991, "Effect of Rib-Angle Orientation on Local Mass Transfer Distribution in a Three-Pass Rib-Roughened Channel," ASME J. Turbomach., **113**, pp, 123–130.

[6] Park, J. S., Han, J. C., Huang, Y., and Ou, S., 1992, "Heat Transfer Performance Comparisons of Five Different Rectangular Channels with Parallel Angled Ribs," Int. J. Heat Mass Transfer, **35**(11), pp. 2891-2903.

[7] Ekkad, S. V., and Han, J. C., 1997, "Detailed Heat Transfer Distribution in Two-Pass Square Channels with Rib Turbulators," Int. J. Heat Mass Transfer, **40**(11), pp. 2525–2537.

[8] Chen, Y., Nikitopoulos, D. E., Hibbs, R., Acharya, S., and Myrum, T. A., 2000, "Detailed Mass Transfer Distribution in a Ribbed Coolant Passage with a 180° Bend," Int. J. Heat and Mass Transfer, **43**, pp. 1479-1492.

[9] Wagner, J. H., Johnson, B. V., and Hajek, T. J., 1991a, "Heat Transfer in Rotating Passage with Smooth Walls and Radial Outward Flow," ASME J. Turbomach., **113**, pp. 42–51.

[10] Wagner, J. H., Johnson, B. V., and Kooper, F. C., 1991b, "Heat Transfer in Rotating Passage with Smooth Walls," ASME J. Turbomach., **113**, pp. 321–330.

[11] Taslim, W. E., Rahman, A., and Spring, S. D., 1991, "An Experimental Investigation of Heat Transfer Coefficients in a Spanwise Rotating Channel with Two Opposite Rib-Roughened Walls," ASME J. Turbomach., **113**, pp. 75–82.

[12] Taslim, M. E., Bondi, L. A., and Kercher, D. M., 1991, "An Experimental Investigation of Heat Transfer in an Orthogonally Rotating Channel Roughened with 45 Deg Criss-Cross Ribs on Two Opposite Walls," ASME J. Turbomach., **113**, pp. 346–353.

[13] Han, J. C., Zhang, Y. M., and Kalkuehler, K., 1993, "Uneven Wall Temperature Effect on Local Heat Transfer in a Rotating Two-Pass Square Channel with Smooth Walls," ASME J. Heat Transfer, **115**(4), pp. 912–920.

[14] Johnson, B. V., Wagner, J. H., Steuber, G. D., and Yeh, F. C., 1994a, "Heat Transfer in Rotating Serpentine Passage with Trips Skewed to the Flow," ASME J. Turbomach., **116**, pp, 113–123.

[15] Johnson, B. V., Wagner, J. H., Steuber, G. D., and Yeh, F. C., 1994b, "Heat Transfer in Rotating Serpentine Passage with Selected Model Orientations for Smooth or Skewed Trip Walls," ASME J. Turbomach., **116**, pp. 738–744.

[16] Parsons, J. A., Han, J. C., and Zhang, Y. M., 1994, "Wall Heating Effect on Local Heat Transfer in a Rotating Two-Pass Square Channel with 90° Rib Turbulators," Int. J. Heat Mass Transfer, **37**(9), pp. 1411–1420.

[17] Parsons, J.A., Han, J. C., and Zhang, Y. M., 1995, "Effects of Model Orientation and Wall Heating Condition on Local Heat Transfer in a Rotating Two-Pass Square Channel with Rib Turbulators," Int. J. Heat Mass Transfer, **38**(7), pp. 1151–1159.

[18] Zhang, Y. M., Han, J. C., Parsons, J. A., and Lee, C. P., 1995, "Surface Heating Effect on Local Heat Transfer in a Rotating Two-Pass Square Channel with 60° Angled Rib Turbulators," ASME J. Turbomach., **117**, pp. 272–280.

[19] Dutta, S., and Han, J. C., 1996, "Local Heat Transfer in Rotating Smooth and Ribbed Two-Pass Square Channels with Three Channel Orientations," ASME J. Heat Transfer, **118**, pp. 578–584.

[20] Dutta, S., Han, J. C., and Lee, C. P., 1996, "Local Heat Transfer in a Rotating Two-Pass Ribbed Triangular Duct with Two Model Orientations," Int. J. Heat Mass Transfer, **39**, pp. 707–715.

[21] Park, C. W., and Lau, S. C., 1998, "Effect of Channel Orientation of Local Heat (Mass) Distributions in a Rotating Two-Pass Square Channel with Smooth Walls," ASME J. Heat Transfer, **120**, pp. 624–632.

[22] Park, C. W., Yoon, C., and Lau, S. C., 2000, "Heat (Mass) Transfer in a Diagonally Oriented Rotating Two-Pass Channel with Rib-Roughened Walls," ASME J. Heat Transfer, **122**, pp. 208–211.

[23] Murata, A., Mochizuki, S., and Takahashi, T., 1999, "Local Heat Transfer Measurement of an Orthogonally Rotating Square Duct with Angled Rib Turbulators," Int. J. Heat and Mass Transfer, **42**, pp. 3047-3056.

[24] Liou, T. M., Chen, M. Y., and Tsai, M. H., 2002, "Fluid Flow and Heat Transfer in a Rotating Two-Pass Square Duct with In-Line 90-deg Ribs," ASME J. Turbomach., **124**, pp. 260-268.

[25] Al-Hadhrami, L., and Han, J. C., 2003, "Effect of Rotation on Heat Transfer in Two-Pass Square Channels with Five Different Orientations of 45° Angled Rib Turbulators," Int. J. Heat Mass Transfer, **46**, pp. 653-669.

[26] Willett, F. T., and Bergles, A. E., 2001, "Heat Transfer in Rotating Narrow Rectangular Ducts with Heated Sides Orientated at 60° to the R-Z Plane," ASME J. Turbomach., **123**, pp. 288-295.

[27] Azad, G. S., Uddin, M. J., Han, J. C., Moon, H. K., and Glezer, B., 2002, "Heat Transfer in a Two-Pass Rectangular Rotating Channel with 45-Deg Angled Rib Turbulators," ASME J. Turbomach., **124**, pp. 251-259.

[28] Al-Hadhrami, L., Griffith, T. S., and Han, J. C., 2003, "Heat Transfer in Two-Pass Rotating Rectangular Channels (AR=2:1) with Five Different Orientations of 45° V-shaped Rib Turbulators," ASME J. Heat Transfer, **125**, pp.232-242.

[29] Griffith, T. S., Al-Hadhrami, L., and Han, J. C., 2002, "Heat Transfer in Rotating Rectangular Cooling Channels (AR=4) with Angled Ribs," ASME J. Heat Transfer, **124**, pp. 617-625.

[30] Lee, E., Wright. L. M., and Han, J. C., 2003, "Heat Transfer in Rotating Rectangular Channels (AR=4:1) with V-Shaped and Angled Rib Turbulators with and without Gaps," ASME Paper No. 2003-GT-38900.

[31] Cho, H. H., Kim, Y. Y., Kim, K. M., and Rhee, D. H., 2003, "Effects of Rib Arrangements and Rotation Speed on Heat Transfer in a Two-Pass Duct," ASME Paper No. 2003-GT-38609.

[32] Agarwal, P., Acharya, S., and Nikitopoulos, D. E., 2003, "Heat/Mass Transfer in 1:4 Rectangular Passages with Rotation," ASME Paper No. 2003-GT-38615.

[33] Han, J.C., Park, J.S., and Lei, C.K., 1985, "Heat Transfer Enhancement in Channels with Turbulence Promoters," ASME J. Engineering for Gas Turbines and Power, **107**, pp. 628-635.

[34] Kline, S. J., and McClintock, F. A., 1953, "Describing Uncertainty in Single-Sample Experiments," Mechanical Engineering, **75**, pp. 3-8.

[35] Al-Qahtani, M., Jang, Y.J., Chen, H.C., and Han, J.C., 2002, "Prediction of Flow and Heat Transfer in Rotating Two-Pass Rectangular Channels with 45-deg Rib Turbulators," ASME Journal of Turbomach., **124**, pp. 242-250.

[36] Su, G., Chen, H.C., Han, J.C. and Heidmann, D., 2004, "Computation of Flow and Heat Transfer in Two-Pass Rotating Rectangular Channels (AR=1:1, AR=1:2, AR=1:4) with 45-Deg Angled Ribs by a Reynolds Stress Turbulence Model," ASME Paper No. 2004-GT-53662.

VITA

Wen-Lung Fu was born on January 8, 1971 in Taiwan. He earned his B.S. degree from Chung Yuan Christian University in 1993 and M.S. degree from Yuan-Ze Institute of Technology in 1995 both in Mechanical Engineering. He started his Ph.D. program at Texas A&M University in January 2002 and graduated in May 2005.

Permanent Mailing Address:

Wen-Lung Fu

C/o Dr. Je-Chin Han

Department of Mechanical Engineering

Texas A&M University

College Station, TX 77843-3123